5-2004

Activity-dependent modulation of neuronal sodium channel expression

Joshua Peter Klein
Yale University.

ACTIVITY-DEPENDENT MODULATION OF NEURONAL SODIUM CHANNEL EXPRESSION

A Dissertation
Presented to the Faculty of the Graduate School
of
Yale University
in Candidacy for the Degree of
Doctor of Philosophy

by

Joshua Peter Klein

Dissertation Director: Stephen G. Waxman, M.D.,Ph.D.

May, 2004

ACTIVITY-DEPENDENT MODULATION OF NEURONAL SODIUM CHANNEL EXPRESSION

Joshua Peter Klein

2004

ABSTRACT

Action potentials initiate via the voltage-dependent opening of plasma membrane-associated sodium channels. The number and type of sodium channels in a neuronal membrane determine the quantity of sodium current that results from a given stimulus. The expression of sodium channels in neurons is plastic, and is not only altered by injury and disease, but also by subtle changes in physiologic environment. In this dissertation, the effect of neuronal activity level on the expression and function of sodium channels is explored within several neuronal populations. First I examine the response of vasopressin-producing magnocellular neurosecretory cells of the supraoptic nucleus to the hyperosmotic setting of chronic diabetes mellitus. Evidence for up-

regulation of sodium channels, and metabolic overactivation leading to apoptosis, in these neurons is presented. Second, I test the effect of electrical stimulation on expression of sodium channels in cultured sensory neurons. And lastly, I demonstrate that there is dysregulated sodium channel expression within cortical neurons in a specific region of the brain in a model of absence epilepsy.

Together, the results of these experiments support the hypothesis that the activity level of a neuron influences its rate of production and expression of sodium channels. Identification of this phenomenon could lead to new therapeutic strategies for 1) limiting end-organ pathogenesis in diabetes (by reducing magnocellular neurosecretory cell sodium channel activity, thereby preventing chronically up-regulated vasopressin secretion), 2) treating pain (by using stimulation to normalize post-injury sodium channel expression and reduce neuronal hyperexcitability), and 3) treating epilepsy (by targeted modulation or block of seizure-initiating sodium channel activity). Development of novel therapeutic approaches will depend on further characterization of the regulatory feedback mechanism that links changes in neuronal activity level with modulation of sodium channel expression.

TABLE OF CONTENTS

ABSTRACT i
TITLE PAGE iii
COPYRIGHT iv
TABLE OF CONTENTS v
LIST OF FIGURES AND TABLES vii
LIST OF ABBREVIATIONS viii
ACKNOWLEDGMENTS ix
DEDICATION xi

CHAPTER 1: INTRODUCTION

1.1 THE VOLTAGE-GATED SODIUM CHANNEL 1
1.2 PLASTICITY OF VGSC EXPRESSION IN INJURY AND DISEASE 2
1.3 ACTIVITY-DEPENDENT MODULATION OF VGSC EXPRESSION 4
1.4 SPECIFIC AIMS 6

CHAPTER 2: SODIUM CHANNEL EXPRESSION IN HYPOTHALAMIC OSMOSENSITIVE NEURONS IN EXPERIMENTAL DIABETES

2.1 SUMMARY 8
2.2 INTRODUCTION 9
2.3 MATERIALS AND METHODS 10
2.4 RESULTS 12
2.4.1 INDUCTION OF DIABETES
2.4.2 UP-REGULATION OF SODIUM CHANNEL MRNA AND PROTEIN
2.4.3 FUNCTIONAL CHANGES IN DIABETIC MNCS
2.5 DISCUSSION 18

CHAPTER 3: APOPTOSIS OF VASOPRESSINERGIC HYPOTHALAMIC NEURONS IN CHRONIC EXPERIMENTAL DIABETES MELLITUS

3.1 SUMMARY 21
3.2 INTRODUCTION 22
3.3 MATERIALS AND METHODS 24
3.4 RESULTS 26
3.4.1 MORPHOLOGICAL CHANGES OCCUR IN DIABETIC MNCS
3.4.2 CASPASE-3 EXPRESSION IS UPREGULATED IN DIABETIC MNCS
3.4.3 DNA FRAGMENTATION OCCURS IN DIABETIC MNCS

3.4.4 QUANTIFICATION OF TUNEL AND VASOPRESSIN STAINING
3.4.4 TUNEL AND VASOPRESSIN DO NOT COLOCALIZE
3.4.5 MICROGLIAL ACTIVITY IS ENHANCED IN DIABETIC MNCS
3.5 DISCUSSION 37

CHAPTER 4: PATTERNED ELECTRICAL ACTIVITY MODULATES SODIUM CHANNEL EXPRESSION IN SENSORY NEURONS

4.1 SUMMARY 42
4.2 INTRODUCTION 43
4.3 MATERIALS AND METHODS 45
4.4 RESULTS 49
4.4.1 EFFECT OF ELECTRICAL STIMULATION ON NEURON SURVIVAL
4.4.2 STIMULATION DOWN-REGULATES SODIUM CHANNEL PROTEIN
4.4.3 STIMULATION DOWN-REGULATES SODIUM CHANNEL MRNA
4.5 DISCUSSION 54

CHAPTER 5: DYSREGULATION OF SODIUM CHANNEL EXPRESSION IN A RODENT MODEL OF ABSENCE EPILEPSY

5.1 SUMMARY 57
5.2 INTRODUCTION 58
5.3 MATERIALS AND METHODS 59
5.4 RESULTS 64
5.4.1 SWD INCIDENCE INCREASES WITH AGE IN WAG/RIJ RATS
5.4.2 SODIUM CHANNEL MRNA IS UP-REGULATED IN EPILEPTIC CORTEX
5.4.3 SODIUM CHANNEL PROTEIN IS UP-REGULATED IN LAYERS II-IV
5.4.4 SODIUM CHANNEL EXPRESSION PARALLELS SWD INCIDENCE
5.5 DISCUSSION 72

CHAPTER 6: CONCLUSIONS

6.1 ACTIVITY-DEPENDENT MODULATION OF VGSC EXPRESSION 76
6.2 MOLECULAR CHANGES WITHIN NEURONS IN THE DIABETIC BRAIN 76
6.3 STIMULATION-DEPENDENT PLASTICITY OF CGSC EXPRESSION 84
6.4 VGSC EXPRESSION AND EPILEPSY 87
6.5 CLINICAL PERSPECTIVES 89

REFERENCES 91

COPYRIGHT PERMISSIONS 112

LIST OF FIGURES AND TABLES

Table 1.1	Voltage-gated sodium channel (VGSC) α-subunits	2
Fig. 1.1	Activity-dependent modulation of VGSC expression: a model	5
Fig. 2.1	Vasopressin expression is up-regulated in diabetic neurons	14
Fig. 2.2	Sodium channel mRNA is up-regulated in diabetic SON neurons	15
Fig. 2.3	Sodium channel protein is up-regulated in diabetic SON neurons	16
Fig. 2.4	Sodium currents are increased in diabetic SON neurons	17
Fig. 2.5	Hyperglycemia, vasopressin, and nephropathy	19
Fig. 3.1	Chronic diabetes induces morphological changes in the SON	30
Fig. 3.2	Caspase-3 is up-regulated in the chronically diabetic SON	31
Fig. 3.3	TUNEL-positive neurons in the chronically diabetic SON	32
Fig. 3.4	Quantification of TUNEL-positive neurons in the diabetic SON	33
Fig. 3.5	TUNEL and vasopressin overlap in the chronically diabetic SON	34
Fig. 3.6	Microglial and astrocytic reactivity in the chronically diabetic SON	35
Table 3.1	Quantification of SON neuronal phenotype	36
Fig. 4.1	NGF withdrawal down-regulates Nav1.8 and Nav1.9	51
Fig. 4.2	Electrical stimulation down-regulates Nav1.8 and Nav1.9 protein	52
Fig. 4.3	Electrical stimulation down-regulates Nav1.8 and Nav1.9 mRNA	53
Fig. 5.1	EEG recordings of absence epileptic WAG/Rij rats	68
Fig. 5.2	Nav1.1 and Nav1.6 mRNA is up-regulated in the WAG/Rij cortex	69
Fig. 5.3	Nav1.1 and Nav1.6 are up-regulated in layer II-IV cortical neurons	70
Fig. 5.4	Sodium channel dysregulation correlates to seizure incidence	71
Fig. 6.1	Neurologically "active" and "passive" responses to diabetes	78
Fig. 6.2	Neuronal activity level modulates VGSC expression	86
Fig. 6.3	Cause or effect: sodium channel expression and epilepsy	88

LIST OF ABBREVIATIONS

AGE	advanced glycosylation end-product
BSA	bovine serum albumin
cAMP	cyclic adenosine monophosphate
CREB	cAMP response element binding protein
DAB	diaminobenzadine hydrochloride
DM	diabetes mellitus
DRG	dorsal root ganglia
GABA	gamma-aminobutyric acid
GFAP	glial fibrillary acidic protein
GLUT	glucose transporter
EEG	electroencephalogram
IGF	insulin-like growth factor
LTD	long term depression
LTP	long term potentiation
MAP	*mitogen activating protein*
MNC	magnocellular neurosecretory cell
NGF	nerve growth factor
NMDA	N-methyl-D-aspartate
NO	nitric oxide
NOS	nitric oxide synthase
PBS	phosphate-buffered saline
PCR	polymerase chain reaction
PKC	protein kinase C
PVN	paraventricular nucleus
SON	supraoptic nucleus
STZ	streptozotocin
SD	standard deviation
SE	standard error
SWD	spike-wave discharge
TUNEL	terminal dUTP nick end labeling
TTX	tetrodotoxin
VGSC	voltage-gated sodium channel
VP	vasopressin
WAG/Rij	Wistar Albino Glaxo from Rijswijk
WM	white matter

ACKNOWLEDGMENTS

I would like to thank Stephen G. Waxman for giving me the opportunity to spend three wonderfully productive and enjoyable years in his laboratory. His encyclopedic knowledge of neurology has been inspiring and his encouragement and guidance have allowed me to pursue my work with enthusiasm and confidence.

I thank my thesis committee, Hal Blumenfeld, Jeffery D. Kocsis, and Robert H. LaMotte, for their critical evaluations of my work, and for their helpful ideas and suggestions.

I thank Joel A. Black and Sulayman D. Dib-Hajj for their constant support, advice, and expert assistance with my experimental work. My friends in the Waxman lab, Matthew J. Craner, Bryan C. Hains, Carl Y. Saab, Ellen K. Wittmack, Theodore R. Cummins, Lynda Tyrrell, Shujun Liu, Pam Zwinger, Cindy Cadoret, and Bart Toftness helped create a pleasant and cooperative working environment.

I would like to thank R. Douglas Fields, Elisabetta Tendi, and members of the Fields Lab at the NIH, and Davender S. Khera, Hrachya Nersesyan, and members of the Blumenfeld lab at Yale, for their hard work on our collaborations.

Funding for my studies was provided by a grant from the National Institute of General Medical Sciences (NIGMS) Medical Scientist Training Program (MSTP), and by the Yale University School of Medicine MD/PhD program. Laboratory work was supported by the Medical Research Service and Rehabilitation Research Service, Department of Veterans Affairs, and by grants from the Paralyzed Veterans of America and Eastern Paralyzed Veterans Association.

I would like to thank James D. Jamieson, Susan Sansone, and Marybeth Brandi in the MD/PhD office for making my years in lab go as smoothly as possible. In addition, I thank Charles A. Greer and Carol Russo of the Yale Interdepartmental Neuroscience Program for their guidance and support.

I would like to thank Harvey Rubin at the University of Pennsylvania, who inspired me to join the MD/PhD program at Yale, and Charles D. Duggan, who first exposed me to scientific research during high school.

I would like to thank my friends in the Yale Medical School classes of 2002 and 2003 (with whom I began medical school in 1998) for their amazing friendship and continued support during my Ph.D. years.

I am indebted to my mother, my brother Jason D. Klein, and my grandmother Sophie Slutsky, along with my extended family, for their love and constant support. I would also like to thank my new family, the Rettingers, for welcoming me into their lives and for their encouragement.

And lastly, I would like to acknowledge my wonderful and beautiful fiancée Meredith L. Rettinger, who was undoubtedly my best discovery during my years in lab.

DEDICATION

To the memory of my father, Marvin Klein, M.D., for his lasting inspiration.

And to my mother, Susan A. Klein, for her strength, courage, love, and support.

CHAPTER 1

INTRODUCTION AND BACKGROUND

1.1 VOLTAGE-GATED SODIUM CHANNELS

Neuronal information transmission occurs by voltage-gated sodium channel (VGSC)-dependent action potential firing. There are at least eight VGSC genes expressed throughout the nervous system, each with different tissue specificities and functional characteristics (Akopian et al., 1996; Black et al., 1996; Catterall, 2000; Dib-Hajj et al., 1998a; Goldin et al., 2000; Kayano et al., 1988; Noda et al., 1986b; Sangameswaran et al., 1996; Schaller et al., 1995; Toledo-Aral et al., 1997) (Table 1.1). The distinct combination of VGSCs present in a neuronal membrane determines its firing pattern and electrical conduction properties. VGSC expression is a dynamic process, and alterations in physiological state as well as injury and disease induce changes in sodium channel expression, which lead to changes in neuronal behavior.

The VGSC itself is a polypeptide whose primary structure consists of a 260 kD α-subunit associated with two β subunits (Isom et al., 1994), β1 (36 kD) (Isom et al., 1992) and β2 (33 kD) (Isom et al., 1995). While sodium currents can be elicited by functional expression of the α-subunit alone (Goldin et al., 1986; Noda et al., 1986a), the β subunits are required for normal physiologic voltage-dependent kinetics (Isom et al., 1992; Isom et al., 1995). The α-subunit is comprised of four internally homologous domains (I-IV), each of which contains six transmembrane segments (S1-S6). The pore,

through which sodium ions flow upon channel opening, is formed by close association of hydrophilic residues within S5 and S6 of each domain. Positively-charged residues on S4 endow the channel with voltage sensitivity.

Table 1.1. Voltage-gated sodium channel (VGSC) α-subunits (Goldin et al., 2000).

Channel	Former name	Expression
Nav1.1	rat I, SCN1A	CNS/PNS
Nav1.2	rat II, SCN2A	CNS/PNS
Nav1.3	rat III	CNS/PNS
Nav1.4	SkM1, μ1	skeletal muscle
Nav1.5	SkM2, H1	heart muscle
Nav1.6	NaCh6, PN4, Scn8a, Cer III	CNS/PNS
Nav1.7	hNE, PN1	PNS/Schwann cells
Nav1.8	SNS, PN3	PNS
Nav1.9	NaN, SNS2, PN5, Scn12a	PNS

1.2 PLASTICITY OF VGSC EXPRESSION IN INJURY AND DISEASE

Neuronal firing is critically dependent on the repertoire of sodium channels within the plasma membrane. Injury-induced changes in expression of multiple sodium channel subtypes can lead to altered firing properties including spontaneous ectopic activity and hyperexcitability (Rizzo et al., 1996). This effect has been studied in dorsal root ganglia (DRG) sensory neurons after a variety of injuries. Molecular analysis has revealed that different sodium channel genes underlie different currents recorded in DRG neurons: Aα/β neurons express tetrodotoxin-sensitive (TTX-S) currents which are generated by Nav1.1, Nav1.6 and Nav1.7, while C-type neurons preferentially express tetrodotoxin-resistant (TTX-R) currents, generated by Nav1.8 and Nav1.9 (Akopian et al., 1996; Cummins et al., 1999).

Following sciatic nerve axotomy, a down-regulation of TTX-R current corresponding to sodium channel genes Nav1.8 and Nav1.9 has been demonstrated in C-type DRG neurons (Cummins and Waxman, 1997; Dib-Hajj et al., 1996; Dib-Hajj et al., 1998a; Sleeper et al., 2000). In addition, a previously silent rapidly-repriming TTX-S current, corresponding to the sodium channel Nav1.3, is expressed in the axotomized neurons. Up-regulation of Nav1.3 has also been demonstrated in dorsal horn neurons following contusion spinal cord injury (Hains et al., 2003). These changes are thought to occur, at least in part, as a result of decreased neurotrophic factor availability in the transected axons. NGF deprivation is known to decrease Nav1.8 expression and its TTX-R current in cultured DRG neurons (Fjell et al., 1999b). These changes in sodium channel expression contribute to the increased firing frequency observed following axotomy. Hyperexcitability leading to ectopic and spontaneous firing may underlie initiation and maintenance of neuropathic pain.

In addition to direct nerve injury, application of inflammatory mediators also alters sodium channel expression in DRG neurons. Carrageenan, which causes localized erythema, edema, and hyperalgesia when injected subcutaneously, induced an up-regulation of Nav1.8 mRNA and TTX-R current in C-type DRG neurons (Tanaka et al., 1998). It is thought that increased peripheral levels of NGF (produced normally by fibroblasts, Schwann cells, and keratinocytes, and by immune cells during inflammation) may cause the up-regulation of Nav1.8 in this model.

Sodium channel plasticity has also been demonstrated in several diseases. In streptozotocin (STZ)-induced diabetes, DRG neurons up-regulate mRNA and protein expression of Nav1.3, Nav1.6, and Nav1.9, and down-regulate expression of Nav1.8, after the onset of allodynia (Craner et al., 2002a). This effect is associated with a significant down-regulation of IGF and its receptor in diabetic DRG neurons (Craner et al., 2002b). There is also evidence for up-regulated VGSC expression within cortical

neurons in experimental epilepsy (Aronica et al., 2001; Bartolomei et al., 1997; Gastaldi et al., 1998; Vreugdenhil et al., 1998). Increases in expression of VGSCs producing persistent currents, in particular, may contribute to the sustained depolarizations characteristic of seizure activity (Segal and Douglas, 1997; Segal, 2002).

In all of these examples, neuronal activity is altered based on changes in transcription of normal sodium channel genes. These so-called "transcriptional channelopathies" are distinct from other channelopathies characterized by either 1) mutations causing abnormal or absent channel protein, or 2) autoimmune and toxic effects causing altered channel function (Waxman, 2001). The ability of a neuron to remodel its electrogenic apparatus by altering the number and ratio of various sodium channels in its membrane is a focus of this dissertation.

1.3 ACTIVITY-DEPENDENT MODULATION OF EXPRESSION

Do changes in neuronal activity induce plasticity of VGSC expression? At the transcriptional level, VGSC gene expression is known to be growth factor dependent (Fjell et al., 1999a), but the effect of afferent stimulation and neuronal firing on VGSC gene expression remains unclear. It has been suggested that neurons adjust their gain and excitability by altering VGSC expression to adapt to, or react to, new input environments (Desai et al., 1999; Spitzer, 1999; Stemmler and Koch, 1999; Waxman, 1999a; Woolf and Salter, 2000). The underlying activity-dependent transcriptional signals for these modifications are only partially understood. There is some evidence that activity-dependent changes in sodium channel expression are mediated through changes in intracellular calcium levels, but much of this data, as will be discussed, is derived from experiments on non-neuronal sodium channels, for example, Nav1.4 in skeletal myotubes (Brodie et al., 1989; Monjaraz et al., 2000; Offord and Catterall, 1989; Sherman and Catterall, 1984; Shiraishi et al., 2001).

Since alterations in physiologic environment influence the functional output of a neuron, a link between neuronal activity level and VGSC gene expression is anticipated (Fig. 1.1). If properly characterized, this link might provide a new paradigm for therapeutic control of neuronal transcriptional sodium channelopathies by activity modulation.

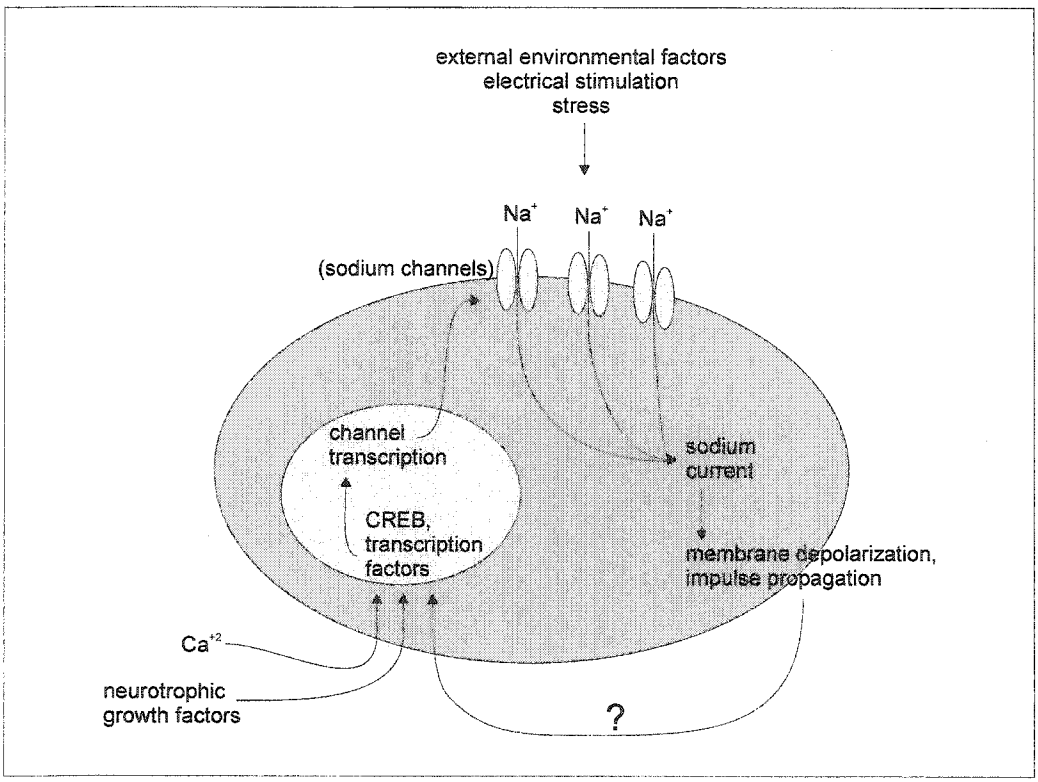

Fig. 1.1. The effect of neuronal activity on voltage-gated sodium channel expression is unknown, but likely involves regulatory feedback (question mark) that either directly or indirectly influences the activity of transcription factors.

1.4 SPECIFIC AIMS

The objective of this dissertation is to identify whether changes in VGSC expression occur in experimental models where neuronal activity levels are altered. In Chapter 2, vasopressin producing neurons of the hypothalamic supraoptic nucleus are studied in the hyperosmotic setting of streptozotocin (STZ)-induced diabetes. In response to elevated serum osmolality, these neurons increase their synthesis of vasopressin. I demonstrate that the increased biosynthetic activity of these neurons is accompanied by up-regulated expression of two sodium channels, Nav1.2 and Nav1.6, and their currents. This molecular reorganization of the electrogenic apparatus enables these neurons to increase their firing, and this increases the depolarization-dependent calcium-mediated release of vasopressin. The long-term effects of this increased demand for vasopressin and up-regulated sodium channel expression are explored in Chapter 3, using 6 month STZ-induced diabetic animals. In these animals, apoptosis was detected in a sub-population of neurons within the supraoptic nucleus, indicating that chronic diabetes induces neuronal loss, possibly as a result of activity-dependent overactivation.

The effect of electrical activity on neuronal VGSC expression is examined in Chapter 4. Cultured embryonic mouse DRG neurons, which normally express high levels of Nav1.8 and Nav1.9, are known to down-regulate expression of these channels after NGF withdrawal. In these experiments I show that, using non-limiting concentrations of NGF, expression of Nav1.8 and Nav1.9 mRNA and protein are down-regulated following electrical stimulation. This finding provides direct evidence that sodium channel expression can be regulated and altered by changes in neuronal activity.

Epilepsy is a condition characterized by abnormally elevated neuronal activity, and therefore provides a useful model for studying activity-dependent changes in VGSC expression. I demonstrate that in a rodent model of absence epilepsy, mRNA and

protein expression of Nav1.1 and Nav1.6 are up-regulated in layer II-IV neurons specifically within the facial somatosensory region of the cortex, compared to controls (Chapter 5). This region of cortex approximately corresponds to the electrophysiologically-determined region of seizure onset in this model. The dysregulated sodium channel expression parallels the increase in seizure frequency and duration observed in these animals.

Activity-dependent modulation of VGSC expression is therefore explored within several neuronal populations, and the functional significance and implications of the observed changes are discussed within each chapter.

CHAPTER 2

SODIUM CHANNEL EXPRESSION IN HYPOTHALAMIC OSMOSENSITIVE NEURONS IN EXPERIMENTAL DIABETES

2.1 SUMMARY

Vasopressin is synthesized by neurons in the supraoptic nucleus of the hypothalamus and its release is controlled by action potentials produced by specific subtypes of voltage-gated sodium channels expressed in these neurons. The hyperosmotic state associated with uncontrolled diabetes mellitus causes elevated levels of plasma vasopressin, which are thought to contribute to the pathologic changes of diabetic nephropathy. We demonstrate here that in the rodent streptozotocin model of diabetes there are increases in expression of mRNA and protein for two sodium channel α-subunits and two β-subunits in the neurons of the supraoptic nucleus. Transient and persistent sodium currents show parallel increases in these diabetic neurons. In the setting of chronic uncontrolled diabetes, these changes in sodium channel expression in the supraoptic nucleus may be maladaptive, contributing to the development of secondary renal complications.

2.2 INTRODUCTION

The role of the central nervous system in the pathophysiology of diabetes mellitus is incompletely understood. Vasopressin is synthesized in magnocellular neurosecretory cells (MNCs) of the supraoptic nucleus (SON) of the hypothalamus and released from the posterior pituitary in response to elevated plasma osmotic pressure. There is now evidence that prolonged elevated levels of vasopressin are a risk factor for the development of diabetic nephropathy, which can lead to end stage renal disease (Ahloulay et al., 1999; Bardoux et al., 1999). The amount of vasopressin released is a function of action potential firing in the MNCs. This firing, which occurs in a characteristic bursting pattern (Andrew and Dudek, 1983) is dependent on the opening of voltage-gated Na^+ channels in the MNCs, and in fact, application of tetrodotoxin (TTX) to dissociated MNCs strongly reduces vasopressin secretion (Sperlagh et al., 1999).

At least eight types of voltage-gated sodium channels are expressed in neurons (Catterall, 2000; Goldin et al., 2000), each with different tissue specificities. These channels consist of an α-subunit which comprises the channel pore and voltage-sensor, and accessory β-subunits (Isom et al., 1994). Supraoptic MNCs express the Nav1.2 and Nav1.6 α-subunits, and β1 and β2 subunits, under physiological conditions (Tanaka et al., 1999). Transcription of these channel subunits is up-regulated and increased numbers of functional subunits are inserted in the membranes of MNCs with chronic salt-loading, a maneuver that results in increased plasma osmolality; the increase in sodium channel expression can result in a lowered threshold for firing in the MNCs (Tanaka et al., 1999).

In this study we asked whether the hyperosmolality associated with diabetes could trigger a change in sodium channel expression in hypothalamic MNCs. After confirming in initial studies that sodium channels Nav1.2 and Nav1.6, but not Nav1.1 and

Nav1.3, are present at significant levels in normal and diabetic SON, we focused on Nav1.2 and Nav1.6 and β1 and β2. We report here that in experimentally-induced diabetes, there is a previously undescribed change in the hypothalamus: molecular and functional alteration of MNCs by up-regulation of expression of specific α- and β-subunit sodium channel genes and insertion of additional functional channels into the membranes of these neurosecretory neurons.

2.3 MATERIALS AND METHODS

Induction of Diabetes. Adult male Sprague-Dawley rats (225-250 g) were injected with streptozotocin (STZ, 60mg/kg i.p., Sigma, St. Louis, Missouri). Plasma glucose (Encore Glucometer, Miles Inc., Elkhart, Indiana) and plasma osmotic pressure (Wescor model 5500, Logan, Utah) were measured at intervals 2-6 weeks post-injection. Ten animals (5 control, 5 diabetic) were studied 2-6 weeks after STZ injection using *in situ* hybridization, 8 animals (4 control, 4 diabetic) using immunocytochemistry, and 10 animals (5 control, 5 diabetic) using patch-clamp electrophysiology.

***In situ* Hybridization**. Rats were anesthetized with ketamine/xylazine (80/5 mg/kg, i.p.) and perfused with 4% paraformaldehyde in 0.14 M phosphate buffer. Brains were postfixed, cryoprotected and serial coronal sections (20 μm) including the supraoptic nucleus were cut. Control and diabetic sections were hybridized with isoform-specific riboprobes (Black et al., 1996) in parallel as described previously (Tanaka et al., 1999). Sense riboprobes yielded no signals on *in situ* hybridization (not shown).

Immunocytochemistry. Brains were postfixed, cryoprotected in PBS, and sections of SON (20 μm) were processed for immunocytochemistry as previously described

(Tanaka et al., 1999) using antibodies to vasopressin (1:1000, Oncogene Research Products, San Diego, CA), or sodium channel subunits Nav1.2 (1:100, Sigma), Nav1.6 (1:100, Alomone, Jerusalem, Israel), and the β2-subunit (1:100, Alomone). Control experiments without primary or secondary antibody incubations showed no staining.

Data Analysis. Quantitative microdensitometry of hybridization and immunostaining signals were performed using a Nikon Eclipse E800 light microscope (20X objective) and IPLab Image Processing software (Scanalytics Inc., Fairfax, Virginia). Signal intensities were obtained by manually outlining the SON and using IPLab integrated densitometry functions to calculate mean signal intensities for the selected areas. Background optical intensity measured adjacent to the SON in each section was subtracted from all signals; the results are expressed as means ± SEM. Diabetic tissue was compared to controls processed in parallel. Control and diabetic groups were compared using non-paired t-tests.

Patch clamp electrophysiology. MNCs in the SON were acutely dissociated from control and diabetic animals as previously described (Tanaka et al., 1999; Widmer et al., 1997). MNCs were recorded in the whole-cell patch-clamp configuration as described previously (Tanaka et al., 1999) within two hours with an EPC-9 amplifier (HEKA electronics, Lambrecht/Pfalz, Germany) using 1-2 MΩ electrodes (85% series resistance compensation). The pipette solution contained (in mM): 140 CsF, 2 $MgCl_2$, 1 EGTA, and 10 Na-HEPES (pH 7.3) and the saline solution (above) was used as extracellular bath. All recordings were conducted at room temperature (~21 °C).

2.4 RESULTS

Induction of diabetes. All animals injected with STZ developed hyperglycemia (>250 μg/dl) and elevated plasma osmotic pressure compared with control animals injected with vehicle (control 294.3±6.5 mOsm; diabetic 314.4±7.6 mOsm; $p<0.01$). Animals were studied 2-6 weeks after injection with STZ. Vasopressin expression was up-regulated in the diabetic SON (Fig. 2.1).

Up-regulation of sodium channel mRNA and protein in the diabetic SON. Because our earlier studies (Widmer et al., 1997) demonstrated that Nav1.2, Nav1.6, β1 and β2 (but not Nav1.1 or Nav1.3) are present in MNCs and are up-regulated by salt-loading, we focused on these channel subunits. *In situ* hybridization using isoform-specific anti-sense riboprobes showed that in control animals, there are moderate levels of mRNA for Na^+ channel α-subunits Nav1.2, Nav1.6, and β-subunits β1 and β2. In diabetic animals, we observed a statistically significant ($p<0.05$) increase in mRNA levels for each of these four Na^+ channel subunits within the SON (Fig. 2.2). There was no change in sodium channel expression within the surrounding neuropil. Immunocytochemical observations using isoform-specific antibodies showed that there are parallel changes in protein for both of the α-subunits and the β2-subunit within the SON (Fig. 2.3).

Functional changes in diabetic MNCs. To determine whether the up-regulated mRNA and protein resulted in an increase in the number and/or density of functional channels inserted into the neuronal membrane, we acutely dissociated MNCs from control ($n=5$) and diabetic ($n=5$) animals and studied them using patch clamp electrophysiology. Control and diabetic MNCs both produced fast, TTX-sensitive sodium currents. The voltage dependence of activation and steady-state inactivation of the transient sodium

current were similar for diabetic and control MNCs (Fig. 2.4A,B). The time constant for inactivation (measured at 0 mV) was similar for MNCs from diabetic (τ=.65±.03 ms, n=31) and control (τ=.67±.03 ms, n=22) animals. However the peak transient current amplitude was 130% greater in MNCs isolated from the diabetic animals (Fig. 2.4C; 13.2±12.2 nA, control, n=23; 30.4±2.9 nA, diabetic, n=34; p<0.001). Since MNCs from diabetic animals showed an increased soma size (measured by cell capacitance; 16.7±1.1 pF, control; vs. 20.0±0.9 pF, diabetic; p<0.05), peak current density (peak amplitude divided by cell capacitance) was also compared. Peak current density in diabetic MNCs was 65% greater (p<0.05) than in control animals (Fig. 2.4D).

Because persistent sodium currents are known to contribute to neuronal bursting (Crill, 1996; Parri and Crunelli, 1998; Taddese and Bean, 2002) and are increased in MNCs exposed to hyperosmolar conditions (Tanaka et al., 1999), we elicited persistent sodium currents by slow ramp depolarizations (233 mV/s) and compared them in control and diabetic MNCs (Fig. 2.4E). Both control and diabetic MNCs produced TTX-sensitive ramp currents that were activated at potentials close to threshold (-65 to -55 mV). The diabetic MNCs exhibited significantly larger ramp currents than control MNCs (218±29 pA, control, n=21; 428±45 pA, diabetic, n=31; p<0.005). The ramp current density was ~50% larger in the diabetic MNCs (21.5±2.0 pA/pF, n=31) than in control cells (14.5±2.5 pA/pF, n=21, P<0.05) (Fig. 2.4D).

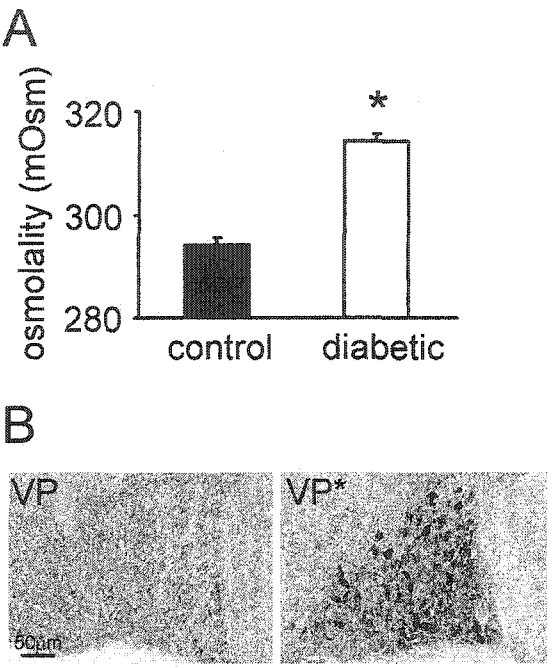

Fig. 2.1. A. Streptozotocin-induced diabetes causes elevated serum osmolality. **B.** MNCs increase their production of vasopressin, as detected by vasopressin antibody immunoreactivity (left panel (VP) = control, right panel (VP*) = diabetic).

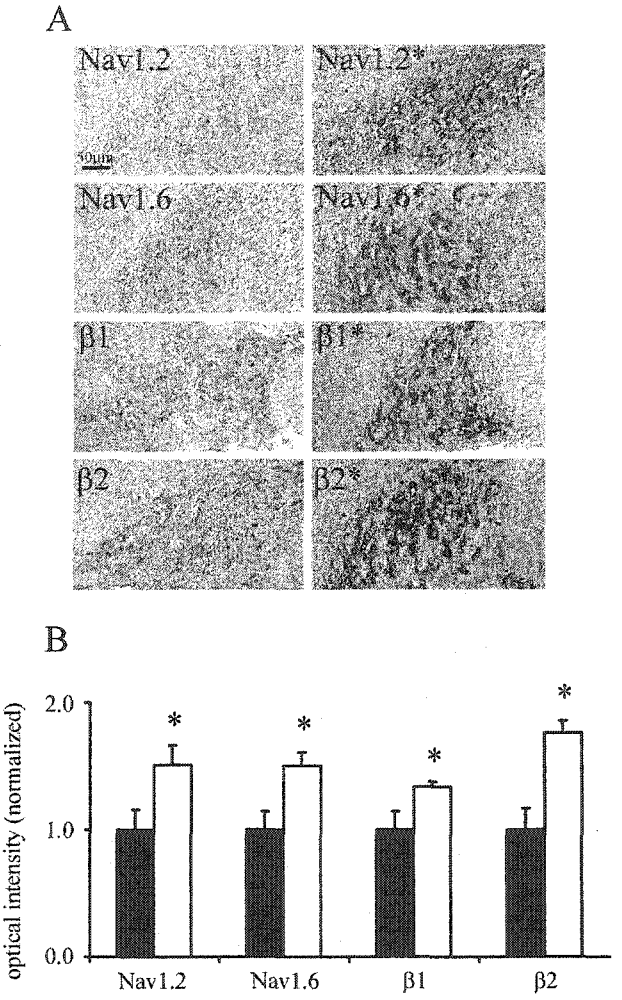

Fig. 2.2. Sodium channel subunit mRNA transcripts are up-regulated in diabetic MNCs. **A**, Moderate levels of Nav1.2, Nav1.6, β1 and β2 were detectable in control SON (no *) and there was a significant up-regulation of each of these transcripts in the diabetic animals (*). The fields of control and diabetic tissue shown were digitally contrast-enhanced to qualitatively illustrate the up-regulation of transcripts, but they do not illustrate the quantitative magnitude of the changes. **B**, Optical intensity measurements from unenhanced images in the histogram provide quantitative comparisons between control (■) and diabetic (□) animals. Optical densities were normalized for each transcript to facilitate comparison of diabetic and control tissue. Error bars indicate SEM, * = $p<0.05$.

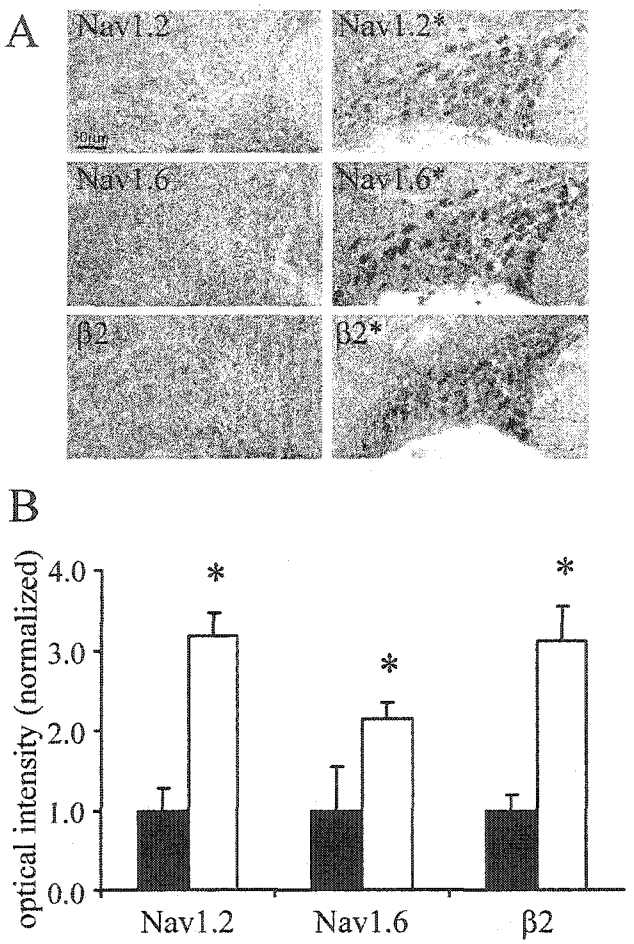

Fig. 2.3. Sodium channel subunit protein is up-regulated in diabetic MNCs. **A**, Moderate levels of Nav1.2, Nav1.6, and β2 were detectable in control SON (no *) and there was a significant up-regulation of each of these proteins in the diabetic animals (*). The fields of control and diabetic tissue shown were digitally contrast-enhanced to qualitatively illustrate the up-regulation of transcripts, but they do not illustrate the quantitative magnitude of the changes. **B**, Optical intensity measurements from unenhanced images in the histogram provide quantitative comparisons between control (■) and diabetic (□) animals. Optical densities were normalized for each channel to facilitate comparison of diabetic and control tissue. Error bars indicate SEM, * = $P<0.05$.

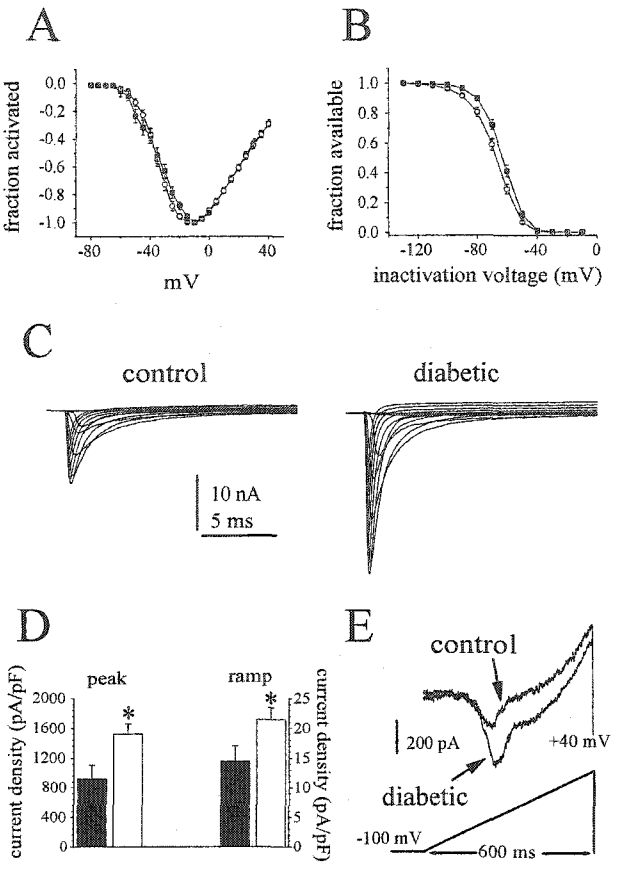

Fig. 2.4. Comparison of sodium currents in control and diabetic MNCs. **A**, The normalized peak current-voltage relationship for control (■; V½ = -28.4±1.7 mV, *n*=16) and diabetic (○; V½ = -31.0±1.5 mV, *n*=28) MNCs are similar. **B**, Comparison of control (■; V½=-62.7±1.2 mV, *n*=22) and diabetic (○; V½=-67.4±1.3 mV, *n*=32) MNC steady-state inactivation. Steady-state inactivation was measured with 500 ms inactivating prepulses. Cells were held at prepulse potentials over the range of -130 to -10 mV prior to a test pulse to 0 mV for 20 ms. Error bars indicate SEM. **C**, Family of traces from representative neurons acutely isolated from control (left panel) or diabetic (right panel) rats. The currents were elicited by 40 ms test pulses to various potentials from -80 to 40 mV. Cells were held at -100 mV. **D**, The peak and ramp current densities (estimated by dividing the maximum currents by the cell capacitance) are larger in diabetic MNCs (□,

n=34) than in control MNCs (■, *n*=23). Error bars indicate SEM, and the * indicates *P*<0.05. **E**, Representative ramp currents elicited in MNCs by slow voltage ramps (600 ms voltage ramp extending from -100 to +40 mV) are shown.

2.5 DISCUSSION

Magnocellular neurosecretory cells (MNCs) are responsible for the synthesis and controlled release of vasopressin. We have demonstrated that MNCs normally coexpress the Nav1.2, Nav1.6, β1 and β2 voltage-gated sodium c3hannel subunits and that in experimental diabetes, the mRNA and protein levels for these sodium channel subunits are elevated. We have also shown that electrophysiological changes parallel these molecular changes.

Neuronal firing patterns are dependent on sodium currents, and persistent currents lower the threshold for firing and predispose neurons to fire spontaneously (Crill, 1996; Parri and Crunelli, 1998; Taddese and Bean, 2002). It is known that electrical activity, cAMP levels, and intracellular calcium influence sodium channel expression in excitable cells (Offord and Catterall, 1989; Sashihara et al., 1997), while activity-dependent phosphorylation state influences the functional properties of the channel (Cantrell and Catterall, 2001; Cukierman, 1996; Li et al., 1993). Consistent with increased transcription and translation of two sodium channel α-subunits and their insertion into the cell membrane, we observed higher amplitudes and densities of two sodium currents (transient and persistent) in MNCs of diabetic rats, similar to the changes that accompany the transition of MNCs to the bursting state in salt-loaded rats (Tanaka et al., 1999). This would be expected to contribute to increased excitability and vasopressin release in diabetes.

Diabetic nephropathy is thought to result from prolonged elevated levels of serum vasopressin (Ahloulay et al., 1999; Bardoux et al., 1999), which raise blood pressure and increase filtration demand to the kidneys (see Fig. 2.5). It has been demonstrated i) that the antidiuretic V2-receptor-dependent effects of vasopressin directly affect glomerular filtration rate and albumin excretion, and ii) that in STZ-injected vasopressin-deficient rats there is no hyperfiltration and decreased renal hypertrophy and albuminuria compared to controls (Bankir et al., 2001; Bouby et al., 1999). In this study we have shown that there is a link between the onset of experimental diabetes (which is associated with vasopressin release (Ahloulay et al., 1999; Bardoux et al., 1999)), and changes in sodium channel transcription and translation which result in the insertion of increased numbers of functional channels in the cell membrane of neurosecretory neurons within the hypothalamus. These changes in expression of sodium channels in the SON represent a previously undescribed change in the brain in experimental diabetes which may represent a component of the pathogenesis of diabetic nephropathy (see Fig. 2.5).

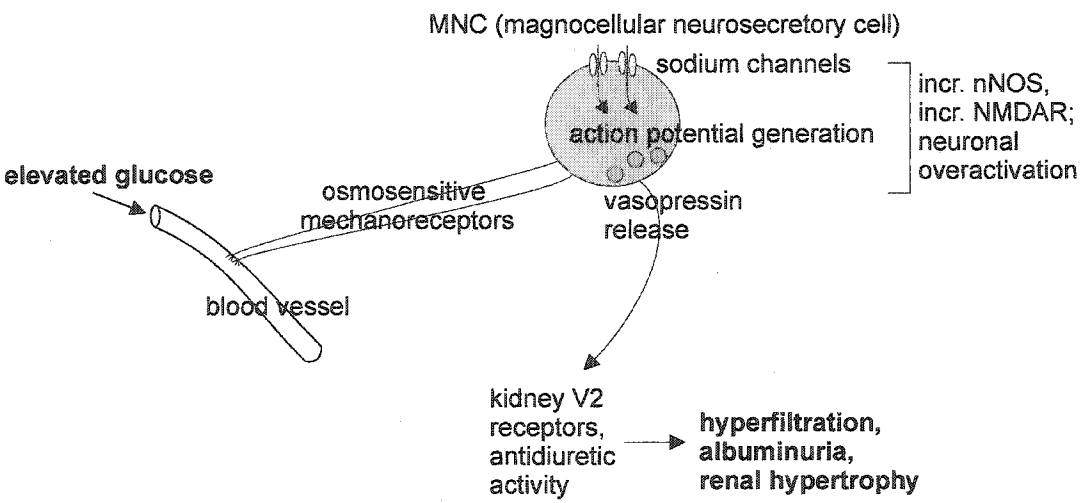

Fig. 2.5. Chronic hyperglycemia induces changes in gene transcription in vasopressinergic MNCs of the hypothalamus and these changes, in turn, can contribute to the development of diabetic nephropathy.

Our results demonstrate up-regulation of sodium channel transcription, and insertion of increased numbers of functional sodium channels in the membranes of MNCs in experimental diabetes. We propose that, in untreated or under-treated diabetes, the SON attempts to correct osmolality and normalize blood pressure by persistent release of vasopressin, which requires sustained impulse activity. As discussed above, action potential activity in MNCs triggers the release of vasopressin, which over time irreversibly damages the microvasculature of the kidney and causes the changes characteristic of diabetic nephropathy. Identification of this change in the brain in experimental diabetes, and of the specific sodium channel subtypes associated with it, may suggest new therapeutic strategies for preventing or delaying the onset of vascular and renal complications of diabetes.

CHAPTER 3

APOPTOSIS OF VASOPRESSINERGIC HYPOTHALAMIC NEURONS IN CHRONIC DIABETES MELLITUS

3.1 SUMMARY

The hyperosmolality associated with diabetes mellitus triggers an increase in neuronal activity and vasopressin production within magnocellular neurosecretory cells of the hypothalamic supraoptic nucleus (SON). In this study, we examined the effect of chronic diabetes on the function and survival of these neurons. After 6 months, but not 6 weeks, of streptozotocin (STZ)-induced diabetes, we observed an increase in the appearance of small hyperchromatic neurons, and a decrease in SON neuronal density. A sub-population of neurons within the SON at this time point demonstrated positive staining for cleaved caspase-3 and TUNEL, two markers of apoptosis. In addition, the number of vasopressin-positive neurons was decreased. Markers for apoptosis did not colocalize with vasopressin immunopositivity; this was probably due to a diabetes-induced degenerative process causing down-regulation of vasopressin expression and/or depletion of neuropeptide. Although the phenotypes of the apoptotic neurons were not identified, other SON neurons including oxytocin-producing neurons are unlikely to be affected by chronic hyperglycemia. Microglial hypertrophy and condensation was also observed in the 6 month diabetic SON. Although up-regulation of vasopressin production in response to acute hyperosmolality is adaptive, prolonged overstimulation of vasopressin-producing neurons in chronic diabetes results in neurodegeneration and apoptosis.

3.2 INTRODUCTION

The diabetic state results in an increase in plasma vasopressin levels, primarily as a result of hyperglycemia-induced hyperosmolality. This effect is observed in humans with diabetes mellitus and in experimental models of diabetes (Bankir et al., 2001; Brooks et al., 1989; Van Itallie and Fernstrom, 1982). While elevated vasopressin levels may be adaptive in the short term, there is evidence suggesting that prolonged elevated levels of vasopressin can cause chronic renal hyperfiltration, albuminuria, and hypertrophy, and ultimately contribute to diabetic nephropathy and renal failure (Ahloulay et al., 1999; Bardoux et al., 1999).

Vasopressin is synthesized in magnocellular neurosecretory cells (MNCs) within the supraoptic nucleus (SON) of the hypothalamus, and released from the neuropituitary in response to elevated plasma osmotic pressure. In diabetes, there is an increased demand on these neurons to produce enough vasopressin to maintain euvolemia and minimize fluid shifts between intracellular and extracellular environments.

Experimental evidence suggests that chronic overactivation of these neurons may have adverse effects on their survival. Ultrastructural studies first demonstrated that in streptozotocin (STZ)-induced diabetes there is an age-dependent progressive degeneration of SON neurons including the appearance of abnormal somata, dendrites, axonal profiles, and cytoplasmic vacuoles (Dheen et al., 1994a). This same study reported a significant increase in mean cross-sectional area and cross-sectional nuclear area of diabetic SON neurons compared to controls (Dheen et al., 1994a). Nuclear and somal hypertrophy is suggestive of increased mRNA and protein synthesis, which reflects the increased demand for, and production of, vasopressin in diabetic MNCs (Crespo et al., 1990). While the diabetic SON is indeed characterized by hypertrophic neurons, Luo et al. (2002) recently observed that in addition, shrunken and hyperchromatic neurons are also present.

Changes in the transcription of several genes in diabetic SON neurons have been examined. After 4 months of STZ-induced diabetes, vasopressin levels in SON neurons remain elevated compared to controls, but there is less up-regulation compared to earlier time points (Luo et al., 2002), suggesting that in chronic diabetes, a functional insufficiency of vasopressin production may develop. The expression of voltage-gated sodium channels Nav1.2 and Nav1.6, which support the bursts of action potentials that release vasopressin, is up-regulated in diabetic SON neurons (Klein et al., 2002). Likewise, the glutamate receptor NMDAR and neuronal nitric oxide synthase (nNOS), which plays a role in the modulation of secretion of vasopressin, are also up-regulated in diabetic SON neurons (Kadowaki et al., 1994; Luo et al., 2002; Serino et al., 1998). In these neurons, NMDAR and nNOS overactivation may be excitotoxic and result in degeneration or apoptosis (Brecht et al., 2001). Following STZ-induced diabetes, neuronal apoptosis has in fact been demonstrated in hippocampal neurons (Li et al., 2002) and retinal ganglion cells (Barber et al., 1998; Zeng et al., 2000).

In the present study we asked whether chronic STZ-induced diabetes leads to apoptotic cell death in vasopressinergic neurons of the SON. We report here that in chronic STZ-induced diabetes, there is increased expression of activated caspase-3 and markers of DNA degradation within SON neurons, compared to age-matched normoglycemic controls. These changes were evident after 6 months of diabetes, but not after 6 weeks of diabetes. We propose that long-term neuronal overstimulation in chronic diabetes induces a heterogenous response in the SON: some neurons degenerate and/or undergo apoptosis while others continue to produce and secrete vasopressin.

3.3 MATERIALS AND METHODS

Induction of diabetes. Adult male Sprague-Dawley rats (225-250g) were injected with streptozotocin (STZ, 60 mg/kg i.p., Sigma, St. Louis, MO). Animals were housed in a 12 h light-dark cycle with free access to water and food. Plasma glucose (Encore Glucometer, Miles Inc., Elkhart, IN) was measured at 6 weeks and 6 months post-injection and compared to control rats injected with saline. In total, 18 animals were used: 5 diabetic and 4 control rats at 6 weeks, and 5 diabetic and 4 control rats at 6 months. All experimental manipulations were carried out in accordance with National Institutes of Health guidelines for the care and use of laboratory animals, and all animal protocols were approved by the Yale University Institutional Animal Care and Use Committee.

Neuronal morphology. All rats were anasthetized with ketamine/xylazine (80/5 mg/kg i.p.) and then underwent intracardiac perfusion with 0.01 M PBS followed by a 4% solution of cold buffered paraformaldehyde. Brains were removed, postfixed and cryoprotected in 30% sucrose in 1 M phosphate buffer solution (PBS), and coronal cryosections (10 μm) of cortex containing the SON were cut. Sections were stained with Cresyl Violet (Sigma). Neuronal area and diameter were determined by outlining individual neurons whose nuclei were visible in the plane of section, using IPLab v3.0 Image Processing software (Scanalytics, Fairfax, VA). Counts of neurons within the SON were performed by arbitrarily selecting an area within the SON and averaging multiple counts (n=6) of neurons from the 6 week and 6 month control and diabetic animals.

Immunocytochemistry. Sections were incubated in blocking solution (5% normal goat serum and 1% BSA in PBS) containing 0.1% Triton X-100 and 0.02% sodium azide at

room temperature for 30 min, then incubated with antibodies to either vasopressin (1:1000, Oncogene Research Products, San Diego, CA), cleaved caspase-3 (1:50, Cell Signaling Technology, Beverly, MA), glial fibrillary acidic protein (GFAP) (1:50, Chemicon, Temecula, CA), or OX-42 (CD11b/c) (1:50, BD Biosciences, Franklin Lakes, NJ) overnight at 4 °C. Sections reacted with the caspase-3 antibody were washed in PBS and incubated with biotinylated goat anti-rabbit serum (1:1000, Sigma) in blocking solution for 3 hours, then washed in PBS and incubated in ExtrAvidin-HRP (1:1000, Sigma) in blocking solution for 3 hours. These sections were then washed again in PBS and exposed to heavy metal enhanced 3,3'-diaminobenzidine•4HCl in 1X peroxide substrate buffer (Pierce, Rockford, IL) for 7 min, washed in PBS, and mounted with Aqua-Polymount (Polysciences, Warrington, PA). Alternatively, for double labeling experiments utilizing fluorescent labels, goat anti-rabbit IgG-Cy3 (1:2000, Amersham, Piscataway, NJ) and goat anti-mouse IgG-Cy2 (1:1000, Molecular Probes, Eugene, OR) secondary antibodies were used. Vasopressin signal was detected using rhodamine epifluorescence illumination (emission wavelength 570-620 nm) and GFAP and OX-42 signals were detected using fluorescein epifluorescence illumination (emission wavelength 516-565 nm).

For detection of terminal d-UTP nick end labeling (TUNEL) of genomic DNA, 10 μm coronal sections of SON that had been previously reacted with vasopressin antibody were incubated sequentially in: PBS, 3% H_2O_2 in methanol for 10 min., PBS, 0.1% Triton X-100 in freshly prepared 0.1% sodium citrate for 15 min., PBS, and a mix of 100 ml label solution (containing fluorescein-dUTP) and 400 ml enzyme solution (containing terminal deoxynucleotidyl transferase, TdT; In Situ Cell Death Detection Kit, Roche, Indianapolis, IN), at room temperature for 3 hours.

Following vasopressin and TUNEL localization, sections were reacted with the nuclear stain Hoechst 33342 (10 μg/ml, Molecular Probes) for 10 min, washed with PBS,

and mounted with Aqua-Polymount. TUNEL positive neurons were detected using fluorescein epifluorescence illumination. Hoechst 33342 signal was observed using ultraviolet (UV) fluorescence illumination. To evaluate colocalization of staining, rhodamine-, fluorescein-, and UV-filtered images were merged using Adobe Photoshop v5.5.

Data Analysis. Quantitative microdensitometry was performed with a Nikon Eclipse E800 light microscope (20X objective) using IPLab software (Scanalytics). Signal intensities were determined by outlining individual neurons, and IPLab integrated densitometry functions were used to calculate mean signal intensities for the selected areas. Only neurons with distinct borders and visible nuclei in the plane of section were counted. Immunopositive neurons were defined as signal greater than 2X background levels and specifically localized within the margins of the neuronal plasma membrane. Immunopositive neurons were counted as a fraction of total neurons in the SON. TUNEL positive neurons were also compared to counts of vasopressin positive neurons in the SON. Data from neuron counting procedures was analyzed using one-way ANOVA with *post-hoc* multiple comparison analysis. Microglial morphology was quantified by comparing the maximum microglial cell diameter including dendritic processes in control and diabetic animals (Kreutzberg, 1996), and analyzed using a nonpaired t-test. An alpha level of 0.05 was used as a threshold for statistical significance. All data is presented as mean ± SE.

3.4 RESULTS

Morphological changes occur in diabetic MNCs. All animals injected with streptozotocin (STZ) developed hyperglycemia (>250 μg/dl) compared to control animals injected with saline. After either 6 weeks or 6 months, tissue sections of supraoptic

nucleus (SON) from control and diabetic animals were stained with Cresyl Violet (Nissl) to examine changes in cellular morphology. In control animals at 6 weeks and 6 months, there was relatively little variation in cell size, with the majority of neurons in the 10-15 μm range (Fig. 3.1A,A',C,C'). In contrast, after 6 weeks of diabetes, there was a change in size distribution of magnocellular neurosecretory cells (MNCs) such that a greater proportion of neurons were larger (15-25 μm) (Fig. 3.1B,B'). After 6 months of diabetes, an even greater heterogeneity of SON size was observed: there was a similar trend toward larger neurons, but in addition, there was an increased proportion of smaller neurons (<10 μm) (Fig. 3.1D,D'), which were not seen in controls or the 6 week diabetic SON. The larger neurons showed nuclear and Golgi distention and cytoplasmic swelling and vacuolization (arrows), while the smaller neurons tended to be hyperchromatic (arrow heads).

Counts of neurons revealed no significant difference between 6 week and 6 month control SONs, or between 6 week diabetic and 6 week control SONs. In the 6 month diabetic animals, neuronal density was significantly decreased, by 34.5% compared to 6 month controls (Fig. 3.1E, *=$p<0.05$).

Cleaved caspase-3 expression is up-regulated in the chronically diabetic SON. Cleaved caspase-3 is the activated form of caspase-3, a critical effector of apoptosis (Cohen, 1997). Immunocytochemistry using an antibody directed against cleaved caspase-3 revealed low levels of caspase-3 immunoreactivity in neurons from control animals at 6 weeks and 6 months, and from diabetic animals at 6 weeks (Fig. 3.2A-C). Six month diabetic animals demonstrated a large up-regulation of cleaved caspase-3 expression, which was visible in the cytoplasmic compartment of the neurons (Fig. 3.2D). 28% of SON neurons in the 6 month diabetic group were immunopositive,

compared to approximately 5% in the other groups (Fig. 3.2E, *=$p<0.05$). In general, the level of immunostaining of neurons in the 6 week diabetic group (Fig. 3.2B) was greater compared to the controls (Fig. 3.2A,C), but many of these moderately stained neurons (Fig. 3.2B) were not above the threshold for inclusion in the immunopositive group.

DNA fragmentation occurs in the chronically diabetic SON. Having demonstrated an up-regulation of caspase-3 in the 6 month diabetic SON, we sought to confirm these findings using an additional marker of apoptosis. The TUNEL assay was used to identify DNA strand breaks, which occur in apoptotic neurons as a result of cleavage of genomic DNA. At 6 months, TUNEL positive neurons were not seen in control MNCs (Fig. 3.3B), but were clearly visible in neurons in the diabetic SON (Fig. 3.3E, arrows). Fig. 3.3A and D are phase-contrasted images of the cells shown in B and E. Fig. 3.3C and F are overlays of 3.3A and B, and 3.3D and E, respectively. TUNEL positive neurons were detected extremely infrequently in the 6 week control, 6 week diabetic, and 6 month control SON, and were significantly increased in 6 month diabetic SON (Fig. 3.4, *=$p<0.05$).

TUNEL and vasopressin are not colocalized in the chronically diabetic SON. It is well established that vasopressin is up-regulated in diabetic MNCs, and it has been hypothesized that neuronal overactivation due to chronic hyperosmotic stimulation may lead to neuronal degeneration and apoptosis. Table 3.1 shows a quantification of neuronal phenotype in control and diabetic animals after 6 weeks and 6 months of diabetes. These measurements indicate that (1) the percent of vasopressin-positive neurons in increased in 6 week diabetic animals; (2) the number of vasopressin-negative neurons in decreased in 6 week and 6 month diabetic animals; (3) the number of vasopressin-positive neurons is decreased in 6 month diabetic animals, and (4) the

number of total SON neurons in decreased in 6 month animals. We then attempted to correlate vasopressin immunoreactivity with TUNEL staining in the 6 month diabetic animals. Vasopressin immunopositive neurons are clearly visible in Fig. 3.5A (arrow heads). TUNEL positive neurons can be seen in Fig. 3.5B (arrows). Hoechst 33342 staining of nuclei is shown in Fig. 3.5C. The vasopressin immunopositive neurons had normal-appearing nuclei (Fig. 3.5C, arrow heads), while the TUNEL positive neurons showed condensed, pyknotic, and irregular nuclei (Fig. 3.5C, arrows). Overlay of Fig. 3.5A-C, as seen in Fig. 3.5D, demonstrated that after 6 months of diabetes, vasopressin positive neurons do not exhibit overlap with TUNEL positive neurons. This result was quantified in Fig. 3.4. The apoptotic neurons appeared to comprise a separate population from the presumably functional vasopressin-producing neurons.

Microglial activity is enhanced in the diabetic SON. Because neuronal density in the 6 month diabetic SON was decreased (Fig. 3.1E), we examined the possibility that microgliosis and/or astrocytosis occurs in conjunction with neuronal degeneration and apoptosis. Vasopressin and either OX-42 (a marker for activated microglia) or GFAP (a marker for reactive astrocytes) were detected simultaneously in tissue slices containing the SON, using fluorescence microscopy. At 6 weeks, the SON from both control and diabetic animals showed similar staining for OX-42 (Fig. 3.6A,B), and GFAP (Fig. 3.6A',B'). At 6 months, GFAP staining in both the control and diabetic SON was modestly increased compared to 6 weeks, and GFAP staining in control and diabetic SON appeared similar at this time point (Fig. 3.6A',B',C',D'). In contrast, OX-42 staining in the 6 month diabetic SON showed hypertrophic and condensed microglia (Fig. 3.6D, arrows), which differed from the normal branched dendritic pattern seen in controls (Fig. 3.6C, arrow heads). The maximum diameter of microglial cells including their dendritic processes was quantified (Fig. 3.6E). Six month diabetic animals demonstrated

truncated processes and reduced maximum cell diameter suggesting microglial activation in these animals.

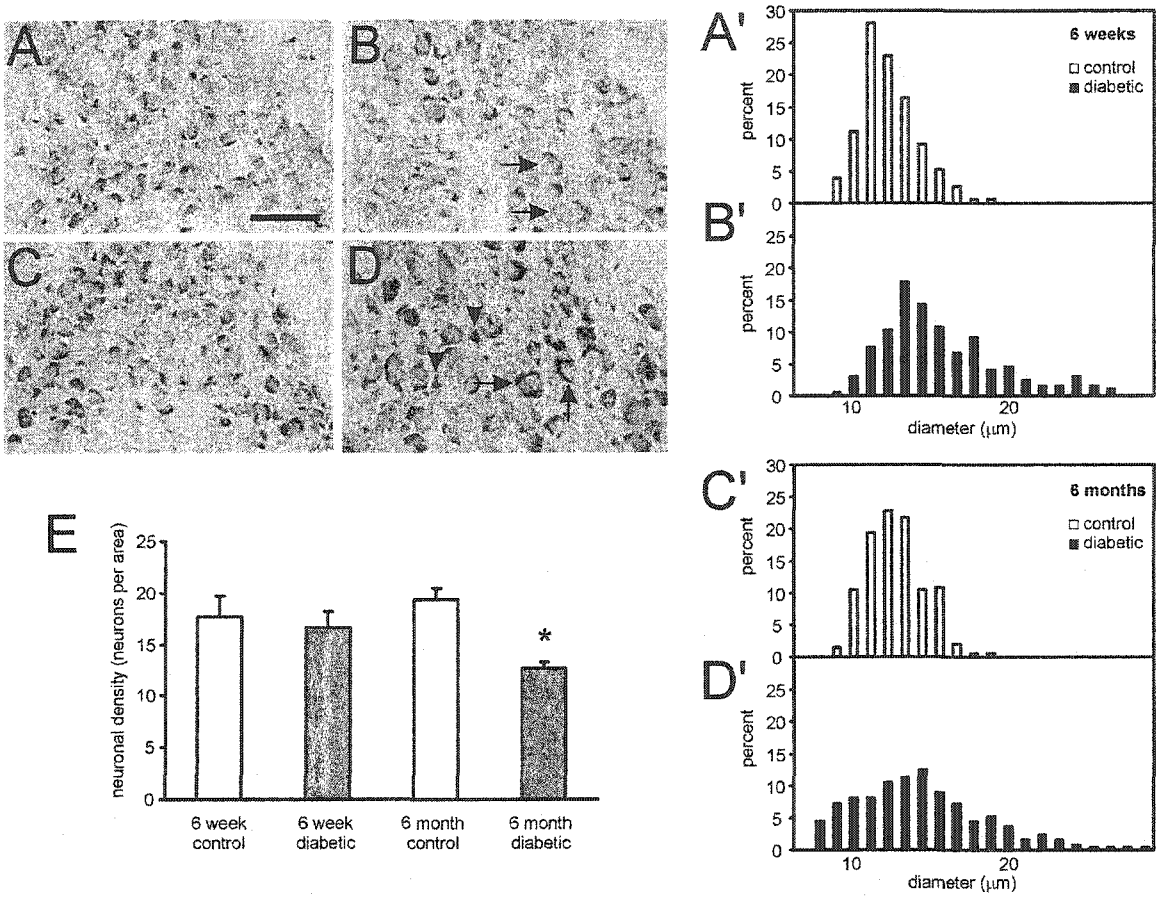

Fig. 3.1. Morphological changes of diabetic neurons. Cresyl violet staining of sections of supraoptic nucleus from 6 week control (**A**) and diabetic (**B**), and 6 month control (**C**) and diabetic (**D**) animals. Arrows in B and D indicate hypertrophic neurons; arrow heads in D indicate shrunken, hyperchromatic neurons. Size frequency histograms corresponding to A-D are shown in **A'-D'**. Neuronal density is quantified in **E**. Scale bar in A = 50 μm. Data are plotted as mean ± SE, * = $p < 0.05$.

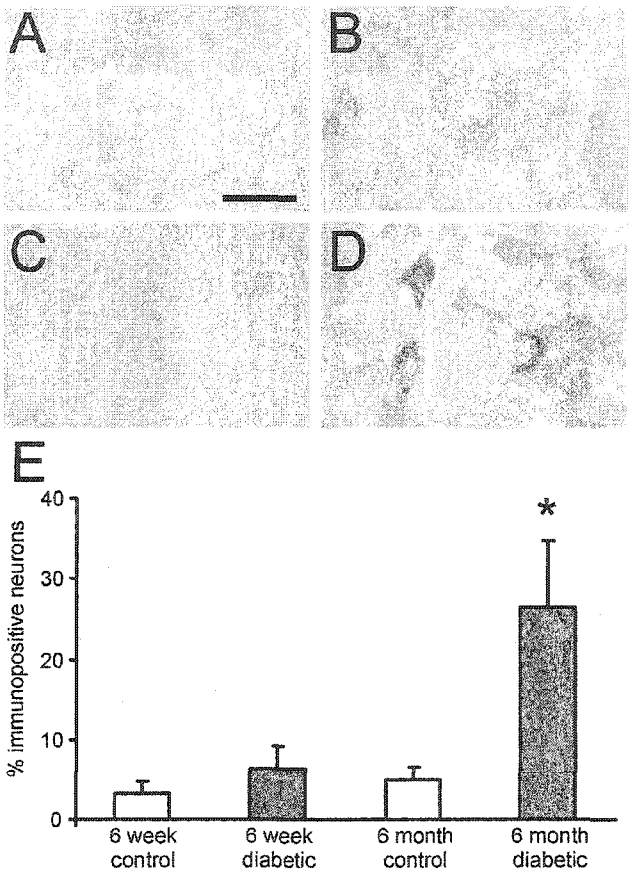

Fig. 3.2. Cleaved caspase-3 immunoreactivity in sections of supraoptic nucleus from 6 week control (**A**) and diabetic (**B**), and 6 month control (**C**) and diabetic (**D**) animals. Images were converted to greyscale and identically digitally contrast-enhanced to qualitatively illustrate differences in immunostaining. Quantitative microdensitometry of unenhanced images was used to obtain data shown in **E**. Neurons defined as immunopositive demonstrated signal greater than 2X background levels with staining specifically localized to within the margins of the plasma membrane. Scale bar in (A) = 50 μm. Data are plotted as mean ± SE, * = $p < 0.05$.

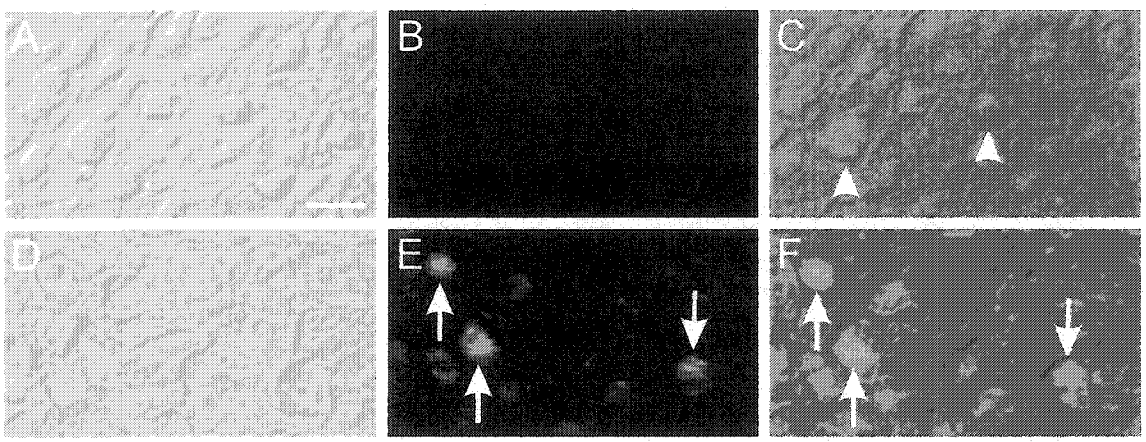

Fig. 3.3. TUNEL assay for apoptosis-related DNA fragmentation. Phase-contrast images of 6 month control (**A**) and diabetic (**D**) supraoptic nucleus are shown to identify neuronal boundaries. TUNEL staining is shown for 6 month control (**B**) and diabetic (**E**) sections. **C** is an overlay of A and B, and **F** is an overlay of D and E. Positive TUNEL staining (E, arrows) occurs within neuronal boundaries (F, arrows), and is not detected in control SON neurons (C, arrow heads). Scale bar in A = 50 μm. Data are plotted as mean ± SE, * = $p < 0.05$.

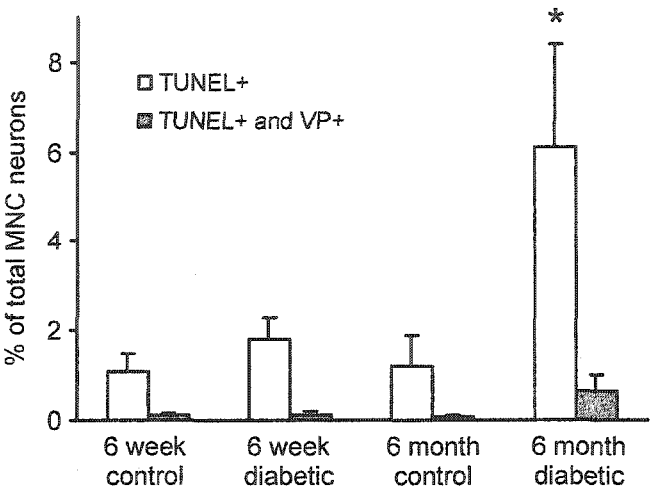

Fig. 3.4. Quantification of TUNEL positive neurons within the supraoptic nucleus of 6 week and 6 month control and diabetic animals (white bars). TUNEL positive neurons demonstrated signal greater than 2X background levels. The percentage of neurons that were both TUNEL positive and vasopressin immunopositive is shown (grey bars). Data are plotted as mean ± SE, * = $p < 0.05$.

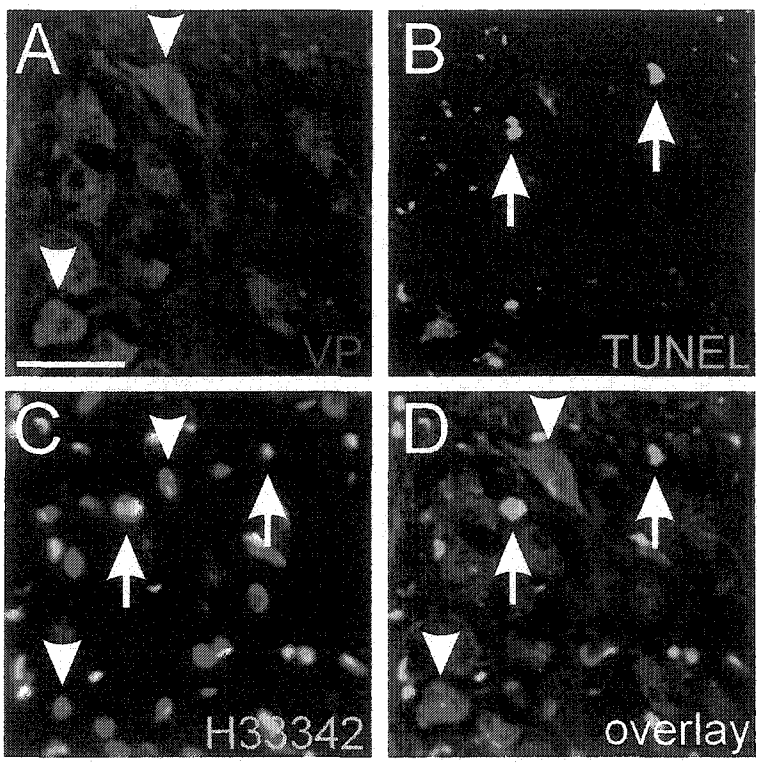

Fig. 3.5. Vasopressin (VP), TUNEL, and Hoechst 33342 (H33342) images from 6 month diabetic supraoptic nucleus. Vasopressin immunopositive neurons are clearly visible in **A** (arrow heads). TUNEL positive cells are visible in **B** (arrows). Hoechst 33342 nuclear stain is shown in **C**. Arrow heads in C showing low intensity nuclear staining correspond to vasopressin immunopositive neurons in A. Arrows in C showing pyknotic, condensed, and hyperchromatic nuclei correspond to TUNEL positive cells in B. Overlay of A, B, and C is shown in **D**; arrow heads correspond to vasopressin immunopositive neurons, arrows correspond to TUNEL positive neurons. Scale bar in A = 50 μm.

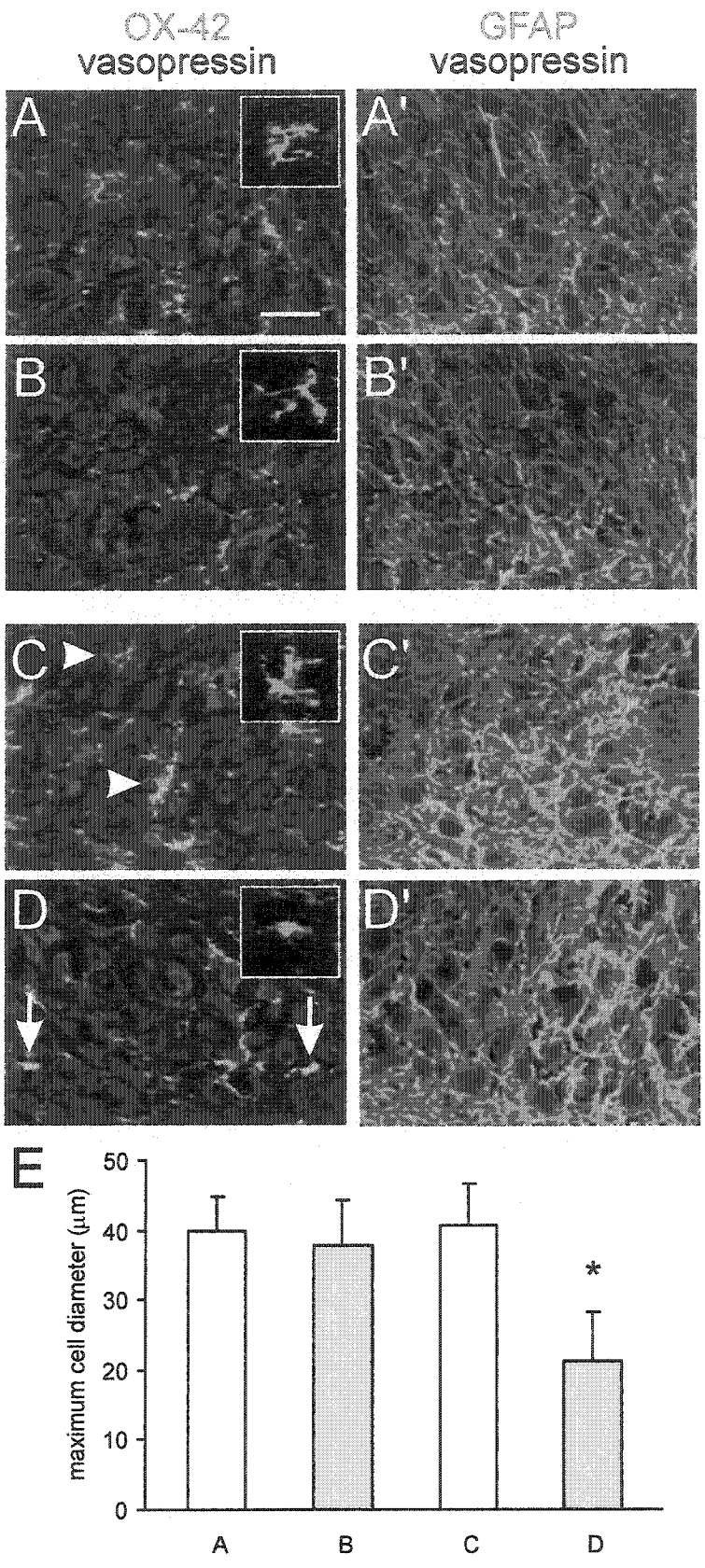

Fig. 3.6. Glial response to chronic diabetes. Sections of supraoptic nucleus were stained with vasopressin (red) and either OX-42 (green, left panels, **A-D**) or GFAP (green, right panels, **A'-D'**). A and A' are from 6 week controls; B and B' are from 6 week diabetics; C and C' are from 6 month controls; and D and D' are from 6 month diabetics. Arrow heads in C show normal branched dendritic microglial morphology. Arrows in D show hypertrophic and condensed microglia. Insets in A-D show greater detail of microglial cells. The histogram in **E** is a quantification of changes in microglial morphology. Six month diabetic animals demonstrate reduced maximum cell diameter suggesting microglial activation. Data are plotted as mean ± SE, * = $p < 0.05$. Scale bar in A = 50 μm.

Table 3.1. Quantification of SON neuronal phenotype. Data is shown as mean ± SE, * = p <0.05; significant difference from corresponding control group.

	VP+	VP-	Total
6 week control	20.0 ± 5.5 (29.3%)	48.3 ± 3.5 (70.7%)	68.3 ± 5.5 (100.0%)
6 week diabetic	24.3 ± 3.3 (40.1%*)	36.3 ± 2.6* (59.9%*)	60.7 ± 3.8 (100.0%)
6 month control	20.0 ± 2.0 (29.9%)	46.6 ± 5.5 (70.1%)	66.7 ± 5.4 (100.0%)
6 month diabetic	14.0 ± 0.8* (27.5%)	37.0 ± 1.5* (72.5%)	51.0 ± 2.2* (100.0%)

3.5 DISCUSSION

The hyperosmolality associated with diabetes mellitus triggers both structural and metabolic changes within magnocellular neurosecretory cells (MNCs) of the hypothalamic supraoptic nucleus (SON). These changes occur, at least in part, as a result of neuronal activation and the demand for increased production and secretion of vasopressin. It is well established that chronic neuronal overactivation can lead, by a variety of mechanisms including nNOS activation and progressive intracellular calcium accumulation, to neuronal degeneration and apoptosis (Brecht et al., 2001; Dawson et al., 1991). In the present study, we asked the question of whether apoptosis occurs among vasopressin-producing neurons after prolonged diabetes. We utilized morphometric and immunocytochemical criteria to examine diabetic SON neurons.

Although we did not label SON neurons that produce and secrete oxytocin, it is unlikely that these neurons are affected by experimental diabetes. Our use of male animals also limited gender effects on oxytocin secretion. Assuming the oxytocin neurons do not become overactivated or undergo apoptosis as a result of chronic diabetes, then our estimates of vasopressin neuron loss in diabetes are, if anything, an underestimate of the actual percentage of vasopressin neurons lost in chronic diabetes.

Our principal findings are that after 6 months of diabetes: (1) small hyperchromatic neurons with condensed and irregular somal and nuclear profiles are present in addition to hypertrophic neurons; (2) neuronal density is significantly decreased in the SON; (3) cleaved caspase-3 immunoreactivity is up-regulated in a sub-population of SON neurons; (4) DNA fragmentation is detectable in some SON neurons; (5) the number of vasopressin-positive neurons is decreased; (6) TUNEL positive neurons do not colocalize with vasopressin-producing neurons; and (7) microglial hypertrophy and condensation is evident. Identification of neuronal apoptosis in the SON after chronic diabetes is an important finding, as tight regulation of plasma osmolality is a

critical physiologic requisite, without which dysregulation of fluid homeostasis will occur.

Analysis of neuronal area and diameter by Cresyl Violet staining provided the first suggestion of neuronal degeneration and apoptosis in this study. The 6 month diabetic SON contained a unique population of neurons that were <10 μm in diameter and appeared hyperchromatic. Neuronal density was also decreased in the 6 month diabetic SON. We reasoned that cell death by an apoptotic mechanism might account for these changes, and assayed for several hallmarks of apoptosis to test this hypothesis.

Caspase-3 is an important regulator of apoptosis, and its proteolytically cleaved form is known to be up-regulated in neurons undergoing apoptosis (Kermer et al., 1999; Srinivasan et al., 1998). In our study, cleaved caspase-3 immunoreactivity was strongly up-regulated in 6 month diabetic SON neurons (Fig. 3.2). The interval over which cleaved caspase-3 yields an immunopositive signal is thought to span the entire active process of neuronal degeneration, and thus may include much of the time course of apoptosis (Brecht et al., 2001). Therefore, the percent of immunopositive neurons reported in Fig. 3.2E may not be an accurate measure of the incidence of apoptosis, and almost certainly represents an overestimate of the rate of neuronal death at any given time point. Morphological assessment of neurons expressing cleaved caspase-3 might be helpful in determining how far along the apoptotic process individual neurons are.

The TUNEL assay is a useful marker for apoptosis-related genomic DNA fragmentation (Gavrieli et al., 1992; Migheli et al., 1995) and was used in conjunction with caspase-3 immunoreactivity in this study as a second marker of apoptosis. DNA fragmentation results from oxidative DNA damage and is a final irreversible step of the apoptotic process (Brecht et al., 2001). Neurons only transiently show positive TUNEL staining and therefore TUNEL positivity may be a more accurate reflection of the incidence of neuronal death compared to caspase-3 immunoreactivity (Duan et al.,

2003). Detection of TUNEL positivity, however, is challenging. Whereas immunocytochemical procedures benefit from signal-boosting amplification steps such as the biotin-avidin-HRP process, the TUNEL reaction is a one-step procedure. In our study, it was necessary to increase the gain (identically for diabetic and control tissue slices) on the microscopic images in order to detect and compare TUNEL positive and TUNEL negative neurons (Fig. 3.3). It is possible, as a result of this manipulation, that our false positive rate was increased, and that the percentages of TUNEL positive neurons shown in Fig. 3.4 are in fact an overestimate. In order to more accurately confirm TUNEL positivity, we used Hoechst 33342 nuclear staining as a means of colocalization with the TUNEL signal (Fig. 3.5). TUNEL positive neurons showed pyknotic and irregular nuclei, which are characteristic of apoptotic cell death (Fig. 3.5C, arrows).

In addition to apoptosis, the decreased neuronal density observed in the chronically diabetic SON could also be due to gliosis, and reflect a relative dilution of neurons by proliferating astrocytes and microglia. Peri-neuronal astrocytes can modulate hormone release by altering their processes. In rats subjected to dehydration (and consequent hyperosmolality), a gross retraction of astrocytic processes has been reported in the SON, which is reversible with hydration (Hawrylak et al., 1998). Detailed ultrastructural analysis of this phenomenon reveals that in dehydrated rats neurovascular astrocytic contacts expand while neuroglial contacts decrease in size (Miyata et al., 2001; Miyata and Hatton, 2002). The increase in terminal-capillary contacts provides a route for increased neuropeptide release.

Like the dehydrated state, chronic diabetes subjects the SON to a hyperosmotic environment, and triggers an increase in vasopressin production and release. Immunocytochemical experiments have shown astrocyte retraction and condensation in the diabetic SON (Luo et al., 2002). In contrast to this response to dehydration,

astrocytes can also hypertrophy following neuronal injury and degeneration. GFAP immunoreactivity in the chronically diabetic SON may therefore reflect multiple (and possibly opposing) factors, and in this study, the pattern of GFAP staining in diabetic SON was not distinguishable from age-matched control SON.

Previous work has shown that microglia within the SON hypertrophy and shorten their processes in response to diabetes (Luo et al., 2002). In the present study, this effect was clearly evident after 6 months of diabetes. Microgliosis and microglial activation can occur in response to a variety of stimuli including neuronal ischemia, inflammation, infection, neoplasia, and neurodegeneration (Kreutzberg, 1996). Neurotoxic overactivation and apoptosis were the likely triggers for microglial proliferation, condensation, and truncation of processes as seen in Fig. 3.6.

Several important questions are raised by this study. First, why were the apoptotic changes not seen at 6 weeks? Because there is no time point at which acute diabetes is delineated from chronic diabetes, it is not possible to conclude that the onset of neuronal apoptosis corresponds to chronic diabetes. Instead, the detection of apoptosis after 6 months of diabetes is indicative of a dynamic process of accumulating neuronal injury which is likely to be present at lower levels, in this case, largely indistinguishable from controls, at the 6 week time point.

Second, as shown in Fig. 3.4, the rate of vasopressin and TUNEL overlap is very low in the diabetic SON. A possible explanation for this is that overstimulated neurons reach a degeneration threshold, where normal function (vasopressin production) is attenuated and the irreversible steps of apoptosis (positive TUNEL signal) begin. The few neurons that demonstrated positive labeling for both vasopressin and TUNEL may have been transitioning between functioning and degenerating states. The molecular changes that account for this transition may result from alterations in intracellular calcium homeostasis, secondary to neuronal overstimulation. Elevated intracellular

calcium levels are known to exist within many diabetic tissues (Levy et al., 1994). Diabetic hippocampal neurons, for example, undergo a slow progressive dysregulation of calcium homeostasis, which at first alters their synaptic function (Biessels et al., 2002; Kamal et al., 1999), and can eventually lead to apoptosis (Li et al., 2002).

Diabetes remains a chronic progressive disease with significant vascular and neurologic complications (Biessels et al., 1994; Donnelly et al., 2000; McCall, 1992). While chronically up-regulated circulating levels of vasopressin can cause glomerular damage within the kidney, we have shown here that chronically overstimulated vasopressin-producing neurons within the SON undergo apoptosis. While up-regulation of vasopressin is adaptive in an acute hyperosmotic state, our results suggest that chronic hyperosmolality may result in a pathologic sequence of neurotoxic events which ultimately lead to neuronal loss.

CHAPTER 4

PATTERNED ELECTRICAL ACTIVITY MODULATES SODIUM CHANNEL EXPRESSION IN SENSORY NEURONS

4.1 SUMMARY

Peripheral nerve injury induces changes in the level of gene expression for sodium channels Nav1.3, Nav1.8, and Nav1.9 within dorsal root ganglion (DRG) neurons, which may contribute to the development of hyperexcitability, ectopic neuronal discharge, and neuropathic pain. The mechanism for this change in sodium channel expression is unclear. Decreased availability of neurotrophic factors following axotomy contributes to these changes in gene transcription, but the question of whether changes in intrinsic neuronal activity levels alone can trigger changes in the expression of these sodium channels has not been addressed. To examine this question, I carried out experiments in which the effect of electrical stimulation on the expression of Nav1.3, Nav1.8, and Nav1.9 was examined using cultured embryonic mouse sensory neurons under conditions in which NGF was not limiting. Expression of Nav1.3 was not significantly changed following stimulation. In contrast, we observed activity-dependent down-regulation of Nav1.8 and Nav1.9 mRNA and protein levels following stimulation, as demonstrated by quantitative PCR and immunocytochemistry. These results show that a change in neuronal activity can alter the expression of sodium channel genes in a subtype-specific manner, via a mechanism independent from NGF withdrawal.

4.2 INTRODUCTION

Action potential generation within neurons is dependent on the activity of voltage-gated sodium channels (VGSCs). At least nine VGSC genes are expressed throughout the nervous system, each with different expression patterns and functional characteristics (Catterall, 2000; Goldin et al., 2000). The precise combination of channels in a neuronal membrane influences its excitability, and injury-induced alterations in the expression of VGSCs can lead to ectopic or spontaneous firing, thereby contributing to hyperalgesia and allodynia (Cummins and Waxman, 1997; Waxman et al., 2000). Because of the importance of sodium channels in action potential generation, and the injury-induced changes in axonal firing, it is difficult to determine whether changes in sodium channel expression are triggered by the abnormal axonal firing patterns, or rather depend entirely on activity-independent means of regulation, such as a response to changing growth factor levels.

Dorsal root ganglia (DRG) sensory neurons express multiple VGSC genes (Black et al., 1996; Caffrey et al., 1992; Sleeper et al., 2000). In addition to tetrodotoxin (TTX)-sensitive sodium channels, DRG neurons produce two unique TTX-resistant channels, Nav1.8 (SNS/PN3) and Nav1.9 (NaN), which are preferentially expressed in small nociceptive sensory neurons (Akopian et al., 1996; Dib-Hajj et al., 1998a; Dib-Hajj et al., 1999a; Sangameswaran et al., 1996).

The maintenance of expression of Nav1.8 and Nav1.9, and of TTX-sensitive sodium channel Nav1.3, in DRG neurons is dependent on the presence of neurotrophic growth factors. *In vitro* and *in vivo* studies have demonstrated a down-regulation of Nav1.8 and Nav1.9 and an up-regulation of Nav1.3 following withdrawal of NGF and GDNF (Black et al., 1999a; Boucher et al., 2000; Cummins et al., 2001; Fjell et al., 1999b) and axotomy (Dib-Hajj et al., 1998a; Sleeper et al., 2000; Waxman et al., 1994). Exogenous administration of specific growth factors can rescue the expression of

Nav1.8 and Nav1.9 within axotomized DRG neurons (Boucher et al., 2000; Cummins et al., 2001; Dib-Hajj et al., 1998b; Fjell et al., 1999a; Leffler et al., 2002).

While changes in neurotrophic growth factor availability can alter sodium channel expression, neurons can also adjust their gain and excitability by modulating sodium channel expression to adapt to, or react to, new input environments or new functional requirements. Evidence from a number of laboratories suggests that neurons can adjust their responsiveness by altering the number or kinetics of sodium channels in their membranes in order to electrically encode the changing range of stimulation to which they are exposed (Desai et al., 1999; Tanaka et al., 1999). It is not known whether impulse activity can regulate sodium channel expression in DRG neurons, although electrical stimulation has been shown to regulate the expression of voltage-gated calcium channels in DRG neurons (Li et al., 1996) and TTX-sensitive sodium channels in skeletal myocytes (Brodie et al., 1989; Offord and Catterall, 1989; Sherman and Catterall, 1984).

In this study, we asked whether the expression of sodium channels Nav1.3, Nav1.8 and Nav1.9 changes in cultured mouse sensory neurons as a result of patterned electrical stimulation. Because growth factors can affect sodium channel expression (Cummins et al., 2001; Dib-Hajj et al., 1998b; Fjell et al., 1999a) and stimulation can trigger release of growth factors (Balkowiec and Katz, 2000, 2002), we attempted to isolate the effect of activity on sodium channel expression independent of growth factor effects by supplying non-limiting amounts of NGF (50 ng/mL). Immunocytochemistry and quantitative PCR were used to identify changes in expression of mRNA and protein for Nav1.3, Nav1.8 and Nav1.9.

4.3 MATERIALS AND METHODS

Cell Culture. DRG neurons from E13.5 day fetal mice were dissociated in 0.125% trypsin and placed into culture media containing 5% horse serum and 50 ng/mL NGF as previously described (Fields et al., 1997). Provision of 50 ng/mL NGF to both stimulated and non-stimulated cultures insured that all neurons were exposed to a high level of NGF. For control experiments demonstrating the effect of NGF withdrawal on the expression of Nav1.3, Nav1.8 and Nav1.9, media without NGF was used during the 5-day period of testing. DRG neurons (125,000 cells per side compartment) were plated in the two side compartments of a 3-multicompartment culture chamber (Campenot, 1977; Fields et al., 1990) and incubated in humidified 10% CO_2 at 37 °C. Shallow parallel scratches (20-25 per plate) in the collagen-coated plastic culture dish helped direct neurite outgrowth from the side compartments into the central compartment. Mitosis of non-neuronal cells was inhibited by adding 13 μM FUDR applied one day after plating. Half of the volume of culture medium was changed every two days. All experimental manipulations were carried out in accordance with NIH guidelines for the care and use of laboratory animals, and all animal protocols were approved by the NIH Institutional Animal Care and Use Committee.

***In Vitro* Electrical Stimulation**. DRG neurons were maintained in culture for 3 weeks prior to electrical stimulation. Culture chambers were randomly assigned to a control (non-stimulated) group and a stimulated group. Extracellular stimulation applied across the barrier between the side compartments and central compartment, which was sufficient to initiate action potentials in the neurons (Fields et al., 1992), was delivered by field electrodes using 5 V, 200 μs biphasic pulses. The stimulation pattern used was as follows: 10 Hz pulses lasting 0.5 s every 8 seconds, 12 hours per day for 5 days. This

stimulation pattern results in increased neuronal firing frequency and activation compared to non-stimulated neurons, and has been previously shown to alter calcium currents (Li et al., 1996). In initial studies, a stimulation pattern of 10 Hz pulses lasting 0.5 s every 2 seconds, 12 hours per day for 40 hours, induced a significant down-regulation of Nav1.8 and Nav1.9 mRNA, but no change in protein. Since the half-life of a sodium channel is estimated to be approximately 1-2 days (Monjaraz et al., 2000; Ritchie, 1988; Schmidt and Catterall, 1986; Waechter et al., 1983), we decided to increase the stimulation time to 5 days in order to allow sufficient time for stimulation-dependent changes in protein levels to be detected.

Immunocytochemistry. Cultures were washed in PBS and fixed for 10 minutes in 2% paraformaldehyde solution. After additional washes with PBS, neurons were incubated in blocking solution (5% normal goat serum and 1% BSA in PBS) containing 0.1% Triton X-100 and 0.02% sodium azide at room temperature for 30 min, then incubated with isoform-specific polyclonal antibodies to Na^+ channel α-subunits Nav1.3 (residues 511-524, 1.19 μg/mL (Hains et al., 2002)), Nav1.8 (residues 1041-1062, 1.80 μg/mL (Black et al., 1999b)), and Nav1.9 (residues 1748-1765, 2.00 μg/mL (Fjell et al., 2000)), overnight at 4 °C. Neurons were washed in PBS and incubated with goat anti-rabbit IgG-Cy3 (1:2000, Amersham Biosciences, Piscataway, NJ) in blocking solution for 3 hours, then washed again in PBS and mounted with Aqua Poly/Mount (Polysciences, Warrington, PA). Incubation without primary or secondary antibodies yielded only background levels of signal (data not shown).

RNA extraction and cDNA synthesis. Total RNA from cultured DRG neurons was extracted using RNeasy mini-columns (Qiagen). The purified RNA was treated with

RNase-free DNase-I (Roche) and re-purified using an RNeasy mini-column (Qiagen). RNA was then eluted in 50 µl of water. First-strand cDNA was reverse transcribed in a final volume of 50 µl using 5 µl purified total RNA, 1 mM random hexamer primer (Roche), 40 U SuperScript II reverse transcriptase (Life Technologies), and 40 U of RNase inhibitor (Roche). The buffer consisted of (in mM): 50 Tris-HCl (pH 8.3), 75 KCl, 3 MgCl2, 10 DTT, and 5 dNTP. The reaction proceeded at 37 °C for 90 min and 42 °C for 30 min, and was then terminated by heating to 95 °C for 5 min. A parallel reaction with identical reagents except for the reverse transcriptase enzyme was performed as a negative control to demonstrate the absence of contaminating genomic DNA (data not shown).

Quantitative PCR. The relative standard curve method was used to quantify and compare RNA extracted from the cultured DRG neurons. An 18S rRNA primer-probe set (Applied Biosystems, Foster City, CA) was used as an endogenous control to normalize the expression level of the sodium channels. Standard curves for 18S rRNA and each sodium channel primer/probe set were constructed using serial dilutions of adult mouse DRG cDNA. One cDNA preparation was used to establish the standard curve for all experiments. Standards and unknowns were amplified in quadruplets. The standard curves for the sodium channel primer/probe sets and endogenous control (rRNA) were constructed from their respective mean critical threshold (C_T) values, and the equation describing the curve was derived using Sequence Detector software v1.6.3 (Applied Biosystems).

Primers and probes for the sodium channel targets were designed using Primer Express software (Applied Biosystems) according to the specifications of the TaqMan protocol (Winer et al., 1999). Sequences are as follows:

Nav1.8 forward 5'-TCAACTTCGACAACGTCGCTAT-3',

reverse 5'-ATACATAATGTCCATCCAGCCTTTG-3',

probe FAM-TACCTCGCGCTTCTCCAGGTGGC-TAMRA;

Nav1.9 forward 5'-CACCATCTGCATCATCGTCAAT-3',

reverse 5'-AGGGTCTAGCGCAATGATCTTG-3',

probe FAM-AACTGGGTTTTCACTGGAATTTTCATAGCGG-TAMRA.

Target specificity was confirmed by nucleotide BLAST search. Probes for sodium channels were synthesized and purified by Applied Biosystems. Primers for the sodium channels and 18S rRNA were used at a final concentration of 900 and 50 nM, respectively, whereas the probes were used at a final concentration of 200 nM. The primer-probe combinations were not limiting at these concentrations. Amplification was done in a 25 μl final volume, under the following cycling conditions: 10 min at 50 °C, and then 40 cycles of 95 °C for 15 s followed by 60 °C for 1 min. An ABI Prism 7700 (Applied Biosystems) was used to run the PCR reaction and data was recorded using Sequence Detector v1.6.3 (Applied Biosystems). Sodium channels and 18S rRNA templates were amplified in separate wells.

Data Analysis. A Nikon Eclipse E800 light microscope was used for sample observation, and quantitative microdensitometry of fluorescent immunostaining signals was obtained using IPLab v3.0 Image Processing software (Scanalytics Inc., Fairfax, Virginia). Signal intensities were determined by outlining individual neurons, and IPLab integrated densitometry functions were used to calculate mean signal intensities for the selected areas. Data from eight side compartments each for the control group and the stimulated group were used to obtain data. Experiments were processed in parallel and differences were assessed by non-paired *t*-tests. Neuron counts per area (Fig. 1) were

quantified by averaging multiple counts (n=6 per group) of neurons within the side compartments of the culture chamber. For the quantitative PCR experiments, differences in mRNA expression between the control and stimulated groups were analyzed using the non-paired t-test (n = 4 control, 4 stimulated). All data are presented as mean ± SE.

4.4 RESULTS

Effect of electrical stimulation on neuron survival. Prior to analyzing the effect of stimulation on sodium channel expression in cultured DRG neurons, we performed several control experiments to distinguish stimulation-dependent changes in channel expression from possible effects on cell survival. Morphometric analyses (Fig. 4.1A) and counts of cultured neurons (Fig. 4.1B) revealed no significant difference in neuron size distribution (n=865 neurons) or density (n=511 neurons) after electrical stimulation. The majority of neurons in culture were within the 25-40 μm diameter range.

As an additional control, we used immunocytochemistry with subtype-specific antibodies and demonstrated the effect of withdrawing NGF from the culture media for 5 days on the expression of Nav1.3, Nav1.8 and Nav1.9. In cultures deprived of NGF, there was a tendency toward an increase in Nav1.3 protein, but this did not reach statistical significance. In contrast, NGF deprivation resulted in significantly reduced levels of Nav1.8 and Nav1.9 protein compared to cultures containing 50 ng/mL NGF (Fig. 4.1C). At the transcript level, withdrawal of NGF induced an 83.3% decrease in Nav1.8 mRNA and a 57.6% decrease in Nav1.9 mRNA as detected by quantitative PCR.

Sodium channel protein is down-regulated by electrical stimulation. Subtype-specific antibodies to Nav1.3, Nav1.8, and Nav1.9 were used to determine the quantity of sodium channel protein in the cultured DRG neurons after stimulation. Fig. 4.2 shows

optical intensity quantification of the results. Stimulated cultures show a significant (p<0.05) down-regulation of Nav1.8 and Nav1.9 protein compared to non-stimulated cultures. Protein expression for Nav1.3 was not statistically different from non-stimulated cultures.

Sodium channel mRNA is down-regulated by electrical stimulation. Having demonstrated a significant change in Nav1.8 and Nav1.9 protein expression, we further examined the expression of these two genes by quantitative PCR analysis of mRNA levels. Stimulation caused a significant (p<0.05) down-regulation of Nav1.8 (to 48.9% of control level) and Nav1.9 (to 63.4% of control level) mRNA (Fig. 4.3).

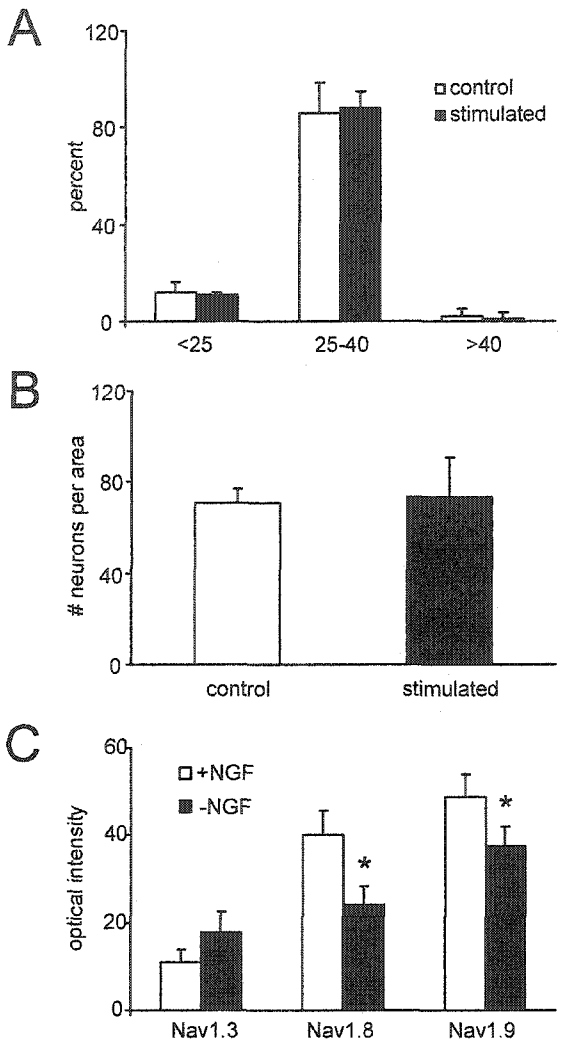

Fig. 4.1. *Electrical stimulation does not influence neuronal survival or size distribution.* **A.** Morphological measurements of cultured neurons do not show significant differences between any of the experimental conditions. The majority of neurons were within the 25-40 μm diameter range. **B.** Counts of cultured neurons in the stimulated and non-stimulated groups showed no significant change in cell number. **C.** The effect of NGF withdrawal on Nav1.3, Nav1.8, and Nav1.9 protein levels is demonstrated by immunocytochemistry. Optical intensity quantification of individual neurons shows a significant down-regulation of Nav1.8 and Nav1.9 protein in cultures without NGF (*) compared to cultures with NGF (no *). Nav1.3 protein levels were not significantly different between +NGF and -NGF cultures. Data are plotted as mean ± SE; * = $p<0.05$.

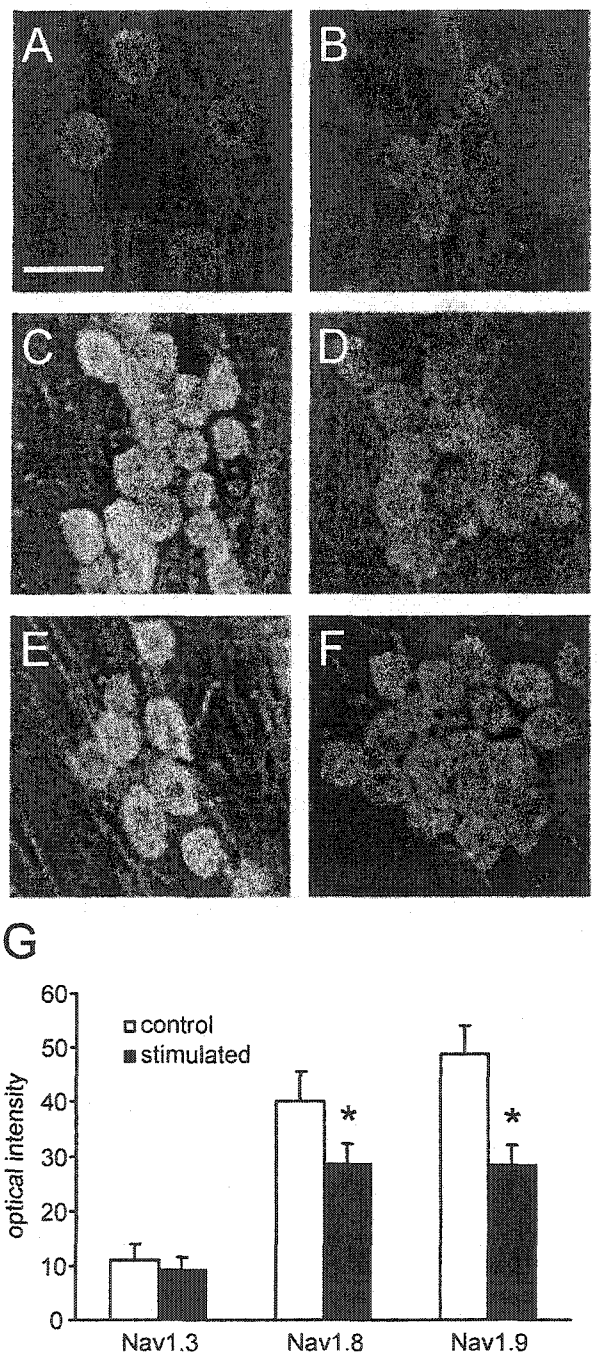

Fig. 4.2. A-F. Representative images demonstrating fluorescent immunoreactivity for Nav1.3, Nav1.8, and Nav1.9. Images were converted to grayscale and digitally contrast-enhanced using identical parameters to qualitatively illustrate the changes in protein expression. **A.** Nav1.3, control (non-stimulated); **B.** Nav1.3, stimulated; **C.** Nav1.8

control; **D**. Nav1.8, stimulated; **E**. Nav1.9, control; **F**. Nav1.9, stimulated; **G**. Optical intensity quantification from unenhanced images of individual neurons shows a significant down-regulation of Nav1.8 and Nav1.9 protein in stimulated cultures (*) compared to non-stimulated cultures (no *). Nav1.3 protein levels were not significantly different between control and stimulated cultures. Scale bar = 50 μm; data are plotted as mean ± SE; * = $p<0.05$.

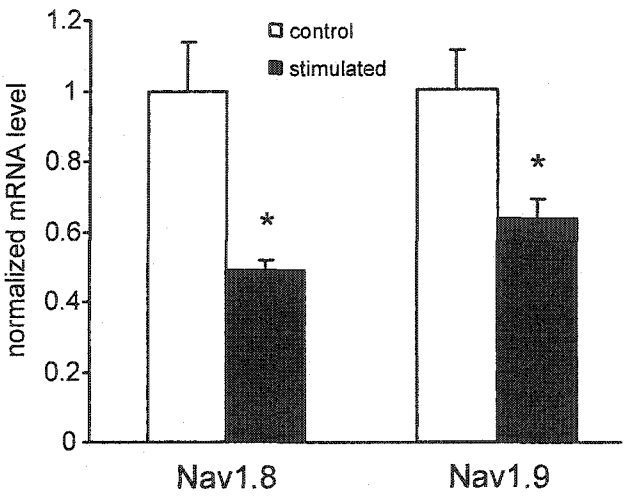

Fig. 4.3. Results of quantitative PCR for Nav1.8 and Nav1.9. Nav1.8 and Nav1.9 mRNAs were both down-regulated in stimulated cultures (*) compared to non-stimulated cultures. Data are plotted as mean ± SE; * = $p<0.05$.

4.5 DISCUSSION

In the present study, we examined the effect of electrical stimulation on the expression of sodium channels Nav1.3, Nav1.8 and Nav1.9 in cultured embryonic mouse DRG neurons. We demonstrated that the expression by DRG neurons of Nav1.8 and Nav1.9, but not of Nav1.3, is regulated by patterned electrical stimulation. There are several mechanisms that may allow a neuron to adapt to changes in the range of afferent or electrical input that it experiences. Calcium-dependent signaling pathways involving CaM kinase II and the MAP kinase cascade have been shown to play an important role in the regulation of CREB-mediated gene transcription (Buonanno and Fields, 1999; Ji and Woolf, 2001; Kornhauser et al., 2002; West et al., 2001; West et al., 2002), and these pathways can be regulated by neuronal firing (Fields et al., 2001). Growth factors, neurotransmitters, and hormones can also exert calcium-independent effects on CREB-mediated transcription.

The intracellular level of calcium and its activity-dependent rate of influx can influence the expression of TTX-sensitive sodium channels (Brodie et al., 1989). Chronic blockade of electrical activity in cultured cardiac myocytes triggers an up-regulation of transcription of sodium channel Nav1.4 (Offord and Catterall, 1989; Sherman and Catterall, 1984). Calcium-mediated down-regulation of sodium channel expression has been demonstrated by increasing electrical stimulation (Chiamvimonvat et al., 1995). Calcium channel activity-dependent regulation of sodium channel expression has also been demonstrated in cultured pituitary GH3 cells (Monjaraz et al., 2000). In this study, calcium channel agonists (Bay K 8644) led to increased peak sodium currents, while antagonists (nimodipine) lowered sodium currents. The regulatory mechanisms linking calcium levels to modulation of sodium channel mRNA transcription and expression remain unknown.

Pain following nerve injury is associated with abnormal bursting activity and increased sensitivity of DRG neurons whose axons have been transected; alterations in VGSC expression are believed to contribute to this phenomenon (Waxman, 1999b; Woolf and Salter, 2000). The number and mix of TTX-sensitive and TTX-resistant sodium channels in the membrane of a neuron may be a determinant of neuronal hyperexcitability; changes in the level of expression of slowly inactivating Nav1.8 sodium currents can result in altered threshold for action potential generation and an increased tendency to fire repetitively (Elliott, 1997; Renganathan et al., 2001; Schild and Kunze, 1997). Moreover, Nav1.9 has a strong effect on membrane potential (Cummins et al., 1999; Herzog et al., 2001) and threshold (Baker et al., 2003) and altered levels of Nav1.9 should thus have important effects on excitability.

Studies that have examined changes in sodium channel expression following inflammation (Djouhri and Lawson, 1999; Tanaka et al., 1998), nerve compression (Dib-Hajj et al., 1999b) and transection (Dib-Hajj et al., 1998a; Okuse et al., 1997) have been limited by the fact that the mechanism of modulation of expression may involve growth factor effects or activity-dependent effects. We have shown here that a change in neuronal activity level is sufficient to modulate the expression of two sodium channels, Nav1.8 and Nav1.9. The down-regulation occurred under cell culture conditions in which NGF was not a limiting factor (50 ng/mL). Because Nav1.3 did not demonstrate an activity-dependent change in expression, it is unlikely that stimulation caused a generalized down-regulation of all sodium channel gene transcripts. Rather, a selective and specific retuning of the electrogenic membrane, which may regulate neuronal gain, occurred in response to changes in input.

We suggest that an activity-dependent down-regulation of Nav1.8 and Nav1.9 proceeds via a molecular mechanism distinct from the mechanism that mediates growth-factor-triggered changes in expression of these channels. If this hypothesis is correct, it

implies the possibility of new therapeutic approaches that might regulate axonal channel expression, and thus excitability, via a previously unstudied activity-dependent pathway.

CHAPTER 5

DYSREGULATION OF SODIUM CHANNEL EXPRESSION IN CORTICAL NEURONS IN A RODENT MODEL OF ABSENCE EPILEPSY

5.1 SUMMARY

Due to the involvement of cortical neurons in spike-wave discharge (SWD) initiation, and the contribution of voltage-gated sodium channels (VGSCs) to neuronal firing, we examined alterations in the expression of VGSC mRNA and protein in cortical neurons in the WAG/Rij absence epileptic rat. WAG/Rij rats were compared to age-matched Wistar control rats at 2, 4, and 6 months. Continuous EEG data was recorded, and percent time in SWD was determined. Tissue from different cortical locations from WAG/Rij and Wistar rats was analyzed for VGSC mRNA (by quantitative PCR) and protein (by immunocytochemistry). SWDs increased with age in WAG/Rij rats. mRNA levels for sodium channels Nav1.1 and Nav1.6, but not Nav1.2, were up-regulated in the facial somatosensory cortex (at AP+0.0, ML+6.0 mm). This region of cortex approximately matches the electrophysiologically determined region of seizure onset. Protein levels for Nav1.1 and Nav1.6 were up-regulated in layer II-IV cortical neurons in this region of cortex. No significant changes were seen in adjacent regions or other brain areas, including the pre-frontal and occipital cortex. Changes in the expression of Nav1.1 and Nav1.6 parallel age-dependent increases in seizure frequency and duration.

5.2 INTRODUCTION

Neuronal excitability is dependent on the activity of voltage-gated sodium channels (VGSCs). Nine VGSC genes are expressed within the nervous system, each with different tissue distribution and functional characteristics (Catterall, 2000; Goldin et al., 2000). The combination of VGSCs present in a neuronal membrane contributes to its electrogenic properties and firing pattern. VGSC expression is a dynamic process, and alterations in physiological state as well as injury induce changes in VGSC expression, which can alter neuronal behavior (Waxman et al., 2000).

Certain types of epilepsy can result from *direct* (sodium channel gene mutations) or *indirect* (changes in genes that affect sodium channel expression) pathways (Aronica et al., 2001; Bartolomei et al., 1997; Gastaldi et al., 1998; Meisler et al., 2001; Noebels, 2002). VGSCs contribute to neuronal bursting (Parri and Crunelli, 1998) and some anticonvulsant drugs act via blockade of specific currents produced by sodium channels (Crunelli and Leresche, 2002; Leresche et al., 1998; Spadoni et al., 2002; Taverna et al., 1998). Alterations in the expression or function of VGSCs that predispose neurons toward repetitive firing and network hyperexcitability may be associated with increased seizure activity (Scharfman, 2002).

Absence seizures have historically been defined as a generalized non-convulsive epilepsy consisting of a sudden arrest of ongoing behavior and impairment of consciousness associated with a rhythmic spike-wave discharge (SWD) firing pattern of thalamic and cortical neurons. The characteristic bilaterally-synchronous spike-wave oscillation, as seen on EEG, results from reverbatory loops of excitation between the cortex and thalamus (Avoli and Gloor, 1982; Blumenfeld and McCormick, 2000; Destexhe et al., 1999). Ablation studies in rodent and feline models of absence epilepsy have demonstrated that an intact cortex and thalamus are necessary for the

electrophysiological transition to SWD firing (Avoli et al., 1983; Avoli et al., 1990; Danober et al., 1998; Vergnes and Marescaux, 1992).

Although SWD is considered a "generalized" seizure discharge, the anatomical region of seizure onset in WAG/Rij (Wistar Albino Glaxo from Rijswijk) rats (a genetic model of absence epilepsy (Coenen et al., 1992)) was recently localized to the facial region of the somatosensory cortex, which lies on the lateral cortex near the coronal plane of bregma (Meeren et al., 2002). SWDs appear to arise from an increase in burst firing in cortical neurons, which causes a large synchronized increase in neuronal firing in thalamocortical networks (Bal et al., 2000; Blumenfeld and McCormick, 2000). SWDs occur most dramatically in the frontal and parietal neocortical regions and corresponding thalamic nuclei with a relative sparing of the limbic and more posterior thalamocortical networks (Blumenfeld and McCormick, 2001; Nersesyan et al., 2002; Vergnes et al., 1990). The underlying molecular and electrophysiological basis of this phenomenon remains unidentified.

Because the cortex has been implicated as a focus for initiation of SWD firing, and because VGSCs can underlie neuronal bursting, we asked whether there are differences in the expression of sodium channel mRNA and protein in the WAG/Rij epileptic cortex compared to non-epileptic controls. We attempted to localize the altered sodium channel expression to a specific region of cortex, and furthermore to a specific population of neurons within the cortical mantle. This data was correlated to EEG recordings in order to establish an age-dependent association between SWD frequency and duration and extent of sodium channel dysregulation.

5.3 MATERIALS AND METHODS

Animals. Adult rats of the WAG/Rij (epileptic) strain were compared to age-matched Wistar rats (control). The WAG/Rij rat colony at our institution originated from the

Radiobiological Institute TNO, in Rijswijk (Reinhold, 1966), and Wistar rats were from Charles River Laboratories (Wilmington, MA). WAG/Rij rats exhibit spontaneous electrographic seizures characterized by bilaterally synchronous and symmetric SWDs. SWDs in these animals occur at a frequency of 7-11 Hz and seizure duration is typically 2-8 seconds. In this study, animals were individually housed and kept on a 12-hour light/dark cycle with unlimited access to food and water, in accordance with NIH guidelines for the care and use of laboratory animals; animal protocols were approved by the Yale University Institutional Animal Care and Use Committee. In total, 25 animals were used: 18 (9 epileptic, 9 control) for quantitative PCR analysis and 7 (4 epileptic, 3 control) for immunocytochemistry. Animals were grouped by age: 2 month (2 epileptic, 2 control), 4 month (3 epileptic, 3 control), and 6 month (4 epileptic, 4 control) rats were used for the PCR experiments, and 4 month rats were used for immunocytochemistry. All animals had electrodes implanted for electrophysiological recording.

EEG recordings and analysis. For EEG recordings, tripolar electrodes (Plastics One Inc., Roanoke, VA) were fixed to the skull. Animals were deeply anesthetized intramuscularly with ketamine (100 mg/kg), xylazine (5.2 mg/kg), and acepromazine (1.0 mg/kg) and placed in a stereotactic frame (David Kopf Instruments, Tujunga, CA). Level of anesthesia was monitored by respiration, heart rate, glabrous skin perfusion, and response to foot pinch. Small burr holes were made in the skull without disturbing the dura and electrodes were secured to the skull using 1.60 mm stainless steel screws (Plastics One). EEG recording electrodes were placed at AP +2.0, ML +2.0 mm, and AP -6.0, ML +2.0 mm and a ground electrode was placed in the midline over the cerebellum. Dental acrylic (Lang Dental Mfg. Co., Wheeling, IL) was used to fix the electrode unit in place. Following a one-week recovery period, continuous EEG data was recorded from awake-behaving rats for two hours per day (between 10:00am and 4:00pm) over a

three-day period for each animal. EEG signals were amplified with a Grass CP 511 unit (Grass-Telefactor, Astro Med, Inc., West Warwick, RI), with band pass filter settings of 1 Hz to 100 Hz. Signals were digitized with a CED Power 1401, and stored and analyzed using Spike 2 software (Cambridge Electronic Design, Cambridge, UK). SWDs were defined as large-amplitude (>400 μV peak-to-peak) rhythmic 7-11 Hz discharges with typical spike-wave morphology lasting >0.5 s. Start and end times for all SWDs were marked, and percent time in SWD firing pattern was then calculated as (sum of SWD interval durations / total recording time) x 100%, for all WAG/Rij (epileptic) and Wistar (control) rats.

RNA extraction and cDNA synthesis. Rats were deeply anaesthetized with CO_2, decapitated, and brains were quickly removed. Twelve plugs of tissue, each measuring approximately 1 mm^3 were dissected from the left and right cortex of each rat using iridectomy scissors. For each hemisphere, three plugs at AP +3,0,-6 and ML +6 mm, and three plugs at AP +3,0,-6 and ML +2 mm were taken (see Fig. 2). Tissue plugs included all six layers of cortex but did not extend into subcortical tissue. Tissue was immediately frozen in dry ice and stored at –80 °C until use.

Total RNA from brain tissue was extracted using RNeasy mini columns (Qiagen). The purified RNA was treated with RNase-free DNase-I (Roche) and re-purified using an RNeasy mini-column (Qiagen). RNA was then eluted in 50 μl of water. First-strand cDNA was reverse transcribed in a final volume of 50 μl using 5 μl purified total RNA, 1 mM random hexamer primer (Roche), 40 U SuperScript II reverse transcriptase (Life Technologies), and 40 U of RNase inhibitor (Roche). The buffer consisted of (in mM): 50 Tris-HCl (pH 8.3), 75 KCl, 3 MgCl2, 10 DTT, and 5 dNTP. The reaction proceeded at 37 °C for 90 min and 42 °C for 30 min, and was then terminated by heating to 95 °C for 5 min. A parallel reaction was performed as a negative control to demonstrate the absence

of contaminating genomic DNA (data not shown) by using all identical reagents except for the reverse transcriptase enzyme.

Quantitative real-time PCR. The relative standard curve method was used to quantify and compare RNA extracted from different regions of cortex in epileptic (WAG/Rij) and control (Wistar) rats. An 18S rRNA primer-probe set (Applied Biosystems) was used as an endogenous control to normalize the expression level of the sodium channels. Standard curves for 18S rRNA and each sodium channel primer/probe set were constructed using serial dilutions of control brain cDNA. Standards and unknowns were amplified in quadruplets. Standard curves for the sodium channel primer/probe sets and endogenous control (rRNA) were constructed from respective mean critical threshold (C_T) values; the equation describing the curve was derived using Sequence Detector software v1.6.3 (Applied Biosystems).

Primers and probes for the sodium channel targets were designed using Primer Express software (Applied Biosystems) according to the specifications of the TaqMan protocol (Winer et al., 1999). Sequences are as follows:

Nav1.1 forward 5'-TCCTGGAGGGTGTTTTAGATGC-3',
reverse 5'-AAAGATTTTCCCAGAAGTCCTGAG-3',
probe FAM-CTGGGCATTTCTGTCCCTGTTTCGACT-TAMRA;

Nav1.2 forward 5'-CATCAAGTCCCTCCGAACGTTA-3',
reverse 5'-GGCAGACCAGAAGTACGTTCATT-3',
probe FAM-CCTTATCCCGATTTGAAGGAATGAGGGTTG-TAMRA;

Nav1.6 forward 5'- AGTAACCCTCCAGAATGGTCCAA-3',
reverse 5'-GTCTAACCAGTTCCACGGGTCT-3',
probe FAM-AATCATCGCAAGAGGTTTCTGCATAGACGG-TAMRA.

Target specificity was confirmed by nucleotide BLAST search. Primers and probes for sodium channels were synthesized and purified by Applied Biosystems. Primers for the sodium channels and 18S rRNA were used at a final concentration of 900 and 50 nM, respectively, whereas the probes were used at a final concentration of 200 nM. The primer-probe combinations were not limiting at these concentrations. Amplification was done in a 25 μl final volume, under the following cycling conditions: 10 min at 50 °C and then 40 cycles of 95 °C, 15 sec, followed by 60 °C, 1 min. An ABI Prism 7700 (Applied Biosystems) was used to run the PCR reaction and data was recorded using Sequence Detector v1.6.3. Sodium channels and 18S rRNA templates were amplified in separate wells. The amount of mRNA in different regions of cortex was reported as the ratio of mRNA in the epileptic rats divided by mRNA in the control rats.

Immunocytochemistry. Rats were anasthetized with ketamine/xylazine (80/5 mg/kg i.p.) and then underwent intracardiac perfusion with 0.01 M PBS followed by a 4% solution of cold buffered paraformaldehyde. Brains from 4 month WAG/Rij and Wistar rats were postfixed and cryoprotected in 30% sucrose in 1 M phosphate buffer solution (PBS), and coronal sections (10 μm) of the cerebral hemispheres, including all regions studied by quantitative PCR, were cut. Slices were mounted onto slides and incubated in blocking solution (5% normal goat serum and 1% BSA in PBS) containing 0.1% Triton X-100 and 0.02% sodium azide at room temperature for 30 min., then incubated with subtype-specific antibodies to Na^+ channel α-subunits Nav1.1 (residues 465-481, 1:100 dilution, Alomone, Jerusalem), Nav1.2 (residues 467-485, 1:100 dilution, Alomone), Nav1.6 (residues 1042-1061, 1:100, Alomone), and a phospho-CREB antibody (1:50, Cell Signaling Technology, Inc., Beverly, MA) overnight at 4 °C. Sections were washed

in PBS and incubated with biotinylated goat anti-rabbit serum (1:1000, Sigma) in blocking solution for 3 hours, then washed in PBS and incubated in avidin-HRP (1:1000, Sigma) in blocking solution for 3 hours. Sections were washed in PBS and exposed to heavy metal enhanced 3,3'-diaminobenzidine•4HCl in 1X peroxide substrate buffer (Pierce, Rockford, Illinois) for 7 min.

Data Analysis. A Nikon Eclipse E800 light microscope was used for sample observation, and quantitative microdensitometry of immunostaining signals was obtained using IPLab v3.0 Image Processing software (Scanalytics Inc., Fairfax, VA). Signal intensities were determined by outlining individual cortical neurons, and IPLab integrated densitometry functions were used to calculate mean signal intensities for the selected areas. Results from identical regions and layers of cortex in WAG/Rij (epileptic) rats were compared to Wistar (control) rats processed in parallel and differences were assessed by non-paired *t*-tests. Immunopositivity was quantified by averaging multiple counts within a defined area ($1.9x10^4\mu m^2$) within layers II-IV. For counts of immunopositive neurons, cells that displayed a signal of >50% above background were scored as positive.

For the EEG data in Fig. 1F and the quantitative PCR data in Fig. 2, differences were analyzed using ANOVA with *post-hoc* Fisher's least significant difference analysis with Bonferroni adjustment. An alpha level of 0.05 was used as a threshold for statistical significance.

5.4 RESULTS

Seizure frequency and duration increase with age in the WAG/Rij model of absence epilepsy. SWDs begin to be seen at approximately 3 months of age in WAG/Rij rats (Coenen and Van Luijtelaar, 1987; Coenen et al., 1992). In the animals we

studied, EEG recordings from WAG/Rij rats showed an age-related increase in the number of seizures per unit time, and in the mean duration of each seizure. Age-matched control Wistar rats did not show SWD activity (Fig. 5.1A). Examples of typical recordings from WAG/Rij rats at different ages are shown in Fig. 5.1B-D. SWDs, consisting of high voltage 7-11 Hz rhythmic spike-wave activity, are shown on an expanded timescale in Fig. 5.1E. To correlate the molecular changes with SWD activity at different ages, we calculated the percentage of time in SWD (Fig. 5.1F). Percent time in SWD depends on both the number of SWDs per minute and the duration of each SWD. Mean seizure durations were 2.8 ± 1.17 s (mean ± SD) at 2 months, 2.6 ± 1.67 s at 4 months, and 3.1 ± 1.83 s at 6 months. Mean SWDs per minute were 0.02 ± 0.017 at 2 months, 0.19 ± 0.080 at 4 months, and 0.14 ± 0.061 at 6 months. Percent time in SWD was 0.11± 0.070 (mean ± SE) at 2 months, 0.51±0.141 at 4 months, and 0.74±0.188 at 6 months (n=23 animals). The difference between 2 month and 4 month, and 2 month and 6 month percent time in SWD was statistically significant. (*=p<0.05, Fig. 5.1F). Although the 6 month WAG/Rij rats had a greater percent time in SWD compared to 4 months, the difference did not reach statistical significance.

Nav1.1 and Nav1.6 mRNAs are up-regulated in epileptic cortex. Sodium channels Nav1.1, Nav1.2, and Nav1.6 were found to be expressed in the cortices of both control and epileptic animals. Nav1.3 was expressed at very low levels in both control and epileptic animals, and Nav1.8, which has been shown to be expressed in CNS tissue in some pathologic conditions (Black et al., 2000) was not detected. Tissue plugs were taken from 6 month old WAG/Rij (epileptic) and age-matched Wistar (control) rat cortex. Quantitative PCR experiments showed a significant up-regulation of Nav1.1 and Nav1.6 mRNA selectively at ML+6 mm in the transverse plane at bregma (n=8 animals, *=p<0.05, Fig. 5.2). This region of cortex approximately matches the

electrophysiologically determined region of seizure onset, as reported by Meeren et al., within the peri-oral area of the somatosensory cortex (Meeren et al., 2002). PCR results for primer/probe sets yielded statistically insignificant differences between matched left and right hemispheric tissue sections; therefore data from bilaterally equivalent tissue sections were combined. Nav1.2 did not show a significant change between WAG/Rij and Wistar rats in any region of cortex tested (Fig. 5.2).

Nav1.1 and Nav1.6 proteins are up-regulated in layer II-IV cortical neurons. Having demonstrated a region-specific up-regulation of Nav1.1 and Nav1.6 mRNA, we next asked whether these changes occurred within a specific population of neurons within the cortex. Immunocytochemical experiments using subtype-specific antibodies for Nav1.1 and Nav1.6 on 4 month WAG/Rij and Wistar rats showed up-regulation of these channels in layer II-IV cortical neurons of WAG/Rij rats. Layer II-IV neurons were identified by their neuronal morphological characteristics and by their proximity to the pial surface superficially. Fig. 5.3A-C shows coronal sections of cortex at bregma and +6 in the transverse plane, demonstrating the significant change in sodium channel expression (for Nav1.1 and Nav1.6, but not Nav1.2) in layers II-IV in epileptic rats. Fig. 5.3D shows cortical staining with phospho-CREB antibody, a marker of transcription activation. The up-regulation of sodium channels Nav1.1 and Nav1.6 is paralleled by an increase in neuronal phospho-CREB immunoreactivity in epileptic cortex layers II-IV (Fig. 5.3D). Fig. 5.3E,F represent a quantification of the sodium channel data (n=4 epileptic, 3 control, and 668 total neurons, *=$p<0.05$). Immunocytochemical experiments done in the absence of primary antibody yielded only non-specific background levels of signal (data not shown). Sodium channel protein expression and pCREB expression in adjacent regions and in other areas of cortex and thalamus did not show a significant difference between epileptic and non-epileptic animals (data not shown).

Age-dependent dysregulation of sodium channel expression in WAG/Rij rats. To further assess the connection between altered sodium channel expression and seizure activity, we examined age-dependent changes in sodium channel mRNA expression. Fig. 5.4 shows the variation in Nav1.1, Nav1.2, and Nav1.6 mRNA levels at AP+0.0, ML+6.0 mm (anatomical location E on Fig. 5.2) with respect to age in the WAG/Rij model compared to Wistar animals. Nav1.1 and Nav1.6 mRNA levels increase progressively over the three time points studied in the WAG/Rij rats.

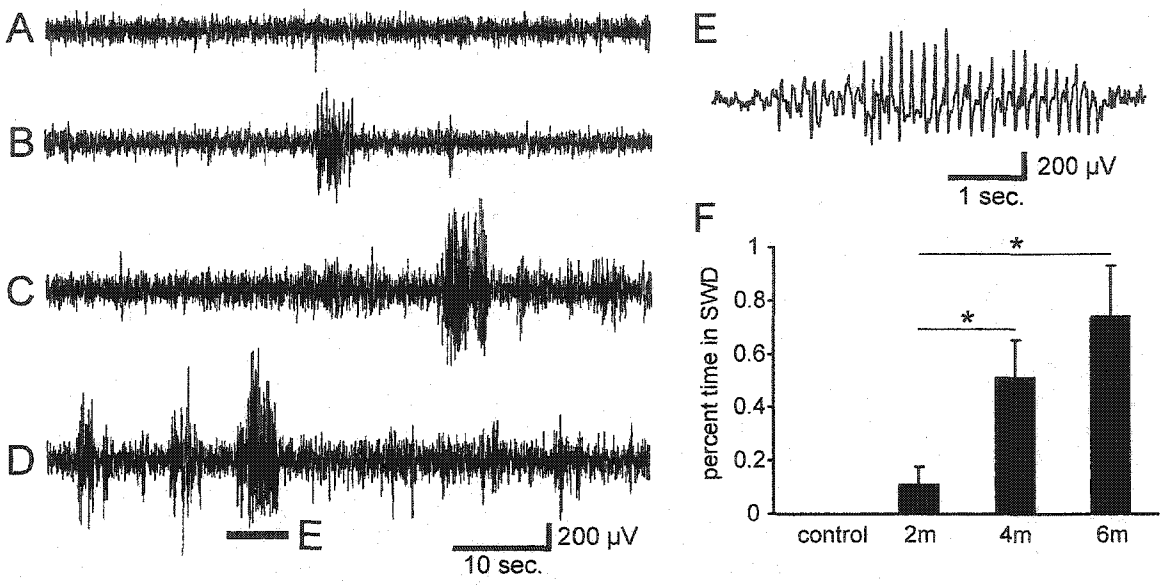

Fig. 5.1. Spike-wave discharges increase with age in WAG/Rij rats. **A**, Typical recording from a Wistar control rat at 7 months of age showing normal EEG activity with no SWDs. **B-D**, Typical examples of EEG recordings from WAG/Rij rats showing SWDs of increasing duration and frequency of occurrence with age (B = 2 month WAG/Rij, C = 4 month WAG/Rij, D = 6 month WAG/Rij). Section expanded in *E* is indicated by horizontal bars. **E**, Segment of data from *D* shown at expanded time scale to demonstrate typical morphology of SWDs. **F**, Control Wistar rats aged 2-6 months exhibited no SWDs (n=10). Percent time spent in SWD firing pattern is shown for WAG/Rij rats at 2 months (n=2), 4 months (n=6), and 6 months (n=5). Each rat was recorded for sessions lasting 2 hours each on 3 consecutive days (6 hours total) just before performing the molecular studies. Data is plotted as mean ± SE, * = $p<0.05$ (4 and 6 month each compared to 2 month, ANOVA with *post-hoc* Fisher's least significant difference analysis with Bonferroni adjustment).

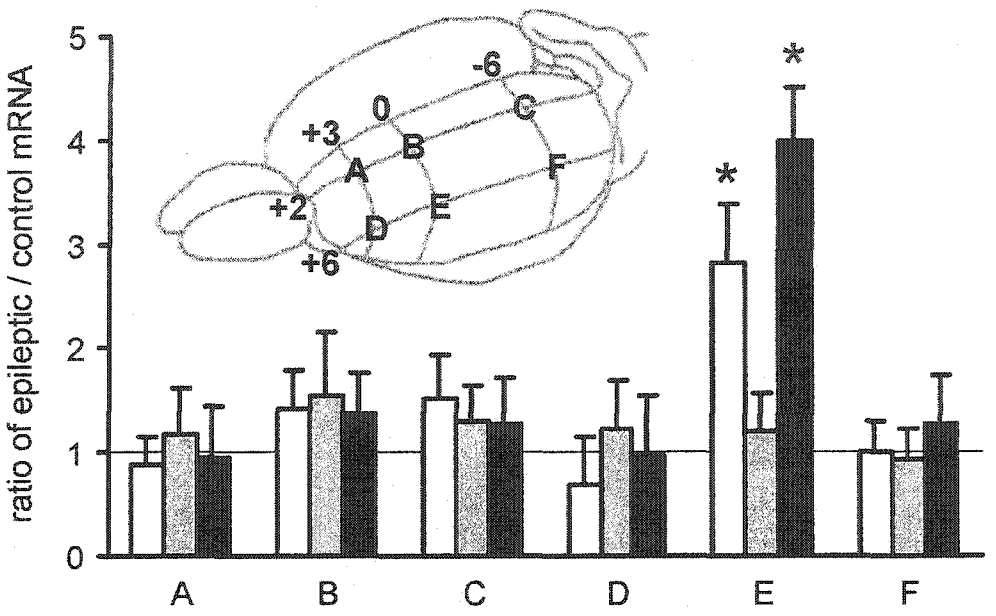

Fig. 5.2. Sodium channel mRNA in WAG/Rij and Wistar cortex. Anatomical locations of tissue plugs used for quantitative PCR analysis are indicated on inset drawing of rat brain. The histogram shows the ratio of sodium channel mRNA levels in the neocortex of 6 month old WAG/Rij (epileptic) rats compared to age-matched Wistar (control) rats. At anatomical location "E", there is a statistically significant increase in Nav1.1 (□) and Nav1.6 mRNA (■), but not Nav1.2 mRNA (▨), in the epileptic animals compared to control animals. Data is plotted as mean ± SE; n = 8 animals, * = $p<0.05$, ANOVA with *post-hoc* Fisher's least significant difference analysis with Bonferroni adjustment.

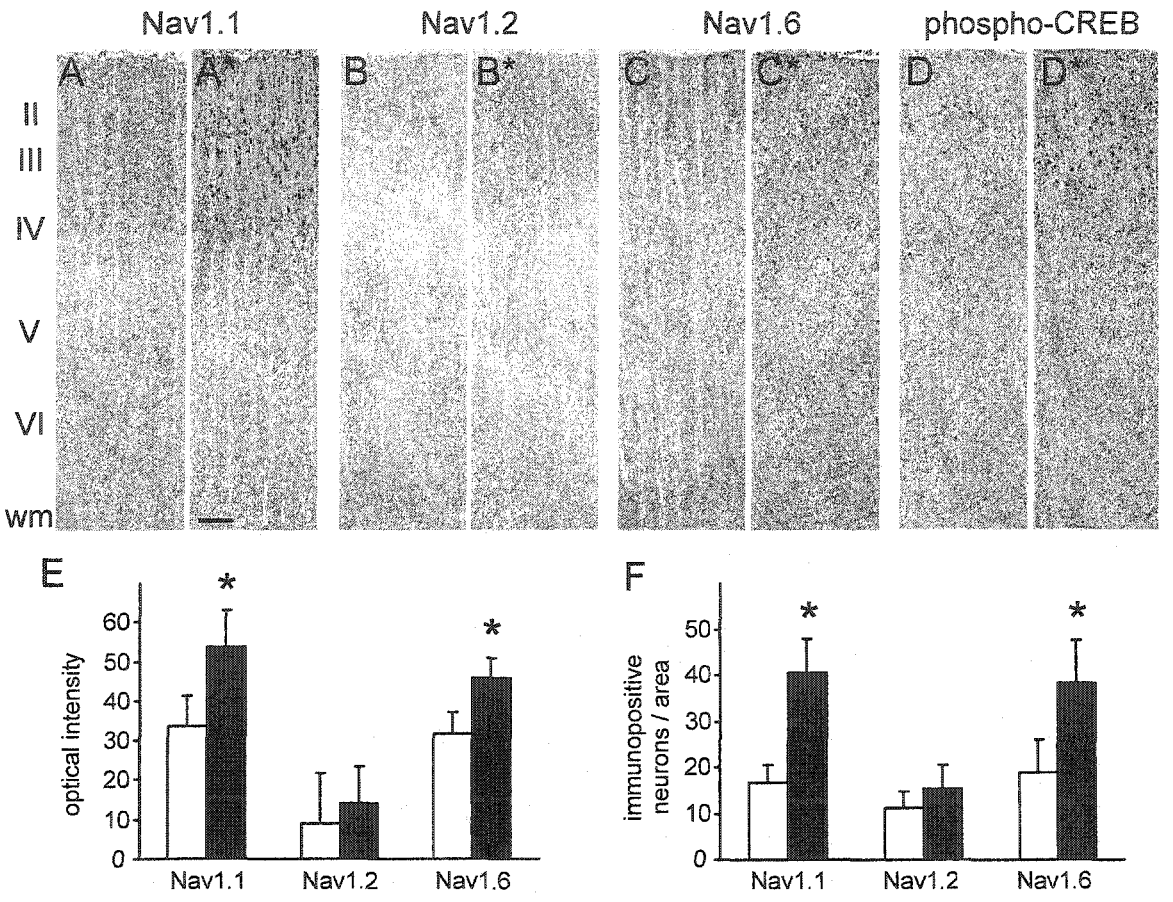

Fig. 5.3. Sodium channel protein in layers II-IV neurons of WAG/Rij and Wistar rat cortex. **A-D**, Coronal sections of cortex at bregma and +6 in the transverse plane (location E in Fig. 2) showing layers of cortical mantle. Immunostaining in control rats (no *) versus WAG/Rij rats (*) for Nav1.1 (A), Nav1.2 (B), Nav1.6 (C), and phopho-CREB (D) antibodies are shown. Pial surface is at the top of image, wm = white matter, scale bar = 100μm. The control and epileptic images were digitally contrast-enhanced using identical parameters to qualitatively illustrate the up-regulation of transcripts. **E**, Optical intensity quantification from unenhanced images of individual neurons in layers II-IV shows increased staining with Nav1.1 and Nav1.6 antibodies in the epileptic animals (■) compared to controls (□), indicating up-regulated sodium channel protein. Layer V-VI pyramidal neurons and neurons in other regions of cortex did not show a significant

change in sodium channel expression between epileptic and control animals (data not shown). F, Quantification of immunopositive neurons for each sodium channel antibody in layers II-IV. Epileptic animals (■) showed increased numbers of Nav1.1 and Nav1.6 immunopositive neurons compared to control animals (□). Data is plotted as mean ± SD; n = 7 animals, * = $p<0.05$, student's t-test.

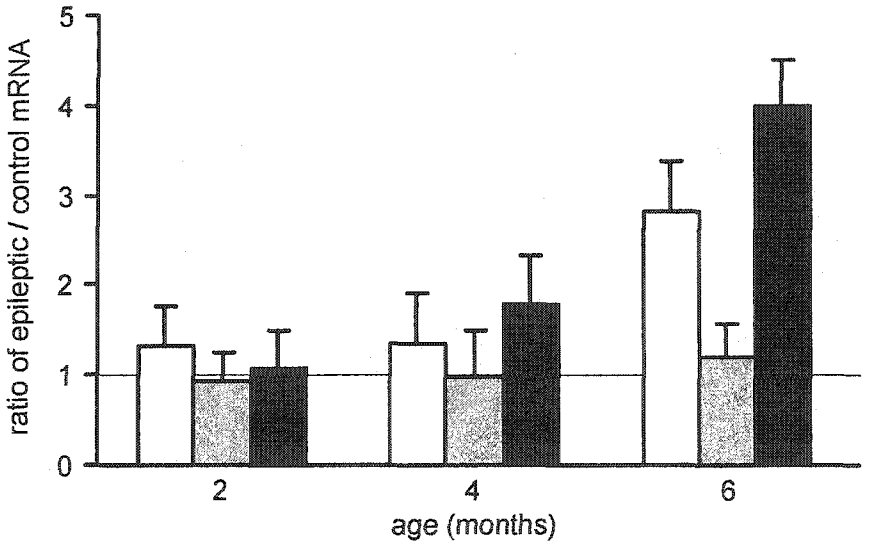

Fig. 5.4. Dysregulated sodium channel expression in layer II-IV cortical neurons parallels age-dependent increase in seizure frequency in WAG/Rij rats. The ratio of expression of sodium channel mRNA levels between epileptic and control rats for Nav1.1 (□) and Nav1.6 (■) mRNA, but not Nav1.2 mRNA (▨), increases from 2 months to 6 months. Data is plotted as mean ± SE.

5.5. DISCUSSION

This study demonstrates for the first time that there is dysregulated expression of voltage-gated sodium channels in cortical neurons in a rodent model of absence epilepsy. We focused on the cortex due to the possible role of the facial somatosensory cortex in initiating seizures, based on previous studies (Meeren et al., 2002). We used quantitative PCR to identify a specific region of cortex where sodium channel mRNA expression was different in epileptic (WAG/Rij) and non-epileptic (Wistar) rats. We then used immunocytochemistry to localize the change in sodium channel expression to a specific population of neurons in the cortex. Our data show that mRNA levels for sodium channel genes Nav1.1 and Nav1.6 are increased in the lateral aspect of the cortex in the plane of bregma and that layer II-IV cortical neurons in this region contain elevated Nav1.1 and Nav1.6, but not Nav1.2, protein. Interestingly, this region of cortex corresponds anatomically to the electrophysiologically-determined region of seizure onset, as reported by Meeren et al., within the facial region of the somatosensory cortex (Meeren et al., 2002). Increased phospho-CREB immunoreactivity in these cortical neurons reflects increased transcription activation and neuronal activity (Buonanno and Fields, 1999) in the epileptic vs. control animals, which may be associated with the observed changes in Nav1.1 and Nav1.6 expression. Although we did not detect qualitative changes in sodium channel expression in subcortical regions such as the thalamus or cerebellum, future quantitative studies of sodium channel expression in subcortical structures will be necessary to determine whether or not changes occur there as well.

Layer II-IV neurons, and the intracortical currents they produce, are a major factor in the generation of SWDs (Kandel and Buzsaki, 1997). Since the rhythmic oscillations of SWDs depend on cortico-thalamic circuits arising in deeper layers of cortex (layers V-VI), it is interesting that the initiation of this pathological firing pattern

correlates to abnormal sodium channel expression in other more superficial layers (layers II-IV) of cortex.

Nav1.1 and Nav1.6, in particular, are thought to be capable of producing a persistent current (Maurice et al., 2001; Raman et al., 1997; Smith et al., 1998) associated with neuronal bursting and hyperexcitability (Parri and Crunelli, 1998; Tanaka et al., 1999). This current could generate bursting in neurons, which could potentially contribute to an epileptic phenotype. The anti-convulsant drugs valproate and lamotrigine reduce the persistent current in cortical neurons (Spadoni et al., 2002; Taverna et al., 1998) and ethosuximide reduces persistent sodium current in thalamic and cortical neurons (Crunelli and Leresche, 2002; Leresche et al., 1998). In addition, Nav1.6 sodium channels populate the neuronal axon hillock and therefore increased channel density at this site could lower the threshold for action potential generation (Jenkins and Bennett, 2001). The developmental and regulatory processes that control the transcription, cellular expression, and plasticity of sodium channel genes in the cortex are unknown, and therefore we cannot conclude whether the changes observed here are a cause or result of the increased neuronal activity.

Burst firing appears to be essential for the generation of SWDs (Bal et al., 2000; Blumenfeld and McCormick, 2000). Dysregulated expression of VGSCs can play a crucial role in enhanced burst firing of cortical and other neurons (Brumberg et al., 2000; Waxman, 2001). In fact, it has been proposed that enhanced burst firing resulting from VGSC-mediated action potentials may constitute a final pathway of electrical hyperexcitability in interictal and ictal activities in epilepsy (Bartolomei et al., 1997; Titan et al., 1995).

At the genetic and molecular level, most forms of epilepsy result from neuronal migrational abnormalities, metabolic defects, or accumulation of inappropriate material that alters neuronal function (Segal, 2002). The WAG/Rij model of absence epilepsy has

an undetermined genetic basis (Coenen et al., 1992; Peeters et al., 1992). Currently, no single sodium channel mutation has been linked or attributed to this model. Because we have demonstrated a change in the expression of two sodium channel genes, it is possible that the molecular defect in WAG/Rij rats occurs upstream of single gene transcription. Altered availability of neurotrophic transcription factors, which can regulate the developmental expression of multiple genes and gene families, may be responsible for the dysregulation of sodium channel expression in this model (Noebels, 2002).

Absence seizures have traditionally been classified as a type of generalized epilepsy (ILAE Classification, 1981). There may, however, be crucial nodes within the brain that are most important for generating these seizures (Blumenfeld, 2003; Blumenfeld et al., 2003). The focal dysregulated expression of Nav1.1 and Nav1.6 reported here is associated with an age-dependent increase in seizures and roughly corresponds to the electrophysiologically-determined region of seizure onset (Meeren et al., 2002). Therefore, although absence seizures cause an impairment of consciousness and involve widespread brain regions, they may in fact initiate as focal electrophysiological events which secondarily generalize. Improved detection methods and more time-sensitive physiological measurements will continue to improve our understanding of this process.

In the WAG/Rij model, we report that an age-related increase in percent time in SWD firing (Fig. 5.1) is associated with a progressive increase in expression of Nav1.1 and Nav1.6 transcripts in layer II-IV cortical neurons in specific regions of cortex (Fig. 5.4). The critical question of whether the changes in sodium channel expression that we observed are a cause or effect of increasing seizure activity remains unanswered by this study. Future experiments examining the effect of either subtype-specific sodium channel blockers, or targeted knock-down of specific sodium channel transcripts, on SWD firing, will be necessary in order to discern whether the changes in expression of

Nav1.1 and Nav1.6 are a primary or secondary effect, and whether these changes have any functional significance.

Understanding the molecular basis for changes in neuronal activity during spike-wave seizures may help direct the development of new treatments for this disorder. Our results raise the possibility that altered expression of Nav1.1 and Nav1.6 in cortical neurons may play a role in either the generation of, or response to, SWD firing seen in absence epilepsy. If the molecular mechanisms of enhanced burst firing can be correlated to specific regional alterations in sodium channel expression in human epilepsy, gene therapy and other molecular approaches to treating severe generalized seizure disorders may be possible.

CHAPTER 6

CONCLUSIONS

6.1 ACTIVITY-DEPENDENT MODULATION OF VGSC EXPRESSION

The preceding chapters present evidence that changes in neuronal activity modulate the expression of VGSCs, which in turn regulate neuronal excitability and responsiveness. This effect was demonstrated within several populations of neurons, in both physiological and pathological conditions. As discussed below, the consequences of these changes are complex; some appear to be adaptive and beneficial, while others may over time contribute to neuronal overactivation and injury, and even drive end-organ damage.

6.2 MOLECULAR CHANGES WITHIN NEURONS IN THE DIABETIC BRAIN

Type I and type II diabetes both result in downstream complications, including renal dysfunction, coronary artery disease, retinopathy, peripheral neuropathy, and stroke, which can compromise quality of life or even be life-threatening (Donnelly et al., 2000). Chronic hyperglycemia, which results from decreased production of insulin in type I diabetes, and increased peripheral resistance to insulin in type II diabetes, disrupts cellular homeostasis and normal physiology. At least four metabolic pathways involving the shunting of excess glucose are known to participate in the generation of hyperglycemic end-organ damage (Brownlee, 2001): 1) The polyol pathway is activated during hyperglycemia, and leads to consumption of NADPH and depletion of GSH,

which lower the threshold for intracellular oxidative injury. 2) Increased formation of advanced glycosylation end-products (AGEs) damages endothelial cells, thus contributing to vascular damage. 3) Diacylglycerol (DAG) activation of protein kinase C (PKC) occurs during hyperglycemia and has adverse effects on blood flow and vascular permeability. 4) Increased shunting of glucose into the hexosamine pathway leads to increased proteoglycan and O-linked glycoprotein synthesis. Over time, the metabolism of excess glucose through these alternative metabolic pathways contributes to vascular and end-organ injury (Donnelly et al., 2000). Metabolic activity within these pathways does not depend on neuronal activity and thus in the aggregate these pathways constitute a neurologically "passive" response to hyperglycemia (Fig. 6.1, left).

While the direct effects of glucose overload and pathogenesis involving these passive metabolic pathways account for much of the pathology associated with diabetes, the results presented in Chapters 2 and 3 suggest that a second neurologically "active" pathway, driven by neuronal activity, may contribute to end-organ pathology.

The diabetic state induces alterations in gene transcription within neurons of the CNS. Although some of the changes (e.g. up-regulated vasopressin production in the diabetic supraoptic nucleus (SON); see Chapter 2) result in altered neuronal function which is beneficial in the acute setting, there is evidence that over time, prolonged changes in neuronal gene transcription within the diabetic brain may be maladaptive, and underlie an "active" response that can drive pathogenesis and end-organ damage (Fig. 6.1, right).

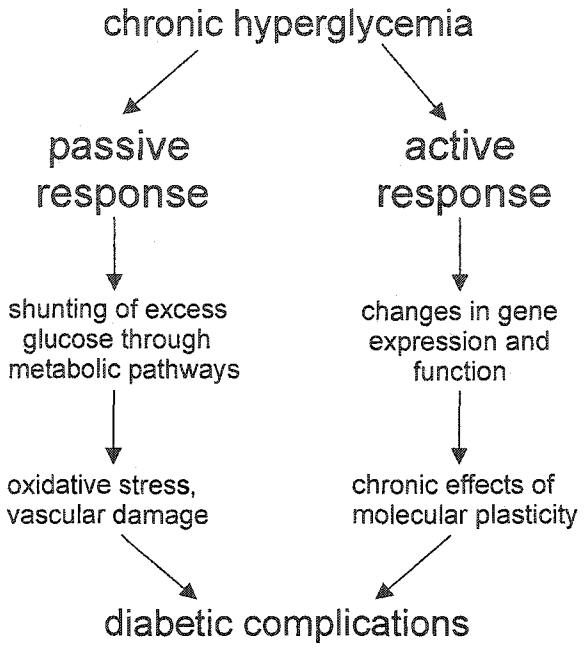

Fig. 6.1. Chronic hyperglycemia induces both neurologically "active" (right) and neurologically "passive" (left) cellular responses.

An increase in serum glucose raises serum osmolality at the rate of 1 mOsm/L per 18 mg/dL glucose. Hyperosmolality triggers both behavioral (polydipsia) and physiological (natriuresis, water retention) responses within the body, which aim to maintain solute balance and minimize fluid shifts between intracellular and extracellular environments. This adaptive response to hyperosmolality is mediated by MNCs within the hypothalamic supraoptic (SON) and paraventricular (PVN) nuclei, which increase their production and secretion of vasopressin when plasma osmolality rises (see Fig. 2.5) (Dheen et al., 1994b; Serino et al., 1998). MNCs are osmosensitive neurons which contain mechanosensitive stretch-inactivated cation channels capable of detecting changes in extracellular osmolality (Chakfe and Bourque, 2000; Voisin and Bourque, 2002). These changes in osmolality are encoded by MNCs as series of action potentials,

which propagate to the MNC terminals within the neuropituitary and regulate the amount of vasopressin released. Action potentials in the MNCs are produced in a characteristic bursting pattern (Andrew and Dudek, 1983), and are generated by the opening of voltage-gated sodium channels (VGSCs). The contribution of sodium channel activation to vasopressin release has been demonstrated by showing that application of the sodium channel blocker tetrodotoxin (TTX) to dissociated MNCs strongly reduces vasopressin secretion (Sperlagh et al., 1999).

The hyperosmolar state is associated with a chronically elevated demand for vasopressin. MNCs adapt to this demand by altering the rate of transcription of the gene for vasopressin (Luo et al., 2002). However, the transition from a quiescent to a bursting state when MNCs are confronted with an increase in osmotic pressure is not just a change in vasopressin synthesis and release – it is accompanied by an up-regulation of activity of VGSC genes and insertion of additional sodium channels in the membranes of the MNCs, a change which lowers the threshold for generation of action potentials. Sodium channel α–subunits Nav1.2 and Nav1.6 are the predominant sodium channel subtypes expressed in MNCs (Tanaka et al., 1999). When MNCs in healthy rats are exposed to oral salt-loading, transcription of the Nav1.2 and Nav1.6 genes is up-regulated and new Nav1.2 and Nav1.6 channels are produced and inserted into the MNC plasma membrane. Increased densities of sodium channels lower the neuronal threshold for firing and poise neurons, including the MNCs (Klein et al., 2002), to fire spontaneously and in bursts (Crill, 1996; Parri and Crunelli, 1998; Taddese and Bean, 2002). The elevated levels of functional sodium channels in the diabetic MNCs also enable greater membrane depolarizations in response to stimulation. As a result, there is greater calcium entry into the neuron which may facilitate vasopressin vesicle fusion and secretion of vasopressin (Scroggs and Fox, 1992). Thus there is a molecular remodeling

of the MNCs that supports the release of vasopressin under hyperosmolar conditions (Tanaka et al., 1999).

The hyperosmolality associated with diabetes has been shown to induce similar changes in MNCs, which have been studied in the STZ-induced diabetic rat model. Expression of the gene for vasopressin is strongly up-regulated within MNCs in diabetes. The transcription of mRNA and synthesis of protein for the Nav1.2 and Nav1.6 sodium channels are also up-regulated in response to the increased osmolality that accompanies hyperglycemia (Figs. 2.2, 2.3) (Klein et al., 2002). Electrophysiological analysis of acutely dissociated MNCs from diabetic animals shows increases in the densities of two distinct sodium currents (transient and persistent), indicating that functional VGSCs have been inserted into the cell membranes of the MNCs (Fig. 2.4) (Klein et al., 2002). Thus, similar to the hyperosmolar state in the absence of diabetes, there is a molecular remodeling of MNCs in untreated diabetes.

The up-regulated expression of VGSCs suggests that the activity level of MNCs should be chronically increased in untreated diabetes. Several studies have examined the expression of markers of neuronal activity within the SON in STZ-induced diabetes and the results support this hypothesis. Expression of c-fos protein (Fos), a marker for neurons with high states of activity, is up-regulated in the SON and PVN after four weeks of STZ-induced diabetes (Zheng et al., 2002). Likewise, neuronal nitric oxide synthase (NOS) mRNA levels are markedly up-regulated in SON and PVN neurons in STZ-induced diabetic rats (Luo et al., 2002; Serino et al., 1998). This increase in NOS expression can be reversed with normalization of glucose by either insulin treatment or dietary restriction (Serino et al., 1998). Because neuronal NOS is activated by calcium influx through NMDA receptors, the expression of the NMDA receptor NMDAR1 has been assessed in STZ-induced diabetes and was found to be up-regulated in SON and PVN neurons (Luo et al., 2002). In the same study expression of the glutamate receptor

GluR2/3 subunit, which endows NMDA receptors with calcium selectivity and limits calcium influx, was found to be down-regulated within the diabetic SON, which might allow further intracellular calcium accumulation (Luo et al., 2002). These findings provide additional support for the idea that in diabetes, increased demand for vasopressin leads to an ensemble of molecular changes which contribute to a high level of activity within vasopressin-producing neurons.

Although short-term rises in vasopressin synthesis and release by MNCs serve an important homeostatic role, sustained elevations in vasopressin levels have been implicated in the development of renal failure (Ahloulay et al., 1999; Bouby et al., 1999; Donnelly et al., 2000), and there is evidence for degeneration of MNCs in the SON which have been driven into a chronically active state in diabetes. The link between high levels of MNC activity and vasopressin release, and renal injury, appears to involve V2 vasopressin receptors, located in the basolateral membrane of principal cells in the renal medullary collecting duct and cortical arcade (Laycock and Hanoune, 1998), which mediate the antidiuretic effect of vasopressin. Activation of the V2 receptor through a G-protein-linked signaling cascade ultimately leads to the expression and insertion of the water channel aquaporin 2 into the apical membrane surface. By introducing water-permeable channels into the renal collecting duct, vasopressin acutely prevents (or limits) a rise in serum osmolality (Bankir et al., 2001). However, long-term overactivation of V2 receptors by chronically elevated serum vasopressin leads to glomerular hyperfiltration, albuminuria, and renal hypertrophy (Bardoux et al., 1999). These structural and physiological changes, which result from chronically increased vasopressin levels, are characteristic of diabetic nephropathy and can progress to renal failure (Fig. 2.5) (Ahloulay et al., 1999; Bouby et al., 1999; Donnelly et al., 2000). Normalization of vasopressin levels prevents the development of these changes and, in

vasopressin-deficient STZ-induced diabetic animals, these changes are not observed (Bardoux et al., 1999).

In addition to contributing to end-organ damage, the changes within hypothalamic neurons may over time contribute to their loss. While short-term changes in MNC activity may be adaptive, more chronic changes, which are associated with prolonged alterations in gene transcription, have been found to be associated with several structural alterations, suggesting that there is degeneration of hypothalamic neurons in the chronically diabetic SON and PVN. These changes were presented in Chapter 3. Other studies have confirmed these findings. Using Cresyl Violet (Nissl) staining, some neurons within the diabetic SON appear hypertrophic and vacuolated, while others are shrunken and hyperchromatic (Luo et al., 2002). These changes become more pronounced with length of time of STZ-induced diabetes. Vasopressin immunoreactivity, while still above control levels, falls off in long term (>2 months) diabetic animals (Luo et al., 2002), providing additional indirect evidence that there may be neuronal damage and functional insufficiency due to chronic overactivation in diabetes. Ultrastructural studies of SON and PVN neurons in prolonged diabetes have demonstrated abnormal axonal profiles, abnormal dendritic morphology, and abnormal somata; after six months of STZ-induced diabetes, substantial neuronal degeneration is present within the SON and PVN (Dheen et al., 1994a).

The molecular changes within hypothalamic MNCs, described above, appear to contribute to the degeneration of these neurons. As discussed above, activation of MNCs triggers an up-regulation of NOS and NMDAR (Luo et al., 2002). Chronic overstimulation of NMDAR can lead to an accumulation of intracellular calcium, which in turn drives the production of NO (Coyle and Puttfarcken, 1993; Dawson et al., 1991). While elevated levels of NO may be protective against damage caused by the accumulation of reactive oxygen species (part of the "passive" response, see Fig. 6.1)

(Brownlee, 2001), high levels of NO can also mediate glutamate toxicity secondary to neuronal overactivation. Chronic diabetes thus may, via the sustained hyperactivity that it produces, trigger the death of vasopressin-producing neurons.

Chronic hyperglycemia therefore triggers changes in the rate of transcription of specific genes within neurons of the hypothalamus and hippocampus, and possibly in other brain regions. It appears that over time these modifications of gene transcription evoke changes in neurons, which contribute to the development of secondary complications of diabetes.

While dietary and medical management of hyperglycemia are often sufficient to delay or prevent the appearance of secondary complications, the changes in neuronal gene transcription discussed in this review may also represent an opportunity for therapeutic intervention. In the hypothalamus, normalization of sodium channel expression or block of abnormal sodium channel activity (Klein et al., 2002; Sperlagh et al., 1999) in MNCs would be expected to decrease vasopressin secretion, and might therefore attenuate the hyperfiltration, albuminuria, and renal hypertrophy associated with increased vasopressin release, thus slowing the onset of diabetic nephropathy (Bardoux et al., 1999).

As the changes in neurons that occur in diabetes become better understood, it appears that the pathogenesis of end-organ damage in diabetes involves two distinct mechanisms: 1) neurologically "passive" shunting of excess glucose through alternative cellular metabolic pathways, which causes diffuse vascular injury and oxidative damage; and 2) "active" modulation of neuronal gene transcription in response to hyperglycemia, which alters neuronal structure and function, and in turn, can lead to physiological deficits (Fig. 6.1). Recognition of the active neuronal pathway may open up new therapeutic approaches, distinct from the classical therapies that work on the passive metabolic pathways, that can slow or prevent end-organ damage in diabetes.

6.3 STIMULATION-DEPENDENT PLASTICITY OF VGSC EXPRESSION

The results described in Chapter 4 provide evidence that the expression of specific sodium channel genes can be modulated by changes in neuronal activity level. Following stimulation consisting of 10 Hz pulses lasting 0.5 s every 2 seconds, 12 hours per day, for 5 days, expression of Nav1.8 and Nav1.9 mRNA and protein was down-regulated, while Nav1.3 was unchanged (Klein et al., 2003a). The differential regulation of transcription of sodium channel subtypes suggests that the activity-dependent modulation of transcription is gene specific, and not the result of a generalized up- or down-regulation of neuronal biosynthetic activity. These results are in concordance with studies examining the effect of a sodium channel activator (scorpion α toxin, which blocks channel inactivation) on sodium channel expression. In these studies, fetal cortical neurons in culture responded to channel activation by decreasing Nav1.1, Nav1.2, and Nav1.3 mRNA levels (Dargent and Couraud, 1990; Giraud et al., 1998; Lara et al., 1996).

The modification of gene transcription in the electrical stimulation model may represent a neuronal adaptation aimed at matching input (stimulation) with output (excitability). Like activity-dependent strengthening of synaptic contacts, remodeling of the neuronal electrogenic apparatus by altering either ion channel density or effective area of excitable membrane, may serve as a means of optimizing information transfer between neurons (Spitzer, 1999; Stemmler and Koch, 1999). Cultured cortical pyramidal neurons have been shown to adjust their voltage-dependent conductances (including VGSCs) in order to increase sensitivity to changes in current injection. By altering these conductances, the neuron maintains a stable firing rate corresponding to changes in input (Desai et al., 1999). The activity-dependent feedback mechanism which regulates the transcription of VGSCs is unknown, but there is evidence that intracellular levels of

calcium may play a role (LeMasson et al., 1993; Liu et al., 1998; Marder et al., 1996; Turrigiano et al., 1994; Turrigiano et al., 1995; Turrigiano, 1999; Turrigiano and Nelson, 2000). It has been proposed that low levels of intracellular calcium, resulting from periods of decreased neuronal firing, trigger a compensatory increase in VGSC expression, which increases neuronal excitability and firing frequency, and in turn, normalizes intracellular calcium levels. Conversely, high levels of intracellular calcium resulting from periods of high activity, trigger a decrease in VGSC expression, which decreases neuronal excitability and firing frequency, and in turn, normalizes intracellular calcium levels (see Fig. 6.2) (Marder and Prinz, 2002; Turrigiano, 1999).

Several experiments support this hypothesis. In cultured rat skeletal myotubes, saxitoxin labeling of sodium channels revealed that blockade of calcium channels by verapamil (as well as blockade of sodium channels by TTX) caused an up-regulation of sodium channel density (Brodie et al., 1989). A similar experiment demonstrated that pharmacological blockade of spontaneous electrical activity in skeletal myotubes caused a 38-83% increase in VGSC density (Sherman and Catterall, 1984). Electrical activity and/or sustained increases in intracellular calcium levels have been shown to decrease the level of VGSC mRNA (Kobayashi et al., 2002; Offord and Catterall, 1989; Shiraishi et al., 2001). This change was paralleled by an increase in cAMP levels, suggesting that stabilization of sodium channel expression and neuronal activity is dependent on a balance between calcium-dependent reduction in cAMP levels (which increases VGSC expression) and direct actions of calcium as a second messenger (which decreases VGSC expression) (Offord and Catterall, 1989). In addition to cAMP-mediated regulation of transcription, other calcium-dependent signaling pathways involving CaM kinase II and the MAP kinase cascade have been shown to regulate CREB-mediated gene transcription (Buonanno and Fields, 1999; Finkbeiner and Greenberg, 1998; Ji and Woolf, 2001; Kornhauser et al., 2002; West et al., 2001; West et al., 2002), and the

activities of these pathways can be modulated by changes in neuronal firing (Fields et al., 2001).

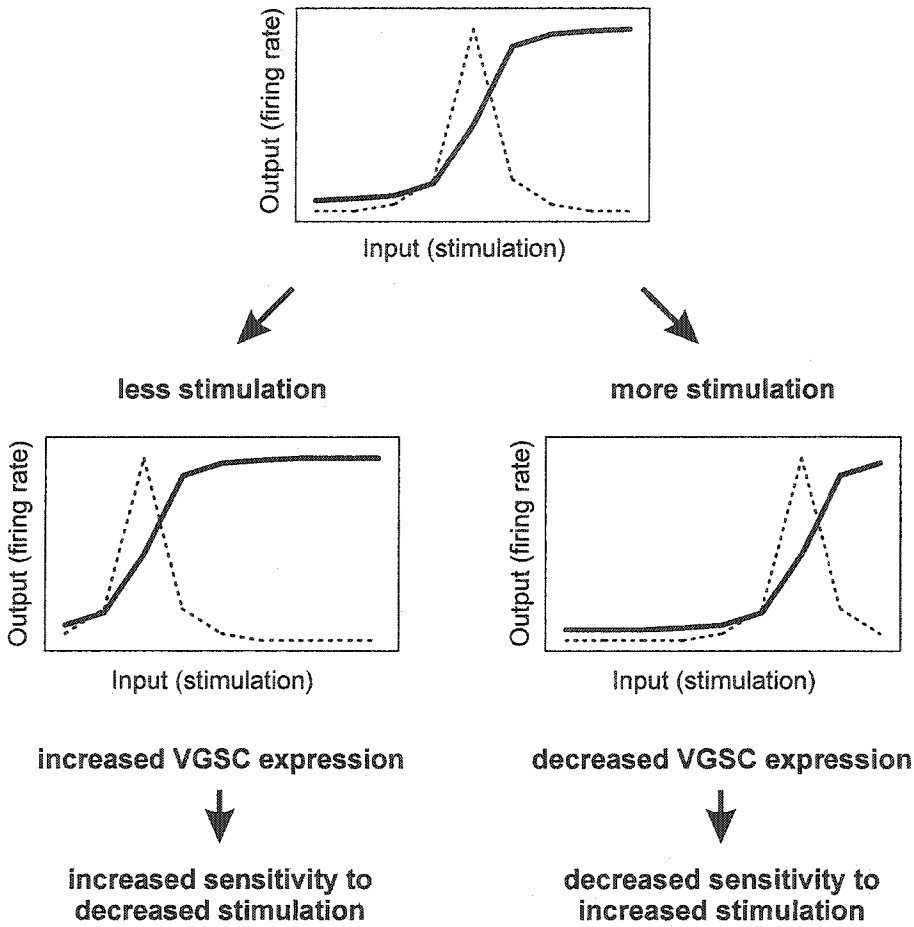

Fig. 6.2. Neuronal activity level (input) regulates expression of VGSCs, which determines neuronal sensitivity and firing rate (output) (Stemmler and Koch, 1999). This activity-dependent retuning of the neuronal response curve may be dependent on intracellular levels of calcium (Desai et al., 1999; Marder and Prinz, 2002; Turrigiano, 1999). Dotted lines represent range of stimulation or input current; solid lines represent output firing rate. Neurons can maintain a consistently wide range of output corresponding to changing input distributions through plasticity of VGSC expression.

These studies, with the results presented in Chapter 4, suggest that VGSC expression is a dynamic process that is continuously modulated by a number of "activity-sensors". Changes in intracellular calcium levels indicate changes in neuronal stimulation and input, and these changes are translated into alterations in the molecular composition of the neuronal electrogenic membrane.

6.4 VGSC EXPRESSION AND EPILEPSY

In Chapter 5, activity-dependent changes in VGSC expression were addressed in the context of epilepsy. WAG/Rij rats, which have spontaneous spike-wave discharges (SWDs) similar to those seen in human absence epilepsy, demonstrated up-regulated expression of Nav1.1 and Nav1.6 mRNA and protein in layer II-IV cortical neurons within the facial somatosensory region (Klein et al., 2003c). This area of cortex matches the electrophysiologically-determined region of seizure onset in this model (Meeren et al., 2002). The dysregulated expression of Nav1.1 and Nav1.6 mRNA and protein parallel the age-dependent increase in SWD firing time in this model (Klein et al., 2003c).

The SWD rhythm is thought to result from interactions between neurons of the GABAergic reticular nucleus and corticopetal thalamic nuclei (Buzsaki et al., 1988; Steriade et al., 1985). Field potential measurements using multi-site depth electrodes in WAG/Rij rats have provided evidence that the currents associated with SWD generation originate through activation of layer II-IV intracortical neuronal networks (Kandel and Buzsaki, 1997). Overexpression of Nav1.1 and Nav1.6 within these neurons could lower the threshold for action potential firing and increase the peak current density upon activation. In addition, Nav1.6 is capable of producing a persistent current (Maurice et al., 2001; Raman et al., 1997; Smith et al., 1998), which can underlie neuronal bursting and hyperexcitability (Parri and Crunelli, 1998; Tanaka et al., 1999).

In the WAG/Rij model of absence epilepsy, it is unclear whether the changes in expression of Nav1.1 and Nav1.6 are a cause or effect of the seizures. In the former case, a molecular defect causing up-regulated expression of Nav1.1 and Nav1.6 could lead to hyperexcitable and seizure-prone neurons (Fig. 6.3, left). In the latter case, a VGSC-independent defect predisposing neurons to SWD firing could trigger an activity-dependent reorganization of the electrogenic membrane, in this case resulting in up-regulated expression of Nav1.1 and Nav1.6 (Fig. 6.3, right).

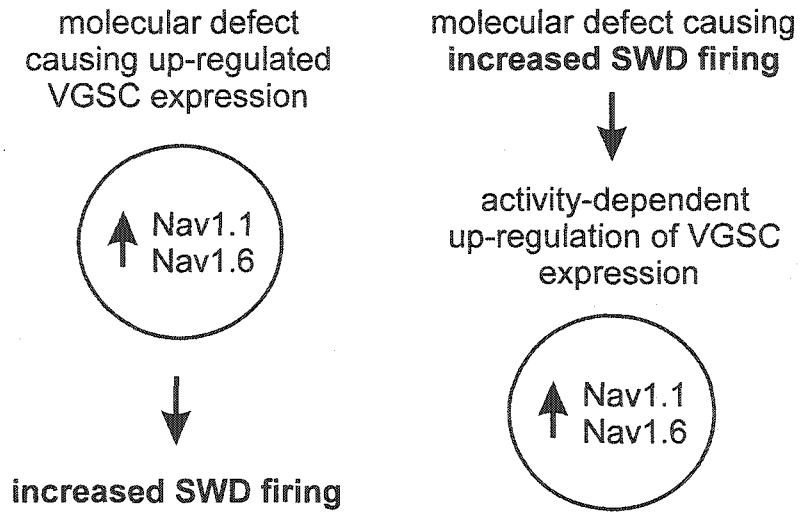

Fig. 6.3. The WAG/Rij model of absence epilepsy has an undetermined genetic basis. A molecular defect resulting in increased expression of Nav1.1 and Nav1.6 (left) could favor hyperexcitability and lead to spike-wave discharge (SWD) initiation. Alternatively, a VGSC-independent molecular defect causing increased SWD firing could trigger secondary activity-dependent changes in neuronal gene transcription leading to up-regulated expression of Nav1.1 and Nav1.6.

There are several approaches that could help dissect the relationship between SWD firing and neuronal VGSC expression in this model. VGSC transcript knock-down strategies or subtype-specific channel blockers could, in the future, help determine the relationship between VGSC expression and SWD firing in layer II-IV cortical neurons in the WAG/Rij model of absence epilepsy.

6.5 CLINICAL PERSPECTIVES

Identification of the dynamic interaction between neuronal activity level and VGSC expression could potentially lead to the development of novel therapeutic strategies for treating diseases and conditions in which sodium channel expression is dysregulated. In diabetes, for example, reversing the up-regulation of Nav1.2 and Nav1.6 that occurs in the supraoptic nucleus would prevent the chronically elevated vasopressin release. This manipulation would be expected to minimize the deleterious effects of vasopressin on the renal glomerulus, and therefore prevent the onset of diabetic glomerulonephritis and renal failure.

Neuropathic pain may result, in part, from injury-induced changes in neuronal sodium channel expression which lead to hyperexcitability and spontaneous firing. In Chapter 4, sodium channel expression was modulated by changes in neuronal activity level by a mechanism independent of changes in growth factor availability. These results suggest that stimulation applied to injured neurons could alter their expression of VGSCs. Currently, functional electrical stimulation, used to either augment or reduce neuronal activity associated with coordinated muscle contraction, is being tested in nerve-injured subjects. It is conceivable that electrical stimulation could be similarly applied to injured nerves, with the hope of reducing pain through modulation of VGSC expression.

Dysregulated sodium channel expression within specific neurons in the epileptic cortex represents another potential target for clinical intervention. As the causality between altered expression of sodium channels and epileptogenesis becomes better elucidated, targeted regulation of sodium channel expression within specific neuronal populations in the brain, using either anti-sense technology or targeted gene knock-down strategies, may be possible. While these approaches are sophisticated, they have the potential to be more specific than current anti-epileptic medications, many of which have systemic side effects and incompletely understood mechanisms of action.

REFERENCES

Ahloulay M, Schmitt F, Dechaux M, Bankir L (1999) Vasopressin and urinary concentrating activity in diabetes mellitus. Diabetes Metab 25:213-222.

Akopian AN, Sivilotti L, Wood JN (1996) A tetrodotoxin-resistant voltage-gated sodium channel expressed by sensory neurons. Nature 379:257-262.

Andrew RD, Dudek FE (1983) Burst discharge in mammalian neuroendocrine cells involves an intrinsic regenerative mechanism. Science 221:1050-1052.

Aronica E, Yankaya B, Troost D, van Vliet EA, Lopes da Silva FH, Gorter JA (2001) Induction of neonatal sodium channel II and III alpha-isoform mRNAs in neurons and microglia after status epilepticus in the rat hippocampus. Eur J Neurosci 13:1261-1266.

Avoli M, Gloor P (1982) Interaction of cortex and thalamus in spike and wave discharges of feline generalized penicillin epilepsy. Exp Neurol 76:196-217.

Avoli M, Gloor P, Kostopoulos G, Gotman J (1983) An analysis of penicillin-induced generalized spike and wave discharges using simultaneous recordings of cortical and thalamic single neurons. J Neurophysiol 50:819-837.

Avoli M, Gloor P, Kostopoulos G, Naquet R (1990) Generalized epilepsy: Neurobiological Approaches. Boston, MA: Birkhauser.

Baker MD, Chandra SY, Ding Y, Waxman SG, Wood JN (2003) GTP-induced tetrodotoxin-resistant Na+ current regulates excitability in mouse and rat small diameter sensory neurones. J Physiol 548:373-382.

Bal T, Debay D, Destexhe A (2000) Cortical feedback controls the frequency and synchrony of oscillations in the visual thalamus. J Neurosci 20:7478-7488.

Balkowiec A, Katz DM (2000) Activity-dependent release of endogenous brain-derived neurotrophic factor from primary sensory neurons detected by ELISA in situ. J Neurosci 20:7417-7423.

Balkowiec A, Katz DM (2002) Cellular mechanisms regulating activity-dependent release of native brain-derived neurotrophic factor from hippocampal neurons. J Neurosci 22:10399-10407.

Bankir L, Bardoux P, Ahloulay M (2001) Vasopressin and diabetes mellitus. Nephron 87:8-18.

Barber AJ, Lieth E, Khin SA, Antonetti DA, Buchanan AG, Gardner TW (1998) Neural apoptosis in the retina during experimental and human diabetes. Early onset and effect of insulin. J Clin Invest 102:783-791.

Bardoux P, Martin H, Ahloulay M, Schmitt F, Bouby N, Trinh-Trang-Tan MM, Bankir L (1999) Vasopressin contributes to hyperfiltration, albuminuria, and renal hypertrophy in diabetes mellitus: study in vasopressin-deficient Brattleboro rats. Proc Natl Acad Sci U S A 96:10397-10402.

Bartolomei F, Gastaldi M, Massacrier A, Planells R, Nicolas S, Cau P (1997) Changes in the mRNAs encoding subtypes I, II and III sodium channel alpha subunits following kainate-induced seizures in rat brain. J Neurocytol 26:667-678.

Biessels GJ, Kappelle AC, Bravenboer B, Erkelens DW, Gispen WH (1994) Cerebral function in diabetes mellitus. Diabetologia 37:643-650.

Biessels GJ, van der Heide LP, Kamal A, Bleys RL, Gispen WH (2002) Ageing and diabetes: implications for brain function. Eur J Pharmacol 441:1-14.

Black JA, Dib-Hajj S, McNabola K, Jeste S, Rizzo MA, Kocsis JD, Waxman SG (1996) Spinal sensory neurons express multiple sodium channel alpha-subunit mRNAs. Mol Brain Res 43:117-131.

Black JA, Cummins TR, Plumpton C, Chen YH, Hormuzdiar W, Clare JJ, Waxman SG (1999a) Upregulation of a silent sodium channel after peripheral, but not central, nerve injury in DRG neurons. J Neurophysiol 82:2776-2785.

Black JA, Fjell J, Dib-Hajj S, Duncan ID, O'Connor LT, Fried K, Gladwell Z, Tate S, Waxman SG (1999b) Abnormal expression of SNS/PN3 sodium channel in cerebellar Purkinje cells following loss of myelin in the taiep rat. NeuroReport 10:913-918.

Black JA, Dib-Hajj S, Baker D, Newcombe J, Cuzner ML, Waxman SG (2000) Sensory neuron-specific sodium channel SNS is abnormally expressed in the brains of mice with experimental allergic encephalomyelitis and humans with multiple sclerosis. Proc Natl Acad Sci U S A 97:11598-11602.

Blumenfeld H, McCormick DA (2000) Corticothalamic inputs control the pattern of activity generated in thalamocortical networks. J Neurosci 20:5153-5162.

Blumenfeld H, McCormick DA (2001) The role of thalamocortical burst firing in the transition from normal activity to epileptic seizures. American Neurological Association, Research Symposium.

Blumenfeld H (2003) From molecules to networks: cortical/subcortical interactions in the pathophysiology of idiopathic generalized epilepsy. Epilepsia 44 Suppl 2:7-15.

Blumenfeld H, Westerveld M, Ostroff RB, Vanderhill SD, Freeman J, Necochea A, Uranga P, Tanhehco T, Smith A, Seibyl JP, Stokking R, Studholme C, Spencer SS, Zubal IG (2003) Selective frontal, parietal and temporal networks in generalized seizures. Neuroimage 19:1556-66.

Bouby N, Hassler C, Bankir L (1999) Contribution of vasopressin to progression of chronic renal failure: study in Brattleboro rats. Life Sci 65:991-1004.

Boucher TJ, Okuse K, Bennett DL, Munson JB, Wood JN, McMahon SB (2000) Potent analgesic effects of GDNF in neuropathic pain states. Science 290:124-127.

Brecht S, Gelderblom M, Srinivasan A, Mielke K, Dityateva G, Herdegen T (2001) Caspase-3 activation and DNA fragmentation in primary hippocampal neurons following glutamate excitotoxicity. Mol Brain Res 94:25-34.

Brodie C, Brody M, Sampson SR (1989) Characterization of the relation between sodium channels and electrical activity in cultured rat skeletal myotubes: regulatory aspects. Brain Res 488:186-194.

Brooks DP, Nutting DF, Crofton JT, Share L (1989) Vasopressin in rats with genetic and streptozocin-induced diabetes. Diabetes 38:54-57.

Brownlee M (2001) Biochemistry and molecular cell biology of diabetic complications. Nature 414:813-820.

Brumberg JC, Nowak LG, McCormick DA (2000) Ionic mechanisms underlying repetitive high-frequency burst firing in supragranular cortical neurons. J Neurosci 20:4829-4843.

Buonanno A, Fields RD (1999) Gene regulation by patterned electrical activity during neural and skeletal muscle development. Curr Opin Neurobiol 9:110-120.

Buzsaki G, Bickford RG, Ponomareff G, Thal LJ, Mandel R, Gage FH (1988) Nucleus basalis and thalamic control of neocortical activity in the freely moving rat. J Neurosci 8:4007-4026.

Caffrey JM, Eng DL, Black JA, Waxman SG, Kocsis JD (1992) Three types of sodium channels in adult rat dorsal root ganglion neurons. Brain Res 592:283-297.

Campenot RB (1977) Local control of neurite development by nerve growth factor. Proc Natl Acad Sci U S A 74:4516-4519.

Cantrell AR, Catterall WA (2001) Neuromodulation of Na+ channels: an unexpected form of cellular plasticity. Nat Rev Neurosci 2:397-407.

Catterall WA (2000) From ionic currents to molecular mechanisms: the structure and function of voltage-gated sodium channels. Neuron 26:13-25.

Chakfe Y, Bourque CW (2000) Excitatory peptides and osmotic pressure modulate mechanosensitive cation channels in concert. Nat Neurosci 3:572-579.

Chiamvimonvat N, Kargacin ME, Clark RB, Duff HJ (1995) Effects of intracellular calcium on sodium current density in cultured neonatal rat cardiac myocytes. J Physiol 483:307-318.

Coenen AM, Van Luijtelaar EL (1987) The WAG/Rij rat model for absence epilepsy: age and sex factors. Epilepsy Res 1:297-301.

Coenen AM, Drinkenburg WH, Inoue M, van Luijtelaar EL (1992) Genetic models of absence epilepsy, with emphasis on the WAG/Rij strain of rats. Epilepsy Res 12:75-86.

Cohen GM (1997) Caspases: the executioners of apoptosis. Biochem J 326:1-16.

Commission on Classification and Terminology of the International League Against Epilepsy (1981) Proposal for revised clinical and electroencephalographic classification of epileptic seizures. Epilepsia 22:489-501.

Coyle JT, Puttfarcken P (1993) Oxidative stress, glutamate, and neurodegenerative disorders. Science 262:689-695.

Craner MJ, Klein JP, Renganathan M, Black JA, Waxman SG (2002a) Changes of sodium channel expression in experimental painful diabetic neuropathy. Ann Neurol 52:786-792.

Craner MJ, Klein JP, Black JA, Waxman SG (2002b) Preferential expression of IGF-I in small DRG neurons and down-regulation following injury. Neuroreport 13:1649-1652.

Crespo D, Ramos J, Gonzalez C, Fernandez-Viadero C (1990) The supraoptic nucleus: a morphological and quantitative study in control and hypophysectomised rats. J Anat 169:115-123.

Crill WE (1996) Persistent sodium current in mammalian central neurons. Annu Rev Physiol 58:349-362.

Crunelli V, Leresche N (2002) Block of thalamic T-type Ca+2 currents by ethosuximide is not the whole story. Epilepsy Currents 2:53-56.

Cukierman S (1996) Regulation of voltage-dependent sodium channels. J Membr Biol 151:203-214.

Cummins TR, Waxman SG (1997) Downregulation of tetrodotoxin-resistant sodium currents and upregulation of a rapidly repriming tetrodotoxin-sensitive sodium current in small spinal sensory neurons after nerve injury. J Neurosci 17:3503-3514.

Cummins TR, Dib-Hajj SD, Black JA, Akopian AN, Wood JN, Waxman SG (1999) A novel persistent tetrodotoxin-resistant sodium current in SNS-null and wild-type small primary sensory neurons. J Neurosci 19:RC43.

Cummins TR, Aglieco F, Renganathan M, Herzog RI, Dib-Hajj SD, Waxman SG (2001) Nav1.3 sodium channels: rapid repriming and slow closed-state inactivation display quantitative differences after expression in a mammalian cell line and in spinal sensory neurons. J Neurosci 21:5952-5961.

Danober L, Deransart C, Depaulis A, Vergnes M, Marescaux C (1998) Pathophysiological mechanisms of genetic absence epilepsy in the rat. Prog Neurobiol 55:27-57.

Dargent B, Couraud F (1990) Down-regulation of voltage-dependent sodium channels initiated by sodium influx in developing neurons. Proc Natl Acad Sci U S A 87:5907-5911.

Dawson VL, Dawson TM, London ED, Bredt DS, Snyder SH (1991) Nitric oxide mediates glutamate neurotoxicity in primary cortical cultures. Proc Natl Acad Sci U S A 88:6368-6371.

Desai NS, Rutherford LC, Turrigiano GG (1999) Plasticity in the intrinsic excitability of cortical pyramidal neurons. Nat Neurosci 2:515-520.

Destexhe A, McCormick DA, Sejnowski TJ (1999) Thalamic and thalamocortical mechanisms underlying 3 Hz spike-and-wave discharges. Prog Brain Res 121:289-307.

Dheen ST, Tay SS, Wong WC (1994a) Ultrastructural changes in the hypothalamic supraoptic nucleus of the streptozotocin-induced diabetic rat. J Anat 184:615-623.

Dheen ST, Tay SS, Wong WC (1994b) Arginine vasopressin- and oxytocin-like immunoreactive neurons in the hypothalamic paraventricular and supraoptic nuclei of streptozotocin- induced diabetic rats. Arch Histol Cytol 57:461-472.

Dib-Hajj S, Black JA, Felts P, Waxman SG (1996) Down-regulation of transcripts for Na channel alpha-SNS in spinal sensory neurons following axotomy. Proc Natl Acad Sci U S A 93:14950-14954.

Dib-Hajj SD, Tyrrell L, Black JA, Waxman SG (1998a) NaN, a novel voltage-gated Na channel, is expressed preferentially in peripheral sensory neurons and down-regulated after axotomy. Proc Natl Acad Sci U S A 95:8963-8968.

Dib-Hajj SD, Black JA, Cummins TR, Kenney AM, Kocsis JD, Waxman SG (1998b) Rescue of alpha-SNS sodium channel expression in small dorsal root ganglion neurons after axotomy by nerve growth factor in vivo. J Neurophysiol 79:2668-2676.

Dib-Hajj SD, Tyrrell L, Cummins TR, Black JA, Wood PM, Waxman SG (1999a) Two tetrodotoxin-resistant sodium channels in human dorsal root ganglion neurons. FEBS Lett 462:117-120.

Dib-Hajj SD, Fjell J, Cummins TR, Zheng Z, Fried K, LaMotte R, Black JA, Waxman SG (1999b) Plasticity of sodium channel expression in DRG neurons in the chronic constriction injury model of neuropathic pain. Pain 83:591-600.

Djouhri L, Lawson SN (1999) Changes in somatic action potential shape in guinea-pig nociceptive primary afferent neurones during inflammation in vivo. J Physiol 520 Pt 2:565-576.

Donnelly R, Emslie-Smith AM, Gardner ID, Morris AD (2000) ABC of arterial and venous disease: vascular complications of diabetes. BMJ 320:1062-1066.

Duan WR, Garner DS, Williams SD, Funckes-Shippy CL, Spath IS, Blomme EA (2003) Comparison of immunohistochemistry for activated caspase-3 and cleaved cytokeratin 18 with the TUNEL method for quantification of apoptosis in histological sections of PC-3 subcutaneous xenografts. J Pathol 199:221-228.

Elliott JR (1997) Slow Na+ channel inactivation and bursting discharge in a simple model axon: implications for neuropathic pain. Brain Res 754:221-226.

Fields RD, Neale EA, Nelson PG (1990) Effects of patterned electrical activity on neurite outgrowth from mouse sensory neurons. J Neurosci 10:2950-2964.

Fields RD, Yu C, Neale EA, Nelson PG (1992) Recording chambers in cell culture. New York: Liss.

Fields RD, Eshete F, Stevens B, Itoh K (1997) Action potential-dependent regulation of gene expression: temporal specificity in Ca^{2+}, cAMP-responsive element binding proteins, and mitogen-activated protein kinase signaling. J Neurosci 17:7252-7266.

Fields RD, Eshete F, Dudek S, Ozsarac N, Stevens B (2001) Regulation of gene expression by action potentials: dependence on complexity in cellular information processing. Novartis Found Symp 239:160-172.

Finkbeiner S, Greenberg ME (1998) Ca2+ channel-regulated neuronal gene expression. J Neurobiol 37:171-189.

Fjell J, Cummins TR, Dib-Hajj SD, Fried K, Black JA, Waxman SG (1999a) Differential role of GDNF and NGF in the maintenance of two TTX-resistant sodium channels in adult DRG neurons. Mol Brain Res 67:267-282.

Fjell J, Cummins TR, Fried K, Black JA, Waxman SG (1999b) In vivo NGF deprivation reduces SNS expression and TTX-R sodium currents in IB4-negative DRG neurons. J Neurophysiol 81:803-810.

Fjell J, Hjelmstrom P, Hormuzdiar W, Milenkovic M, Aglieco F, Tyrrell L, Dib-Hajj S, Waxman SG, Black JA (2000) Localization of the tetrodotoxin-resistant sodium channel NaN in nociceptors. NeuroReport 11:199-202.

Gastaldi M, Robaglia-Schlupp A, Massacrier A, Planells R, Cau P (1998) mRNA coding for voltage-gated sodium channel beta2 subunit in rat central nervous system: cellular distribution and changes following kainate-induced seizures. Neurosci Lett 249:53-56.

Gavrieli Y, Sherman Y, Ben-Sasson SA (1992) Identification of programmed cell death in situ via specific labeling of nuclear DNA fragmentation. J Cell Biol 119:493-501.

Giraud P, Alcaraz G, Jullien F, Sampo B, Jover E, Couraud F, Dargent B (1998) Multiple pathways regulate the expression of genes encoding sodium channel subunits in developing neurons. Brain Res Mol Brain Res 56:238-255.

Goldin AL, Snutch T, Lubbert H, Dowsett A, Marshall J, Auld V, Downey W, Fritz LC, Lester HA, Dunn R, et al. (1986) Messenger RNA coding for only the alpha subunit of the rat brain Na channel is sufficient for expression of functional channels in Xenopus oocytes. Proc Natl Acad Sci U S A 83:7503-7507.

Goldin AL, Barchi RL, Caldwell JH, Hofmann F, Howe JR, Hunter JC, Kallen RG, Mandel G, Meisler MH, Netter YB, Noda M, Tamkun MM, Waxman SG, Wood

JN, Catterall WA (2000) Nomenclature of voltage-gated sodium channels. Neuron 28:365-368.

Hains BC, Black JA, Waxman SG (2002) Primary motor neurons fail to up-regulate voltage-gated sodium channel Na(v)1.3/brain type III following axotomy resulting from spinal cord injury. J Neurosci Res 70:546-552.

Hains BC, Klein JP, Saab CY, Craner MJ, Black JA, Waxman SG (2003) Upregulation of sodium channel Nav1.3 and functional involvement in neuronal hyperexcitability associated with central neuropathic pain after spinal cord injury. J Neurosci 23:8881-8892.

Hawrylak N, Fleming JC, Salm AK (1998) Dehydration and rehydration selectively and reversibly alter glial fibrillary acidic protein immunoreactivity in the rat supraoptic nucleus and subjacent glial limitans. Glia 22:260-271.

Herzog RI, Cummins TR, Waxman SG (2001) Persistent TTX-resistant Na+ current affects resting potential and response to depolarization in simulated spinal sensory neurons. J Neurophysiol 86:1351-1364.

Isom LL, De Jongh KS, Patton DE, Reber BF, Offord J, Charbonneau H, Walsh K, Goldin AL, Catterall WA (1992) Primary structure and functional expression of the beta 1 subunit of the rat brain sodium channel. Science 256:839-842.

Isom LL, De Jongh KS, Catterall WA (1994) Auxiliary subunits of voltage-gated ion channels. Neuron 12:1183-1194.

Isom LL, Ragsdale DS, De Jongh KS, Westenbroek RE, Reber BF, Scheuer T, Catterall WA (1995) Structure and function of the beta 2 subunit of brain sodium channels, a transmembrane glycoprotein with a CAM motif. Cell 83:433-442.

Jenkins SM, Bennett V (2001) Ankyrin-G coordinates assembly of the spectrin-based membrane skeleton, voltage-gated sodium channels, and L1 CAMs at Purkinje neuron initial segments. J Cell Biol 155:739-746.

Ji RR, Woolf CJ (2001) Neuronal plasticity and signal transduction in nociceptive neurons: implications for the initiation and maintenance of pathological pain. Neurobiol Dis 8:1-10.

Kadowaki K, Kishimoto J, Leng G, Emson PC (1994) Up-regulation of nitric oxide synthase (NOS) gene expression together with NOS activity in the rat hypothalamo-hypophysial system after chronic salt loading: evidence of a neuromodulatory role of nitric oxide in arginine vasopressin and oxytocin secretion. Endocrinology 134:1011-1017.

Kamal A, Biessels GJ, Urban IJ, Gispen WH (1999) Hippocampal synaptic plasticity in streptozotocin-diabetic rats: impairment of long-term potentiation and facilitation of long-term depression. Neuroscience 90:737-745.

Kandel A, Buzsaki G (1997) Cellular-synaptic generation of sleep spindles, spike-and-wave discharges, and evoked thalamocortical responses in the neocortex of the rat. J Neurosci 17:6783-6797.

Kayano T, Noda M, Flockerzi V, Takahashi H, Numa S (1988) Primary structure of rat brain sodium channel III deduced from the cDNA sequence. FEBS Lett 228:187-194.

Kermer P, Klocker N, Labes M, Thomsen S, Srinivasan A, Bahr M (1999) Activation of caspase-3 in axotomized rat retinal ganglion cells in vivo. FEBS Lett 453:361-364.

Klein JP, Craner MJ, Cummins TR, Black JA, Waxman SG (2002) Sodium channel expression in hypothalamic osmosensitive neurons in experimental diabetes. NeuroReport 13:1481-1484.

Klein JP, Waxman SG (2003) The brain in diabetes: molecular changes in neurons and their implications for end-organ damage. Lancet Neurol 2:548-554.

Klein JP, Tendi EA, Dib-Hajj SD, Fields RD, Waxman SG (2003a) Patterned electrical activity modulates sodium channel expression in sensory neurons. J Neurosci Res 74:192-198.

Klein JP, Hains BC, Craner MJ, Black JA, Waxman SG (2004a) Apoptosis in vasopressinergic hypothalamic neurons in chronic diabetes mellitus. Neurobiol Dis, in press.

Klein JP, Khera DS, Nersesyan H, Kimchi EY, Waxman SG, Blumenfeld H (2004b) Dysregulation of sodium channel expression in cortical neurons in a rodent model of absence epilepsy. Brain Res, in press.

Kobayashi H, Shiraishi S, Yanagita T, Yokoo H, Yamamoto R, Minami S, Saitoh T, Wada A (2002) Regulation of voltage-dependent sodium channel expression in adrenal chromaffin cells: involvement of multiple calcium signaling pathways. Ann N Y Acad Sci 971:127-134.

Kornhauser JM, Cowan CW, Shaywitz AJ, Dolmetsch RE, Griffith EC, Hu LS, Haddad C, Xia Z, Greenberg ME (2002) CREB transcriptional activity in neurons is regulated by multiple, calcium-specific phosphorylation events. Neuron 34:221-233.

Kreutzberg GW (1996) Microglia: a sensor for pathological events in the CNS. Trends Neurosci 19:312-318.

Lara A, Dargent B, Julien F, Alcaraz G, Tricaud N, Couraud F, Jover E (1996) Channel activators reduce the expression of sodium channel alpha-subunit mRNA in developing neurons. Brain Res Mol Brain Res 37:116-124.

Laycock JF, Hanoune J (1998) From vasopressin receptor to water channel: intracellular traffic, constraint and by-pass. J Endocrinol 159:361-372.

Leffler A, Cummins TR, Dib-Hajj SD, Hormuzdiar WN, Black JA, Waxman SG (2002) GDNF and NGF reverse changes in repriming of TTX-sensitive Na(+) currents following axotomy of dorsal root ganglion neurons. J Neurophysiol 88:650-658.

LeMasson G, Marder E, Abbott LF (1993) Activity-dependent regulation of conductances in model neurons. Science 259:1915-1917.

Leresche N, Parri HR, Erdemli G, Guyon A, Turner JP, Williams SR, Asprodini E, Crunelli V (1998) On the action of the anti-absence drug ethosuximide in the rat and cat thalamus. J Neurosci 18:4842-4853.

Levy J, Gavin JR, 3rd, Sowers JR (1994) Diabetes mellitus: a disease of abnormal cellular calcium metabolism? Am J Med 96:260-273.

Li M, West JW, Numann R, Murphy BJ, Scheuer T, Catterall WA (1993) Convergent regulation of sodium channels by protein kinase C and cAMP-dependent protein kinase. Science 261:1439-1442.

Li M, Jia M, Fields RD, Nelson PG (1996) Modulation of calcium currents by electrical activity. J Neurophysiol 76:2595-2607.

Li ZG, Zhang W, Grunberger G, Sima AA (2002) Hippocampal neuronal apoptosis in type 1 diabetes. Brain Res 946:221-231.

Liu Z, Golowasch J, Marder E, Abbott LF (1998) A model neuron with activity-dependent conductances regulated by multiple calcium sensors. J Neurosci 18:2309-2320.

Luo Y, Kaur C, Ling EA (2002) Neuronal and glial response in the rat hypothalamus-neurohypophysis complex with streptozotocin-induced diabetes. Brain Res 925:42-54.

Marder E, Abbott LF, Turrigiano GG, Liu Z, Golowasch J (1996) Memory from the dynamics of intrinsic membrane currents. Proc Natl Acad Sci U S A 93:13481-13486.

Marder E, Prinz AA (2002) Modeling stability in neuron and network function: the role of activity in homeostasis. Bioessays 24:1145-1154.

Maurice N, Tkatch T, Meisler M, Sprunger LK, Surmeier DJ (2001) D1/D5 dopamine receptor activation differentially modulates rapidly inactivating and persistent

sodium currents in prefrontal cortex pyramidal neurons. J Neurosci 21:2268-2277.

McCall AL (1992) The impact of diabetes on the CNS. Diabetes 41:557-570.

Meeren HK, Pijn JP, Van Luijtelaar EL, Coenen AM, Lopes da Silva FH (2002) Cortical focus drives widespread corticothalamic networks during spontaneous absence seizures in rats. J Neurosci 22:1480-1495.

Meisler MH, Kearney J, Ottman R, Escayg A (2001) Identification of epilepsy genes in human and mouse. Annu Rev Genet 35:567-588.

Migheli A, Attanasio A, Schiffer D (1995) Ultrastructural detection of DNA strand breaks in apoptotic neural cells by in situ end-labelling techniques. J Pathol 176:27-35.

Miyata S, Takamatsu H, Maekawa S, Matsumoto N, Watanabe K, Kiyohara T, Hatton GI (2001) Plasticity of neurohypophysial terminals with increased hormonal release during dehydration: ultrastructural and biochemical analyses. J Comp Neurol 434:413-427.

Miyata S, Hatton GI (2002) Activity-related, dynamic neuron-glial interactions in the hypothalamo-neurohypophysial system. Microsc Res Tech 56:143-157.

Monjaraz E, Navarrete A, Lopez-Santiago LF, Vega AV, Arias-Montano JA, Cota G (2000) L-type calcium channel activity regulates sodium channel levels in rat pituitary GH3 cells. J Physiol 523 Pt 1:45-55.

Nersesyan H, Hyder F, Rothman D, McCormick D, Blumenfeld H (2002) Comparison of BOLD fMRI and electrophysiology recordings during spike-wave seizures in WAG/Rij rats. Society for Neuroscience, Abstracts.

Noda M, Ikeda T, Suzuki H, Takeshima H, Takahashi T, Kuno M, Numa S (1986a) Expression of functional sodium channels from cloned cDNA. Nature 322:826-828.

Noda M, Ikeda T, Kayano T, Suzuki H, Takeshima H, Kurasaki M, Takahashi H, Numa S (1986b) Existence of distinct sodium channel messenger RNAs in rat brain. Nature 320:188-192.

Noebels JL (2002) Sodium channel gene expression and epilepsy. Novartis Found Symp 241:109-120.

Offord J, Catterall WA (1989) Electrical activity, cAMP, and cytosolic calcium regulate mRNA encoding sodium channel alpha subunits in rat muscle cells. Neuron 2:1447-1452.

Okuse K, Chaplan SR, McMahon SB, Luo ZD, Calcutt NA, Scott BP, Akopian AN, Wood JN (1997) Regulation of expression of the sensory neuron-specific sodium channel SNS in inflammatory and neuropathic pain. Mol Cell Neurosci 10:196-207.

Parri HR, Crunelli V (1998) Sodium current in rat and cat thalamocortical neurons: role of a non-inactivating component in tonic and burst firing. J Neurosci 18:854-867.

Peeters BW, Kerbusch JM, Coenen AM, Vossen JM, van Luijtelaar EL (1992) Genetics of spike-wave discharges in the electroencephalogram (EEG) of the WAG/Rij inbred rat strain: a classical mendelian crossbreeding study. Behav Genet 22:361-368.

Raman IM, Sprunger LK, Meisler MH, Bean BP (1997) Altered subthreshold sodium currents and disrupted firing patterns in Purkinje neurons of Scn8a mutant mice. Neuron 19:881-891.

Reinhold HS (1966) Quantitative evaluation of the radiosensitivity of cells of a transplantable rhabdomyosarcoma in the rat. Eur J Cancer 2:33-42.

Renganathan M, Cummins TR, Waxman SG (2001) Contribution of Na(v)1.8 sodium channels to action potential electrogenesis in DRG neurons. J Neurophysiol 86:629-640.

Ritchie JM (1988) Sodium-channel turnover in rabbit cultured Schwann cells. Proc R Soc Lond B Biol Sci 233:423-430.

Rizzo MA, Kocsis JD, Waxman SG (1996) Mechanisms of paresthesiae, dysesthesiae, and hyperesthesiae: role of Na+ channel heterogeneity. Eur Neurol 36:3-12.

Sangameswaran L, Delgado SG, Fish LM, Koch BD, Jakeman LB, Stewart GR, Sze P, Hunter JC, Eglen RM, Herman RC (1996) Structure and function of a novel voltage-gated, tetrodotoxin-resistant sodium channel specific to sensory neurons. J Biol Chem 271:5953-5956.

Sashihara S, Waxman SG, Greer CA (1997) Downregulation of Na+ channel mRNA in olfactory bulb tufted cells following deafferentation. NeuroReport 8:1289-1293.

Schaller KL, Krzemien DM, Yarowsky PJ, Krueger BK, Caldwell JH (1995) A novel, abundant sodium channel expressed in neurons and glia. J Neurosci 15:3231-3242.

Scharfman HE (2002) Epilepsy as an example of neural plasticity. Neuroscientist 8:154-173.

Schild JH, Kunze DL (1997) Experimental and modeling study of Na+ current heterogeneity in rat nodose neurons and its impact on neuronal discharge. J Neurophysiol 78:3198-3209.

Schmidt JW, Catterall WA (1986) Biosynthesis and processing of the alpha subunit of the voltage-sensitive sodium channel in rat brain neurons. Cell 46:437-444.

Scroggs RS, Fox AP (1992) Multiple Ca^{2+} currents elicited by action potential waveforms in acutely isolated adult rat dorsal root ganglion neurons. J Neurosci 12:1789-1801.

Segal MM, Douglas AF (1997) Late sodium channel openings underlying epileptiform activity are preferentially diminished by the anticonvulsant phenytoin. J Neurophysiol 77:3021-3034.

Segal MM (2002) Sodium channels and epilepsy electrophysiology. Novartis Found Symp 241:173-180.

Serino R, Ueta Y, Tokunaga M, Hara Y, Nomura M, Kabashima N, Shibuya I, Hattori Y, Yamashita H (1998) Upregulation of hypothalamic nitric oxide synthase gene expression in streptozotocin-induced diabetic rats. Diabetologia 41:640-648.

Sherman SJ, Catterall WA (1984) Electrical activity and cytosolic calcium regulate levels of tetrodotoxin-sensitive sodium channels in cultured rat muscle cells. Proc Natl Acad Sci U S A 81:262-266.

Shiraishi S, Shibuya I, Uezono Y, Yokoo H, Toyohira Y, Yamamoto R, Yanagita T, Kobayashi H, Wada A (2001) Heterogeneous increases of cytoplasmic calcium: distinct effects on down-regulation of cell surface sodium channels and sodium channel subunit mRNA levels. Br J Pharmacol 132:1455-1466.

Sleeper AA, Cummins TR, Dib-Hajj SD, Hormuzdiar W, Tyrrell L, Waxman SG, Black JA (2000) Changes in expression of two tetrodotoxin-resistant sodium channels and their currents in dorsal root ganglion neurons after sciatic nerve injury but not rhizotomy. J Neurosci 20:7279-7289.

Smith MR, Smith RD, Plummer NW, Meisler MH, Goldin AL (1998) Functional analysis of the mouse Scn8a sodium channel. J Neurosci 18:6093-6102.

Spadoni F, Hainsworth AH, Mercuri NB, Caputi L, Martella G, Lavaroni F, Bernardi G, Stefani A (2002) Lamotrigine derivatives and riluzole inhibit INa,P in cortical neurons. NeuroReport 13:1167-1170.

Sperlagh B, Mergl Z, Juranyi Z, Vizi ES, Makara GB (1999) Local regulation of vasopressin and oxytocin secretion by extracellular ATP in the isolated posterior lobe of the rat hypophysis. J Endocrinol 160:343-350.

Spitzer NC (1999) New dimensions of neuronal plasticity. Nat Neurosci 2:489-491.

Srinivasan A, Roth KA, Sayers RO, Shindler KS, Wong AM, Fritz LC, Tomaselli KJ (1998) In situ immunodetection of activated caspase-3 in apoptotic neurons in the developing nervous system. Cell Death Differ 5:1004-1016.

Stemmler M, Koch C (1999) How voltage-dependent conductances can adapt to maximize the information encoded by neuronal firing rate. Nat Neurosci 2:521-527.

Steriade M, Deschenes M, Domich L, Mulle C (1985) Abolition of spindle oscillations in thalamic neurons disconnected from nucleus reticularis thalami. J Neurophysiol 54:1473-1497.

Taddese A, Bean BP (2002) Subthreshold sodium current from rapidly inactivating sodium channels drives spontaneous firing of tuberomammillary neurons. Neuron 33:587-600.

Tanaka M, Cummins TR, Ishikawa K, Dib-Hajj SD, Black JA, Waxman SG (1998) SNS Na+ channel expression increases in dorsal root ganglion neurons in the carrageenan inflammatory pain model. NeuroReport 9:967-972.

Tanaka M, Cummins TR, Ishikawa K, Black JA, Ibata Y, Waxman SG (1999) Molecular and functional remodeling of electrogenic membrane of hypothalamic neurons in response to changes in their input. Proc Natl Acad Sci U S A 96:1088-1093.

Taverna S, Mantegazza M, Franceschetti S, Avanzini G (1998) Valproate selectively reduces the persistent fraction of Na+ current in neocortical neurons. Epilepsy Res 32:304-308.

Titan LM, Otoom S, Alkadhi KA (1995) Endogenous bursting due to altered sodium channel function in rat hippocampal CA1 neurons. Brain Res 680:164-172.

Toledo-Aral JJ, Moss BL, He ZJ, Koszowski AG, Whisenand T, Levinson SR, Wolf JJ, Silos-Santiago I, Halegoua S, Mandel G (1997) Identification of PN1, a

predominant voltage-dependent sodium channel expressed principally in peripheral neurons. Proc Natl Acad Sci U S A 94:1527-1532.

Turrigiano G, Abbott LF, Marder E (1994) Activity-dependent changes in the intrinsic properties of cultured neurons. Science 264:974-977.

Turrigiano G, LeMasson G, Marder E (1995) Selective regulation of current densities underlies spontaneous changes in the activity of cultured neurons. J Neurosci 15:3640-3652.

Turrigiano GG (1999) Homeostatic plasticity in neuronal networks: the more things change, the more they stay the same. Trends Neurosci 22:221-227.

Turrigiano GG, Nelson SB (2000) Hebb and homeostasis in neuronal plasticity. Curr Opin Neurobiol 10:358-364.

Van Itallie CM, Fernstrom JD (1982) Osmolal effects on vasopressin secretion in the streptozotocin-diabetic rat. Am J Physiol 242:E411-417.

Vergnes M, Marescaux C, Depaulis A (1990) Mapping of spontaneous spike and wave discharges in Wistar rats with genetic generalized non-convulsive epilepsy. Brain Res 523:87-91.

Vergnes M, Marescaux C (1992) Cortical and thalamic lesions in rats with genetic absence epilepsy. J Neural Transm Suppl 35:71-83.

Voisin DL, Bourque CW (2002) Integration of sodium and osmosensory signals in vasopressin neurons. Trends Neurosci 25:199-205.

Vreugdenhil M, Faas GC, Wadman WJ (1998) Sodium currents in isolated rat CA1 neurons after kindling epileptogenesis. Neuroscience 86:99-107.

Waechter CJ, Schmidt JW, Catterall WA (1983) Glycosylation is required for maintenance of functional sodium channels in neuroblastoma cells. J Biol Chem 258:5117-5123.

Waxman SG, Kocsis JD, Black JA (1994) Type III sodium channel mRNA is expressed in embryonic but not adult spinal sensory neurons, and is reexpressed following axotomy. J Neurophysiol 72:466-470.

Waxman SG (1999a) The molecular basis for electrogenic computation in the brain: you can't step in the same river twice. Mol Psychiatry 4:222-228.

Waxman SG (1999b) The molecular pathophysiology of pain: abnormal expression of sodium channel genes and its contributions to hyperexcitability of primary sensory neurons. Pain Suppl 6:S133-140.

Waxman SG, Dib-Hajj S, Cummins TR, Black JA (2000) Sodium channels and their genes: dynamic expression in the normal nervous system, dysregulation in disease states. Brain Res 886:5-14.

Waxman SG (2001) Transcriptional channelopathies: an emerging class of disorders. Nat Rev Neurosci 2:652-659.

West AE, Chen WG, Dalva MB, Dolmetsch RE, Kornhauser JM, Shaywitz AJ, Takasu MA, Tao X, Greenberg ME (2001) Calcium regulation of neuronal gene expression. Proc Natl Acad Sci U S A 98:11024-11031.

West AE, Griffith EC, Greenberg ME (2002) Regulation of transcription factors by neuronal activity. Nat Rev Neurosci 3:921-931.

Widmer H, Amerdeil H, Fontanaud P, Desarmenien MG (1997) Postnatal maturation of rat hypothalamoneurohypophysial neurons: evidence for a developmental decrease in calcium entry during action potentials. J Neurophysiol 77:260-271.

Winer J, Jung CK, Shackel I, Williams PM (1999) Development and validation of real-time quantitative reverse transcriptase-polymerase chain reaction for monitoring gene expression in cardiac myocytes in vitro. Anal Biochem 270:41-49.

Woolf CJ, Salter MW (2000) Neuronal plasticity: increasing the gain in pain. Science 288:1765-1769.

Zeng XX, Ng YK, Ling EA (2000) Neuronal and microglial response in the retina of streptozotocin-induced diabetic rats. Vis Neurosci 17:463-471.

Zheng H, Li YF, Weiss M, Mayhan WG, Patel KP (2002) Neuronal expression of fos protein in the forebrain of diabetic rats. Brain Res 956:268-275.

COPYRIGHT PERMISSIONS

Figures 2.2, 2.3, and 2.4 were reproduced with permission from the journal *NeuroReport*, published by Lippincott Williams & Wilkins (Klein et al., 2002).

Figures 3.1, 3.2, 3.3, 3.4, 3.5, 3.6, and Table 3.1 were reproduced with permission from the journal *Neurobiology of Disease*, published by Elsevier (Klein et al., 2004a).

Figures 4.1, 4.2, and 4.3 were reproduced with permission from the *Journal of Neuroscience Research*, published by Wiley (Klein et al., 2003a).

Figures 5.1, 5.2, 5.3, and 5.4 were reproduced with permission from the journal *Brain Research*, published by Elsevier (Klein et al., 2004b).

Figures 2.5 and 6.1 were reproduced with permission from the journal *Lancet Neurology*, published by Elsevier (Klein and Waxman, 2003).